EXPERIMENTAL AND NUMERICAL STUDY ON THE CYCLIC BEHAVIOR OF CONNECTIONS IN STORAGE RACK STRUCTURES

by

Rahman Shahshenas

B.S., Civil Engineering, Boğaziçi University, 2006

M.S., Civil Engineering, Boğaziçi University, 2009

Submitted to the Institute for Graduate Studies in
Science and Engineering in partial fulfillment of
the requirements for the degree of
Doctor of Philosophy

Graduate Program in Civil Engineering

Boğaziçi University

2015

ACKNOWLEDGEMENTS

Many people have contributed to shape the content and structure of this thesis. It is therefore my great pleasure to thank those who contributed and supported me in the process to write this thesis.

First of all, I would like to thank my advisor, Prof. Gülay Altay, without whose sympathy, patience and guidance, the accomplishment would have been impossible. Since the beginning of my undergraduate and graduate studies at Bogaziçi University, she has been more than an advisor in addition to providing me with invaluable guidance, support and encouragement throughout the preparation of this thesis.

I would also like to thank Prof. M. Cengiz Dökmeci for his kind and supportive attitude to me and showing high interest and valuable advice to my thesis. I would like to acknowledge Prof. Hilmi Luş, Assist Prof. Serdar Soyöz, and Assist Prof. Özden Barlas Çağlayan, members of the examining committee for their efforts in reviewing the thesis.

I am grateful to ÜÇGE DRS for providing me with sponsorship and Çoşkunöz Metal-Form for calibrating tensile test results which eased my job greatly. I also thank my family-my mother, my father, my sister and brothers- for the support they have given me throughout my life. I also express my gratefulness to my friends Ahmet Emre Öcal and Akin Saka for conducting laboratory tests that could last days and nights, and Yavuz Tokmak for his help and guidance throughout numerical analyses and thesis editing. Thanks are also to Yilmaz Yuva and Ibrahim Korkut for encouraging research works of the author.

I cannot find the proper words to thank my beloved one Canan Eliçin Shahshenas, who has been the source of inspiration for me from the very beginning. I wouldn't have been able to finish this work without her support, encouragement, help, patience, and love.

I will always feel grateful to everyone who contributed to this thesis. Any remaining mistakes are my own.

ABSTRACT

EXPERIMENTAL AND NUMERICAL STUDY ON THE CYCLIC BEHAVIOR OF CONNECTIONS IN STORAGE RACK STRUCTURES

Contrary to buildings which serve live loads lower than the self-weight, storage racks support much higher live loads. In unbraced frames of storage racks, the lateral stiffness and the stability along down-aisle direction are provided by means of beam-to-upright and base connections which are neither pinned nor fixed connections. Beam-to-upright connections govern the structural performance and stability of the whole system. Therefore, estimating the behavior of a connection, having knowledge about the failure modes and rotation capacity are of great importance. This study presents the main results of an experimental program on the response of beam-to-upright connections of racks commonly used in the Turkish market. To create reliable references for comparing the results, beam-depth and end-connector types were tested for 2 different types of specimens, altogether 18 specimens were tested. Monotonic and slow quasi-static reversed cyclic tests were performed. Interlocked boltless beam-to-upright connections cause difficulties in collecting the data and measuring the parameters; therefore the testing procedures and originally developed set-up for beam-to-upright connections were proposed and modeled with FE models developed in *SAP2000* v.15 software to establish reliable references. Numerical investigations were used to verify experimental results and to introduce a model of such connections. To simulate the test and to model the connection, *ANSYS* v.14 software was used. The semi-rigid nature of this type of connections which primarily is due to the unpredictable distortions at different components of the joint requires a nonlinear simulation through advanced analyses. *ANSYS* software results showed a good match with moment-rotation curve results with respect to initial stiffness, ultimate strength and the level of ductility.

ÖZET

RAF DEPOLAMA SİSTEMLERİNDEKİ BAĞLANTILARIN SİSMİK DAVRANIŞI ÜZERİNE DENEYSEL VE SAYISAL BİR ÇALIŞMA

Öz ağırlıklarından daha az olan hareketli yükleri taşıyan binaların aksine depo rafları öz ağırlıklarından çok daha fazla yükleri taşımaktadır. Çaprazsız raf depolama çerçevelerinde koridor doğrultusundaki yanal rijitlik ve stabilite, yârı-rijit davranışı gösteren geçmeli kiriş-kolon birleşimler ile sağlanmaktadır. Bu elemanlar birleşim bölgesini oluşturmaktadır ve depo raflarında birleşimin davranışını kestirirken dönme kapasitesi ve olası mafsal noktaları önem taşımaktadır.Bu çalışmada endüstride yaygın olarak kullanılan rafların kiriş-kolon birleşimlerinin davranışları üzerine deneysel bir programın sonuçları sunulmaktadır. Sonuçları kıyaslamak için güvenilir referanslar yaratma amacıyla kiriş derinliği ve uç-bağlantı türleri 2 tip birleşim için değiştirilmiş ve değişik tiplerde toplamda 18 numune test edilmiştir. Bulonsuz iç içe geçmeli kiriş-kolon bağlantışı veri toplamayı zorlaştırmaktadır dolayısıyla kiriş-kolon bağlantışı için test yöntemleri ve özgün olarak geliştirilen deney düzeneği verilmiştir. Deney sonuçlarını doğrulamak amacıyla sayisal kontroller SAP2000 analiz programında yapılmış ve çesitli parametreleri göz önünde bulundurarak bu gibi mekanik bağlantıların modelleme yaklaşımı açıklanmıştır. Testlerin simülasyonu ve modellenmesi için ANSYS sonlu elemanlar yazılımı kullanılmıştır. Esas olarak düğüm noktalarının değişik bölgelerde öngörülemez bozulmalara uğramasından kaynaklanan bu gibi birleşimlerin yarı-rijit davranışı, bu çalışmayı doğrusal ve elastik olmayan analizlere yönlendirmiştir. Analiz sonuçlar, dikkate alınan ilk rijitlik, nihai dayanım ve süneklik oranı test sonuçlarıyla uyumluluk göstermiştir.

TABLE OF CONTENTS

LIST OF FIGURES

LIST OF TABLES

LIST OF SYMBOLS

a	Lever arm for load F
C_s	Seismic response coefficient
D_l	Dead load
E	Modulus of elasticity
F	Connection rotational spring constant
F	Displacement applied by dynamic actuator
F	Vertical load
F_a	Site coefficient
F_v	Site coefficient
f_y	Yield stress
H	Distance between LVDTs
I_b	Moment of inertia of the beam segment
I_c	Moment of inertia of the column segment
I_p	Building importance factor
K_e	Elastic stiffness
LL	Live load
L_b	The length of beam segment
L_c	The length of column segment
M	Moment
PL	Product load
$PL_{Average}$	Average weight of stored pallet
$PL_{Maximum}$	Maximum weight of stored pallets
PL_{RF}	Pallet mass participation coefficient
Q_y	Yield force
q	Behavior factor
R	Response modification factor
S	Constant connection stiffness
S_{D1}	Design earthquake spectral response acceleration at short periods

S_{DS}	Design earthquake spectral response acceleration at a 1 second period
S_s	The mapped spectral accelerations for short periods
S_{MS}	The maximum considered earthquake spectral response accelerations for short period
S_{M1}	The maximum considered earthquake spectral response accelerations for 1 sec period
S_1	The mapped spectral accelerations for 1-second period
T	Fundamental period of the rack structure
V	Base shear
W_s	Seismic weight

$\delta*$	Control Deformation
δ_1	Deflection measured by LVDT #3
δ_2	Deflection measured by LVDT #4
δ_y	Yield displacement
ε_{eng}	Engineering strain
ε_{ln}	Logarithmic strain
σ_{eng}	Engineering stress
σ_{true}	True stress
Θ	The angle between the column and connecting beam
Φ	Radius of curvature

LIST OF ACRONYMS/ABBREVIATIONS

AISC	American Institute of Steel Construction
AISI	American Iron and Steel Institute
ASCE	American Society of Civil Engineers
ASD	Allowable Stress Design
ATC	Applied Technology Council
DBYYHY	Deprem Bölgelerinde Yapılacak Yapılar Hakkında Yönetmelik
FEM	Finite Element Method
FEM	The Federation Europeenne de la Manotention (the Seismic design of static steel pallet racks)
FEMA	Federal Emergency Management Agency
ICBO	International Conference of Building Officials
LC	Load Cell
LVDT	Linear Valuable Displacement Transducer
NEHRP	National Earthquake Hazards Reduction Program
NSF	National Science Foundation
RC	Reinforced Concrete
RMI	Rack Manufacturers Institute
TDY	Turkish Seismic Design Code
TS	Türk Standardı
UBC	Uniform Building Code

1. INTRODUCTION

Steel storage rack structures are widely used in industry for storing and retrieving goods placed on pallets. They are freestanding and act as structures in their own right. Storage racks are designed to carry pallet loads and to resist placement and impact forces from forklift trucks. They are heavily loaded and designed as lightly as possible in the prevailing competitive industry.

Different types of racks are available on the market like as selective racks and drive-in racks. Drive-in racks require less floor space by storing pallets on rail beams, one after the other, with no space between them. The forklift truck drives into the rack to store the pallets on the first-in, last-out principle. With the increasing price of land, drive-in racks are a more economical solution to selective rack when storing the same good. Briefly, minimum available land for construction in big cities leads to high rise buildings and structures and similarly minimum available space for industrial sector leads to rack structures for storing goods.

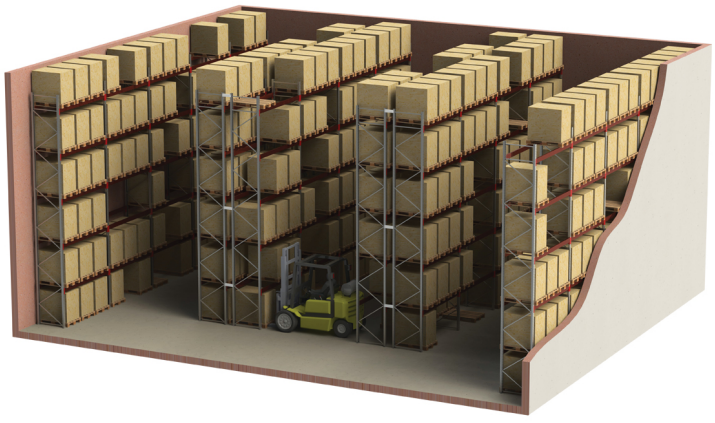

Figure 1.1. Typical Drive in Storage Rack System.

As a consequence, the number of large warehouses which is housing rack structures has grown significantly in last fifty years. Therefore, large factories and shopping markets use engineered warehouses for the optimal space and storage rack systems inside the warehouse which are the most convenient structures to store the goods as

shown in Figure 1.1.

Rack structures typically are subjected to the self-weight, pallet loads, fire loads, impact loads caused by forklifts and seismic forces.

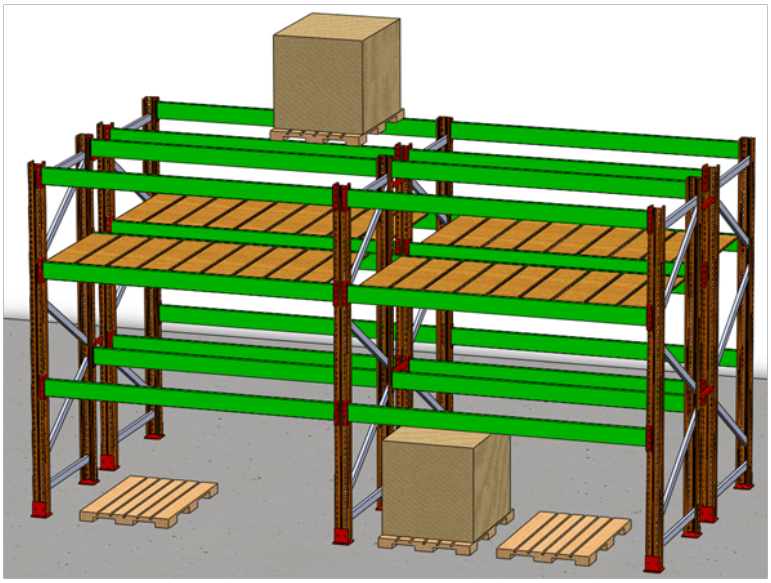

Figure 1.2. Typical Back-to-Back Storage Rack Structure.

Pallets are designed to carry the maximum pallet design load when all racks are fully loaded. Among all kinds of stored goods, hazardous materials pose additional problems in case of failures such as fire. Problems due to earthquakes, impact of drive-in cars, over loading and at the end the majority of failures are the result of instability effects. As a consequence of such failures, safety of not only economic loss of goods but more importantly safety of occupants is a major concern.

Earthquakes can cause storage racks to collapse or overturn if they are not properly designed, installed, loaded, and maintained, hence resulting economic losses due to spill or topple off of stored goods on the rack structures. During an earthquake, life safety is dependent on the structural performance of the host buildings and the structural performance of the storage racks. Not only the building itself but also the storage racks may pose a life-safety risk for the occupants and workers unless designed in compliance with the available codes. The earthquake resistant design methodology of the rack system depends on the structural behavior of rack structure and the stored

contents. Life safety performance level in the "Seismic Considerations for Steel Storage Racks Located in Areas Accessible to the Public" - FEMA 460 is achieved under three conditions.

- Failure of components that could result in rack collapse or contents shedding, must be prevented.
- Rack overturning must be prevented.
- There must be no loss of stored items from rack shelves supported 2.5 m or more above the floor.

Loss of life and economical losses caused by collapse of rack structures are crucial for developing countries where there is less developed or no design code at all, whereas for developed countries since the code compliance structures are generally the case, the emphasis is more on the reduction of direct and indirect economic losses.

Rack systems operated by industrial trucks represent approximately 70% of the total yearly racking industry market. In 2003, estimated pan-European sale value for the racking industry exceeded 1.2 Billion Euro. On the other hand, the current estimated yearly loss due to accidental impact is 600 million Euros. Moreover the losses due to consequent fires far exceed this value. Economic losses are expected to continue to rise due to competitive pressure in logistic industry, resulting in higher driving speeds of industrial trucks within the racking environment (Castiglioni 2005). The use of such systems is scaling up pursuant to the need of huge warehouses and storing space. Consequently, the number of collapses has increased in larger scale. Although relatively few damaging earthquakes have occurred, rack damage and content spillage during several earthquakes in California, like the 1987 Whittier, 1989 Loma Prieta, 1992 Landers, 1994 Northridge and 2001 Nisqually earthquake, caused comparatively high damage in existing rack systems (FEMA 460, 2005).

1.1. Definition of the Problem

There are two types of drive-in rack systems, namely, braced and un-braced frames. Braced frames are not desirable due to loading and unloading problems because of bracing elements which most of the time obstruct the openings. In unbraced rack frames the longitudinal directions and the transverse directions are called the *down-aisle* direction and the *cross-aisle* direction, respectively. Un-braced frames, in the other words, moment frames are typically used as the lateral load carrying system in the down-aisle direction and braced frames are typically used as the framing system in the cross-aisle direction as shown in Figure 1.3.

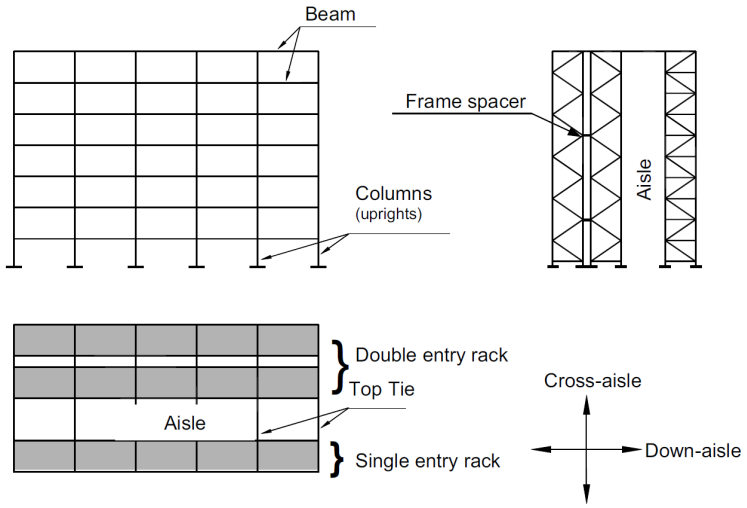

Figure 1.3. Typical Configuration of Unbraced Pallet Rack Structures.

These unbraced storage rack frames are composed of cold formed steel elements that permit easy installation and un-installation by the practical interlocking connections. In the down-aisle direction moment connections are used and called as beam-to-upright connections. The behavior of those beam-to-upright connections which are the major lateral resistance elements for the frames and their moment rotation characteristics need to be determined either through experimental or numerical tests in order to be defined as moment connection, however in reality connections in general behave semi-rigid.

The rotational behavior of beam-to-upright joints is well recognized as being

intermediate between the two extreme situations called as rigid and pinned. When all the different parts in the joint are sufficiently stiff, the joint is rigid, and there is no difference between the respective rotations at the ends of the members connected at this joint. The joint without any stiffness behaves just as a simply supported beam is pinned joint. The simplest means for representing the concept is a rotational spring between the ends of the two connected members. The rotational stiffness is the parameter that links the transmitted moment to the relative rotation, which is the difference between the absolute rotations of the two connected members. When this rotational stiffness is zero or relatively small, the joint falls back into the pinned joint class. In contrast, when the rotational stiffness is infinite or relatively high the joint falls into the rigid class. In all intermediate cases the joint belongs to the semi-rigid joint class (Jaspart 1999).

The semi-rigid beam-to-upright connection is characterized by the rotational capacity of the connection. "FEMA 460" presents a simple analytical model for the displacement based seismic design of storage racks in the down-aisle direction. The model is aimed at developing simplified equations for fundamental period, the base shear, and the top lateral displacement of storage racks in down-aisle direction as a function of the beam-to-upright rotational characteristics at a given target design lateral displacement. The most important parameters to derive the analytical model are the rotational stiffness and the rotational capacity. "FEMA 460 Appendix A" proposes tests at the target displacement for determining the parameters. In designing connection of light steel rack structures contrary to the design of standard steel structures, tests on beam-to-upright must be performed in the preliminary design phase, since the behavior parameters cannot be estimated in advance. Those test procedures as described in Rack Manufacturer Institute (RMI 2008) and EN15512-2009 are for determining the design parameters; however, the seismic behavior of the beam-to-upright connection cannot be predicted due to semi-rigid behavior. Furthermore, presenting a standard test procedure is another problem due to variety of connection types. The connection types for every manufacturer are quite unique and are special to the manufacturer in the rack industry.

Typical beam-to-upright connections are tested under quasi static loading and behavior parameters are predicted. Main results of experimental and numerical study on the responses of beam-to-upright commonly used in Turkey are presented. In this thesis study, the behavior of beam-to-upright connections under monotonic and reversed cyclic loading is investigated by determining moment-rotation curves, and the level of semi-rigid behavior.

1.2. Approaching the Problem

Since the seismic behavior of beam-to-upright connections is not well defined, experiment is the most effective way of approaching the problem. A great amount of experimental work directed toward achieving a better understanding of the performance of beam-to-upright to seismic excitations has been done in recent years in structural laboratories described in the next section.

For the earthquake response of structures, detailed knowledge of strength and deformation characteristics of the elements and assemblies forming the structural system is required. Experiments which reproduce the field conditions are needed to provide information for the test set-up development. This information is also used to develop analytical models that form the basis for determination of seismic behavior.

Today's standard in designing rack structures is to use American specifications such as "Rack Manufacturers Institute Specifications for the Design, Testing, and Utilization of Industrial Steel Storage Rack, RMI 2008 and Steel Static Storage Systems-Adjustable Pallet Racking Systems-Principles for Structural Design EN15512-2009" in Europe; however, many countries including Turkey do not have standard produced for the sections and systems and since each beam-to-upright connection is unique type of connection, that needs experimental and numerical studies to be conducted for the behavior under seismic loading. The need for research in connections comes from the parameters uniqueness defined for special type of connections used in national practice.

To address the above stated problems, different types of the recommendations

and the structural performance of beam-to-upright connections must be well defined. In order to produce prescriptive design guidelines of such connections, research studies need to be conducted.

Storage rack structures are currently designed in accordance with RMI 2008 along with the added provisions of "National Earthquake Hazards Reduction Program NEHRP, Minimum Design Loads for Buildings and Other Structures ASCE 7-10 and International Building Code IBC 2012. Moreover, EN 15512-2009" is used for design of storage rack structures in European countries. "RMI 2008 and EN 15512" are used together with added provisions to design building structures. The consequences of the added provisions are to cause an upper limit to be imposed on the period of rack structural behavior under seismic conditions, and cause large base shear forces to be predicted in the resulting structural analysis since the seismic behavior of rack structures during earthquakes had not been rationally explained (RMI 2008).

The imposition of large base shear forces has been the requirement since early 1970's, when the "Unified Building Code 1997" first introduced provisions to be applied to seismic behavior of steel storage racks. The current cap that results from current provisions imposes an upper limit of 0.6 seconds on the period of the rack structural response where it is well known that typical storage rack may have periods of 2 to 4 seconds in the down aisle direction. Further, it is well known that rack periods, rack damping, and overall rack structural behavior is very dependent on the beam-to-upright connectors and connections and their moment-rotation characteristics that are the key and integral component of rack structures (RMI 2008).

1.2.1. Background

There are a few studies on the seismic performance of storage rack systems in comparison to the other research areas under cold formed steel systems. Experimental and analytical studies have been conducted and the results are often consistent as observed in some studies (Bajoria 2006). Current codes recommend component tests in addition to analytical procedures for the analysis and design of a system. Analytical

procedures are mostly given in the Appendices of the codes.

The lateral stiffness of rack structures along down-aisle direction is influenced by the distortions that occur at the beam-to-upright connections. In these procedures, the distortions are represented by simple rotational springs and the constant of the spring is to be determined by tests.

(Krawinkler *et al.*, 1979) performed cantilever tests on 20 different beam-to-upright subassemblies of standard pallet rack structures; the objective of study was to acquire basic information on the response characteristics that positively affects the seismic behavior of racks. The results indicated that the behavior of the beam-to- post connections can be represented by rotational springs whose characteristics should be determined experimentally and ideally, strength, stiffness and ductility of these springs should be determined by means of subassembly (portal) tests using cyclic loading. The cantilever test, which is much simpler to carry out and results are in more reliable measurements of moments, could be used as an alternative. A further result is that because of local deformations at the beam-to-post connections, hysteresis loops have a pinched shape similar to that obtained in reinforced concrete elements with high shear.

(Markazi *et al.*, 1997) studied boltless semi-rigid connections which consist of end plates welded to each end of a beam and an interlocking arrangement to engage with perforated columns. The influence of the flexibility of the beam and the column used in the derived tests on the stiffness determined experimentally and the effects of dimensional changes on moment-rotation characteristics were considered. The study results state that a beam end connector is subjected to combine axial load and bending moment. Also, the moment-rotation characteristic of a joint is determined not only by the design of beam end connector but also the efficiency of the accompanying members, in particular the upright.

(Godley, 1997) investigated the need for ductility in the connector, in order to allow some plastic design of the pallet beams using analytical equations on braced and unbraced rack systems. Godley (1997) derived the equations on the basis of the

assumption that in unbraced rack systems the sway of the frame is proportional to the load and reaches the maximum specified value of 0.02 rad at the design load which give the worst condition, a further assumption is that all the sway rotation must be absorbed by the connectors which is also a conservative assumption. The study indicated that a connector requires to exhibit different degrees of ductility depending on the strength and span of the beam as well as on the strength of the connector itself and the ductility required is independent of the stiffness of the connector.

(Kotha and Peköz, 2000) studied the behavior of cold-formed pallet storage racks with semi-rigid beam-to-upright connections and with flexible upright bases through finite element analyses. A general moment-rotation relationship was established to model the beam-to-upright connection stiffness of pallet storage racks.

(Baldassino and Bernuzzi, 2000) performed a numerical study on the analysis and behavior of steel pallet rack systems, the study recommended a semi-continuous frame model for an optimal design analysis. Results of elastic second order linear and non linear analyses pointed out a relatively low sensitivity of the rack ultimate capacity in comparison with that at the service condition.

(Bernuzzi and Castiglioni, 2001) performed 11 monotonic and 11 cyclic tests on two different types of beam-to-upright connections manufactured in Europe. Monotonic tests results showed that the nodal zones appear generally characterized by adequate ductile behavior and collapse is never achieved and tests have been stopped in correspondence of high levels of rotation. As to cyclic tests, it has been pointed out the relevant differences in the form of the hysteresis loops of rack joints in comparison with the ones associated with traditional steel components and the non-negligible influence of the connection systems on the joint behavior. The results of the cyclic tests exhibited pronounced pinching behavior associated with slippage and plastic deformations of the connectors leading to significant reduction energy dissipation capacity with increasing number of response cycles.

(Harris and Hancock, 2002) studided the stability in the down-aisle direction of

high rise storage racks which is provided by the beam-to-column and base-plate connections. They performed a complex test rig using two hydraulic actuators. Preliminary results show that the joints remain rigid to a point when they become semi-rigid. The values of joint stiffnesses back-calculated from second-order elastic analyses are much higher than those determined from simple cantilever tests.

(Bernuzzi *et al.*, 2004) studied seismic response of rack systems by performing experiments on two types of beam-to-column connection manufactured in Italy. The study focused on a basic single-bay storey or two-storey rack and multistory multiple-bay structures individually. The analyses have shown that rack structures may supply a limited-post elastic response but they exit the elastic field at very low values of horizontal action.

(Bajoria, Talikoti, 2006) performed two series of tests with different set-up, conventional cantilever method and a newly proposed double cantilever method and the results were verified by a full scale frame test. The results obtained from the cantilever test were found to match well with the full scale frame test. the results indicate that the shear to moment ratio in an actual frame is better represented by newly proposed method, confirmed by finite element analysis. Godley and Beale (2008) within the scope of study on the effect of looseness investigated the behavior of the beam end connector by monotonic moment-rotation test to determine the stiffness and strength and looseness. The proposed procedure appears to work well. The only obvious improvement would be to combine the looseness and bending tests into a single cyclic test that would measure the stiffness and strength of the connector in both directions as well as its looseness.

(Sarawit and Peköz, 2006) stated that the semi-rigid nature of beam to column connection is primarily due to the distortion of the column walls, tearing of the column perforation, and distortion of the beam end connector. The study indicates that the storage rack stability depends significantly on the behavior of this connection, thus it is important to have the means for predicting it and designs of these connections vary widely; making it is impossible to develop a general analytic model. Therefore, beam to

column connection tests are usually done to determine the relationship of the moment at the joint M and the change in angle between the column and the connecting beam θ.

The results of down-aisle shake table tests performed by Filliatrault *et al.*, 2007 on steel pallet type storage racks incorporating two different teardrop beam-to-upright connectors allowed the estimation of beam-to-upright connector rotational stiffness values from measured dynamic characteristics of storage racks. Both bolted and teardrop connectors tested to date had their beam-to-upright connector stiffness values reduce with excitation amplitude. Therefore, the dynamic testing should be performed at various excitations amplitudes.

The moment-rotation behavior of the connections was experimentally investigated (Gilbert and Rasmussen 2010) and can be broken into three distinct phases. The moment-rotation relationship is modeled using multilinear elastic nonlinear plastic moment-rotation curve.

A finite-element model of drive-in racks is introduced and shown to accurately reproduce the 3D behavior of the tested rack structure. Further calibration of the model against dynamically loaded tests is presented in Gilbert *et al.*, (2009). Based on the tests and finite element analysis, the companion paper (Zhang *et al.*, 2012) presents the derivation of a reliability-based design methodology for drive-in racks subjected to horizontal impact loads.

(Gilbert *et al.*, 2012) conducted full-scale tests on a complete drive-in rack system to obtain the load transfer and relative stiffness under various horizontal loading conditions. Differences in behavior were observed for the loaded and unloaded racks, caused mainly by the increased stiffness provided by the pallets and the base plates when the rack is loaded. Therefore, the pallets provided substantial stiffness to the rack.

(Zhao *et al.*, 2014), tested 17 groups of three identical specimens, subjected to

hogging static loading in a single cantilever test setup. The results have shown that tearing of the upright wall and cracking of tab is the governing failure mode and the thickness of upright relative to the thickness of tabs determines the failure mode. Thickness of upright, the depth of beam and the number of tabs are main factors in determining initial stiffness and moment capacity of connections. The importance of tabs has been highlighted at this study compared to former studies.

1.3. Scope of the Study

Since the rack structures are unbraced in down-aisle direction, lateral stiffness is usually provided by beam-to-upright joints rather than by braces in that direction to allow loading and unloading of pallets by forklifts. There are three main components in forming the joint, pallet beam, upright and the part attaching the beam into upright, called hook-in end connector. These mechanically interlocked assemblies are primarily boltless. The hooks on the end-connector are placed in the perforations available on the upright and form the connection, many types of bonded, frictional and frictionless contacts develop in between the surfaces. The performance of hooks, end-connector surfaces, and even performance of the perforation of the upright influence the behavior of joint and characterize the parameters.

The main parameters in this research are the structural behavior of the joint including the moment-rotation, the yield and the ultimate moment capacity, the energy dissipation through inelastic action in the joint and the different buckling modes of the components. Tearing of the hooks and crashing of the perforation, buckling of the end-connector and pallet beam, bending of the upright at joint region are a number of predicted failure modes.

The objective of the study is to understand the behavior of beam-to-upright connections of rack systems under earthquake loads. Therefore, the performance of the connections forming the structural system of the rack structure is experimentally as well as analytically investigated. Key features of tests are discussed and the main parameters characterizing the joint moment-rotation curve under monotonic and cyclic

reversal loading are given in the following chapters.

1.4. Threshold Sensitivity

To address the behavior of racking systems, the following framework is proposed to compare with other structural systems. There are three significant topics in the design of all buildings; safety, economy and regulations. When these three topics perquisites are considerably met, the rate of efficiency of the project is rising up. For example, for design of a building, the designs are started by architects and engineers who know the standard and regulations; they design in accordance with design codes. In the other hand, they must meet the budget restrictions. However, for rack systems there is not such procedure due to main reasons stated in the preceding section. Unfortunately, the situation in this area is not less efficiency but also inefficiency.

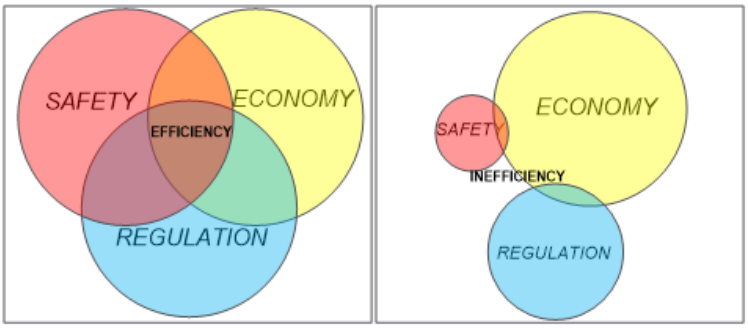

Figure 1.4. a) A General Consideration of Efficiency for Reinforced Concrete and Steel Buildings b) Current Situation of Racking Systems.

From a general perspective, the sustainable objectives of this study derive from, and map onto the problems defined in the preceding section: to address the consequences of earthquakes by considering safety, economy and regulations in design of rack systems. A significant amount of literature focuses on these objectives individually specially on safety topic.

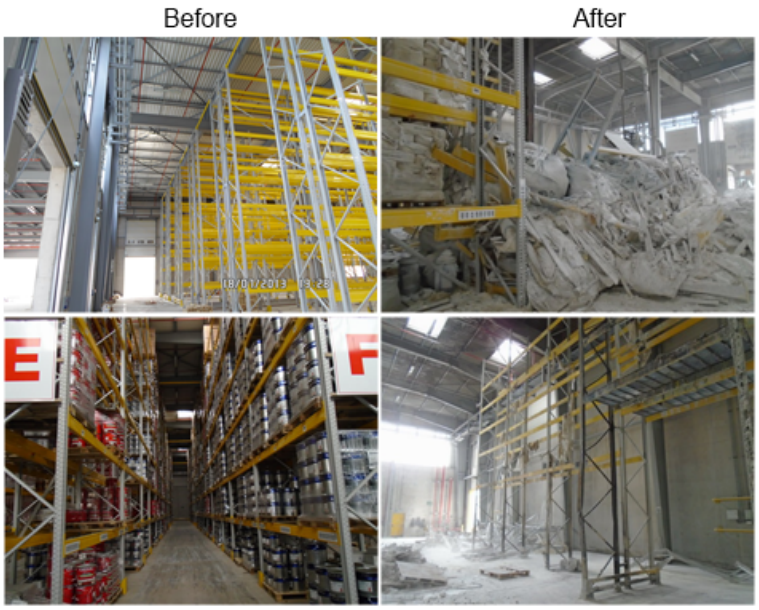

Figure 1.5. Rack Collapse Due to Incorrect Design.

The proposed operations and processes required to be performed in the design phase for increasing the efficiency of the rack project. The efficiency is not a matter of economy only, but also significantly a matter of life safety thanks to intensive standards which have been issued by relevant community composed of engineers, manufacturers, academic and governmental authorities.

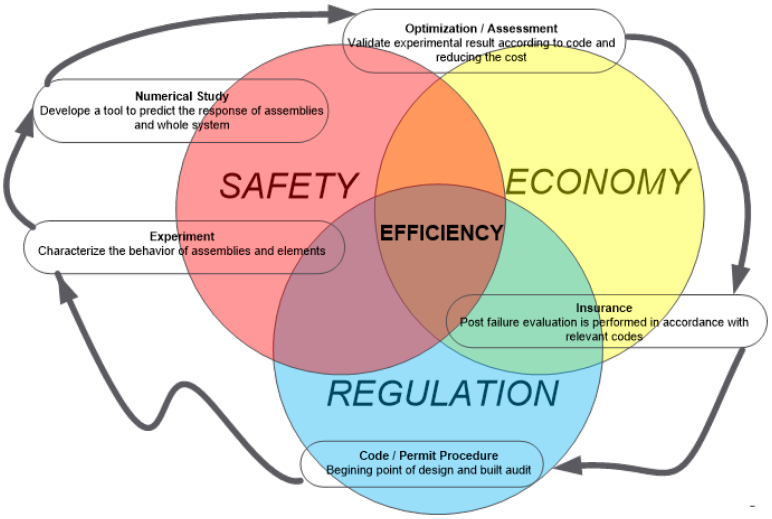

Figure 1.6. Validate the Efficiency by Proposed Framework for Rack Systems.

1.5. Identification of Storage Rack System

Cold-formed steel structures are steel structural products that are made by bending flat sheets of steel into shapes which support more than the flat sheets. In this study, the behavior of the connections of rack structures is investigated. For steel storage racks, lateral stiffness in down-aisle direction is usually provided by beam-to-column joints, since the rack structures are un-braced in that direction to allow for loading and unloading of pallets.

It was highlighted that steel storage rack systems are framed structures constructed from cold-formed steel sections and for connecting the pallet beams into uprights hook-in end connectors are generally used. These mechanically connected assemblies are primarily boltless; however a bolt is mounted in the assembly to retain the end connector in-place. There are different types of beam end connectors with different geometries. In hook-in connections the pallet beam is welded into the end connector to be readily attached into the upright.

Figure 1.7. Drive in Storage Rack System.

Main components of a typical racking system are listed below;

- Upright; perforated column section
- Pallet Beam; a horizontal member linking adjacent frames and lying in the hori-

zontal direction parallel to the main aisle.

- Beam End-Connector; Mostly L-shape connector, welded to or otherwise formed as an integral part of the beams, which has hooks engaged in the holes or slots in the upright.
- Spine bracing; Sway bracing in the vertical plane parallel to the main aisle of the rack linking adjacent frames.
- Frame Spacer; short link element in between two single entry rack.
- Top Tie; long link element at the top to connect two single entry racks together.

The configuration of a typical unbraced pallet rack is shown in Figure 1.8 in which the down-aisle stability is provided solely by the restraining effect of the beam end connectors. In the cross-aisle direction, stability is provided by bracing in the frames. Restraint against lateral loading is provided in the down-aisle direction by portal frame action of the pallet beam.

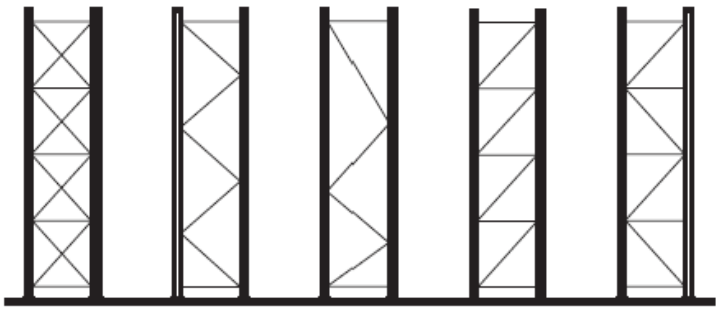

Figure 1.8. Typical Forms of Upright Frames.

Pairs of upright are generally placed along the length of 1.5 m - 2.0 m spacing for supermarkets and 2.0 m - 4.0 m for standard warehouses. The uprights which usually are connected by hollow section diagonal bolted or welded to the uprights. The spacing between the columns along cross-aisle is approximately 0.5 m - 1.2 m. Since the beams thanks to the taps on the end-connector can be easily fitted into the slots in the upright, and uprights are usually pre-punched at factory to take the pallet beams at various levels, it is a simple process of installing and modifying the configuration. Usually, above the pallet beams, shelves or wooden pallets are placed to support the contents. The average weight of each pallet is varied from 500 kg up to 3000 kg consistent with

the needs of the storing in the warehouse.

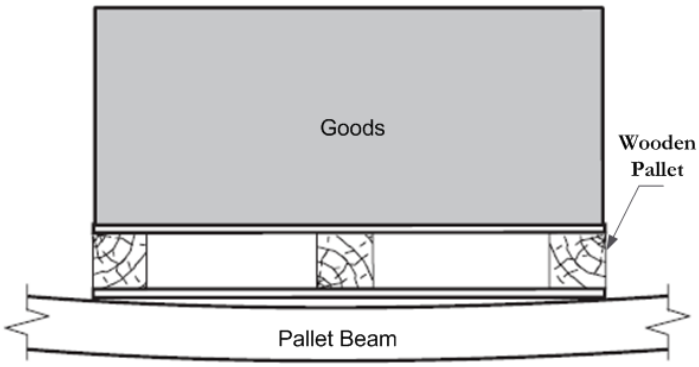

Figure 1.9. Typical Wooden Pallet Used in Storage Racks.

1.6. Codes and Standards for Storage Racks

In preceding sections it was highlighted that the rack systems are not classified as building structures, so, apparently there are a few differences in the common approach and the design philosophy is recognized. Accordingly, design committees have distinguished the design of rack systems from building systems rather than plugging it into the appendix parts of the existing regulations. Even, the relevant associations to deal with the standards, is separated from national and international building code institutes. Otherwise rack buildings or the clad warehouses where racking systems support goods besides roof and cladding of the structure, all other racking systems are not classified as building. All over the world, practically there are a few standards for the design of racking systems, content of some of them is substantially design guide rather than being design code. For this reason it is necessary to explain how to consider the peculiarities of such kind of construction work when they are to be designed for seismic actions, because these peculiarities influence significantly the response to earthquakes and don't allow a designer to follow exactly the same approach for ordinary steel structures, which is stated in the various Building Regulations.

There are regulations and guidelines available dealing with the seismic aspect of racking systems which are listed below;

- FEM 10.2.08, The Seismic Design of Static Steel Pallet Racks.
- RMI, Rack Manufacturer Institute 2008, Specification for the Design, Testing and Utilization of Industrial Steel Storage Racks.
- AISI S-100, Specification for the Design of Cold-Formed Steel Structural Members.
- AISI S110-07/S1-09 (2012) : AISI STANDARD Standard for Seismic Design of Cold-Formed Steel Structural Systems - Special Bolted Moment Frames with Supplement No. 1.
- FEMA 460, Seismic Considerations for Steel Storage Racks Located in Areas Accessible to the Public.

In Europe, "the Federation Europeenne de la Manutention" (FEM) performed standard development research activities for the European Union (EU). One result is the 2005 FEM seismic design standard, FEM 10.2.08, The Seismic Design of Static Steel Pallet Racks. Current FEM work includes analytical research, static and dynamic element testing as well as shake-table testing. Stub-column tests and beam-to column connection tests for moment-rotation characteristics and properties have been conducted, using test facilities at the University of Trento and Politecnico di Milano in Italy. At the National Technical University in Athens, full-scale steel pallet racks have been tested at ground accelerations up to failure. This research indicates that movement of merchandise within packaged unit loads, movement of unit loads or packages on a pallet and movement of pallets on pallet beams within the rack occur even at relatively low ground accelerations. Specific sliding tests have been developed to improve the understanding of these phenomena and their influence on damping, period, and overall structural behavior (Castiglioni, 2005).

In the late 1960s, RMI engaged Professor George Winter of Cornell University to undertake analysis and testing needed to provide a sound basis for the development of a more rigorous standard for the industry. Professor Winter was chosen because of his national and international reputation and his demonstrated expertise in the structural behavior of cold-formed light-gage steel structures. The RMI membership and several other organizations provided financial and engineering support for the research effort

that included analysis and testing related to the expanding range of products made by the growing number of industry members. The results of the work conducted by Professor Winter and his graduate students provided the basis for a new RMI standard, Interim Specification for the Design, Testing, and Utilization of Industrial Steel Storage Racks, which was issued in 1972 and which required earthquake loads to be considered in a manner mimicking the approach to building structures as stated in the Uniform Building Code (UBC) promulgated by the International Conference of Building Officials (ICBO). In the UBC, design seismic forces for different types of building structures were based on K factors. The K factors for ordinary moment frame building structures braced framed structures were 1.0 and 1.33, respectively. These were the factors used to define the seismic forces in 1972 edition of the RMI standard in the down-aisle and cross-aisle directions, respectively (FEMA 460, 2005).

Since the early 1970s, in the U.S., RMI has sponsored many analytical and experimental storage rack research projects conducted at Cornell University. These studies have included full-scale, component, and element tests focusing on, hot-rolled and cold-formed structural elements, beams, columns, perforations, beam-to-column connectors and connections, base plates, flexural and torsional-flexural buckling, and testing and loading protocols. During the late 1970s and early 1980s, major research projects were undertaken, including subassembly tests at Stanford University and full-scale shake-table testing at the University of California/Berkeley using El Centro 1940 records, by URS/Blume (John A Blume and Associates, 1973; and Chen, Scholl, and Blume, 1980a, 1980b, and 1981), with funding from the RMI membership and a large grant from the National Science Foundation (NSF). The results of that testing, along with analytical studies, provided important baseline information about storage rack seismic performance, helped identify topics for further research, and articulated issues needing further study.

Storage racks are typically made of cold-formed steel members; therefore, their design depends on the thorough understanding and application of the American Iron and Steel Institute's (AISI) Specification for the Design of Cold-Formed Steel Structural Members. Other storage rack members are made with hot-rolled steel structural

sections using the applicable seismic provisions of the American Institute of Steel Construction's (AISC) Specification for Structural Steel Buildings, Allowable Stress Design, and Load and Resistance Factor Design Specification for Structural Steel Buildings. AISI is currently developing a standard for the seismic design of structures using cold-formed steel members that may provide detailing requirements for the design of storage racks subjected to seismic loads.

1.6.1. Considering Seismic Response Coefficient in Codes

There are different definitions of seismic loads for racks available in different codes. A description of RMI procedure for determining seismic loads is presented below. Also provided for the purposes of comparison the following figures of the seismic fore coefficients in the down-aisle direction have been adjusted for each of the applicable codes and standards.

1.6.2. Calculation of Seismic Response Coefficient in RMI

Knowing the fundamental period of the rack structure, the seismic response coefficient is calculated from;

$$C_s = \frac{S_{D1}}{TR} \begin{cases} not\,be\,greater\,than\ \frac{S_{DS}}{R} \\ not\,be\,less\,than\ 0.044 S_{DS} \end{cases} \tag{1.1}$$

where S_{D1} is the Design earthquake spectral response acceleration at short periods, S_{DS} is the Design earthquake spectral response acceleration at a 1 second period, R is the Response modification factor R = 4.0 in the braced direction and R = 6.0 in the unbraced direction. Higher values may be used if substantiated by tests, T is the Fundamental period of the rack structure in each direction under consideration established using the structural properties and deformation characteristics of the resisting elements in a properly substantiated analysis. For the unbraced direction (moment

frame), the period shall be determined using a connection stiffness.

$$S_{DS} = {}^{2}\!/_{3}\, S_{MS} \Leftrightarrow S_{MS} = F_a S_S \tag{1.2}$$

$$S_{D1} = {}^{2}\!/_{3}\, S_{M1} \Leftrightarrow S_{M1} = F_v S_1 \tag{1.3}$$

where S_{MS} is the maximum considered earthquake spectral response accelerations for short period, S_{M1} is the maximum considered earthquake spectral response accelerations for 1 sec period, F_a is the site coefficient defined in Table 1.1, F_v is the site coefficient defined in Table 1.2, S_s is the mapped spectral accelerations for short periods, S_1 is the mapped spectral accelerations for 1-second period.

Table 1.1. F_s Values (RMI 2008) Values of Site Coefficient F_a as a Function of Site Class and Mapped Spectral Response Acceleration at Short Periods $(S_s)^a$.

SITE	MAPPED SPECTRAL RESPONSE ACCELERATION AT SHORT PERIODS				
CLASS	$S_s \leq 0.25$	$S_s = 0.50$	$S_s = 0.75$	$S_s = 1.00$	$S_s \geq 1.25$
A	0.8	0.8	0.8	0.8	0.8
B	1.0	1.0	1.0	1.0	1.0
C	1.2	1.2	1.1	1.0	1.0
D	1.6	1.4	1.2	1.1	1.0
E	2.5	1.7	1.2	0.9	0.9
F	Note b	Note b	Note b	Note b	Note b

Table 1.2. F_v Values (RMI 2008) Values of Site Coefficient F_a as a Function of Site Class and Mapped Spectral Response Acceleration at Short Periods $(S_1)^a$.

SITE	MAPPED SPECTRAL RESPONSE ACCELERATION AT SHORT PERIODS				
CLASS	$S_s \leq 0.25$	$S_s = 0.50$	$S_s = 0.75$	$S_s = 1.00$	$S_s \geq 1.25$
A	0.8	0.8	0.8	0.8	0.8
B	1.0	1.0	1.0	1.0	1.0
C	1.7	1.6	1.5	1.4	1.3
D	2.4	2.0	1.8	1.6	1.5
E	3.5	3.2	2.8	2.4	2.4
F	Note b	Note b	Note b	Note b	Note b

The seismic design forces shall not be less than;

$$V = C_s I_p W_s \tag{1.4}$$

$$I_p = \begin{cases} 1.5 \rightarrow \ for\, essential\, facilities \\ 1.5 \ \rightarrow significantly\, hazardous\, material\, stored \\ 1 \rightarrow all\, other\, structures \end{cases} \tag{1.5}$$

$$W_s = (0.67 \times PL_{RF} \times PL) + DL + 0.25 \times LL \tag{1.6}$$

Table 1.3. Seismic Force Direction.

Seismic Force Diretion	PLRF
Cross-Aisle	1.0
Down-Aisle	$PL_{Avarage}/PL_{Maximum}$

where $PL_{Avarage} = PL_{Maximum}$ is the for warehouse retail stores, open to the general public, for all other types of warehousing it is the maximum total weight of product expected on all the beam levels in any row divided by the number of beam levels in that row.

Table 1.4. Site Class Definitions (RMI 2008).

		AVERAGE PROPERTIESC1:G1 IN TOP 100 feet. AS PER SECTION 1615.1.5		
SITE CLASS	SOIL PROFILE NAME	Soil shear wave velocity, $\bar{v}_s$(ft/s)	Standard penetration resistance. $\bar{N}$	Soil undrained shear strength, $\bar{s}_u$, (psf)
A	Hard rock	$\bar{v}_s > 5.000$	N/A	N/A
B	Rock	$2.500 < \bar{v}_s \leq 5.000$	N/A	N/A
C	Very dense soil and soft rock	$1.200 < \bar{v}_s \leq 2.500$	$\bar{N} > 50$	$\bar{s}_u$2.000
D	Stiff soil profile	$600 \leq \bar{v}_s \leq 1.200$	$15 \leq \bar{N} \leq 50$	$1.000 \leq \bar{s}_u \leq 2.000$
E	Soft soil profile	$\bar{v}_s$ ¡ 600	$\bar{N} < 15$	$\bar{s}_u < 1.000$
F		Any profile with more than 10 feet of soil having the following characterics: 1. Plasticity index Pl > 20. 2. Moisture content w ≥ 40%. And 3. Undrained shear strength $\bar{s}_u$ < 500 psf		
G		Any profile containing soils having one or more of the following characterics 1. Soils vulnerable to potential failure or collapse under seismic loading such as liquefiable soils. Quick and highly sensitive clays. Collapsible weakly cemented soils. 2. Peats and/or highly organic clays (H > 10 feet of peat and/or highly organic clay where H = thickness of soil) 3. Very high plasticity clays (H > 25 feet with palsticity index PI > 75) 4. Very thick soft/medium stiff clays (H > 120 feet)		

The 1991 edition of the NEHRP Recommended Provisions introduced design values for storage racks in the chapter on architectural, mechanical, and electrical components. The design seismic forces were independent of period and the lateral force coefficient, based on allowable stress design (ASD), was 0.40 for areas of highest seismicity. In the 1994 Provisions, design values for storage racks were significantly revised to be more consistent with the RMI seismic design criteria. R values of 6 and 4 were assigned for storage racks in the down-aisle direction and the cross-aisle direction, respectively. Further, an importance factor of 1.5 was assigned for racks in areas accessible to the public. The R factor values of 6 and 4 were basically a translation of the UBC Kvalues from the early 1970s. Note that the first several editions of the NEHRP Recommended Provisions focused almost entirely on building structures; however, by the mid-1990s formal recognition was given to the fact that storage rack structures (and some other structures) are neither building structures nor architectural, mechanical, or electrical elements or components. Starting in the 1997 NEHRP Recommended Provisions, non-building structures including storage racks as well as cooling and stor-

age towers, which had been treated in the chapter on architectural, mechanical, and electrical components were now covered in a separate non-building structures chapter.

The design procedures given in Pr FEM 10.2.08 apply to all types of static pallet racks fabricated from steel members for the seismic load case that are supported by floors lying on the ground. They do not apply to mobile storage systems. The approach to the seismic design is based upon the philosophy of prEN 1998-1 (Eurocode 8). The reference to the design, tests and quality control of components and materials is expressly based on FEM 10.2.02. In case of clad racks, where the racking system is supporting roof and walls, this Code gives relevant information in addition to the National Building Regulation. In moment resisting frames the dissipative zones are located in the beams or in the beam-to-column connections, and in the bottom of the columns. A behavior factor q=2 in general can be assumed for regular unbraced racks in down-aisle direction. For the racks with tension-only bracing, the behavior factor q=1.5 is applicable for ductility class Low with no specific overstrength requirements for connections and the behavior factor q=4 is applicable for ductility class High and Medium. For normal bracing racks, in which the braces work for tension and also compression, the behavior factor is 2.5 and 2 respectively for high and medium ductility classes.

No design procedure is given in Turkish seismic code where the storage racks are classified as non-building structures. The seismic modification factor is specified as R=4 for industrial storage racks. The importance factor is identified as “other structures” of building type structures. The subjects not covered in Turkish seismic code are;

- No special design consideration for the structures without diaphragm.
- No consideration for down-aisle and cross-aisle lateral behavior.
- Semi-rigid connections of rack systems are not taken into account.
- Dynamic effects/slip failure of pallets is not included.
- Irregular configuration and loadings of rack systems are not included.
- Damages and local buckling failures under gravity are not considered.

The guidelines are entirely inadequate for seismic design of racks in Turkish codes. In proceeding section a comparison of seismic loads defined in different regulations and guidelines is shown.

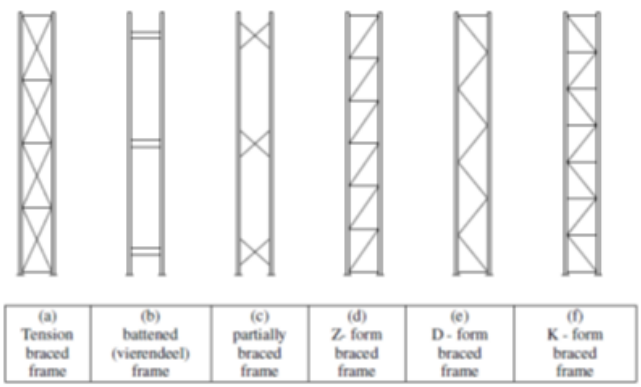

(a) Tension braced frame	(b) battened (vierendeel) frame	(c) partially braced frame	(d) Z- form braced frame	(e) D - form braced frame	(f) K - form braced frame

Frame type	Structural type	Detailing rules for dissipative elements	MAXIMUM q factor	
			Regular Rack	not regular rack
a	diagonal bracing with tension diagonals	tension diagonal 5.2 diagonal connections 5.1.1	4	3.2
	diagonal bracing with tension and compression diagonals		2.5 (class DCH)	2.0
			2.0 (class DCM)	1.6
b	dissipative battened frame can be used, provided that the requirements of moment resisting frames met; otherwise q = 1.5 must be assumed			
c			1.0	1.0
d-e-f	low dissipative		1.5	1.5

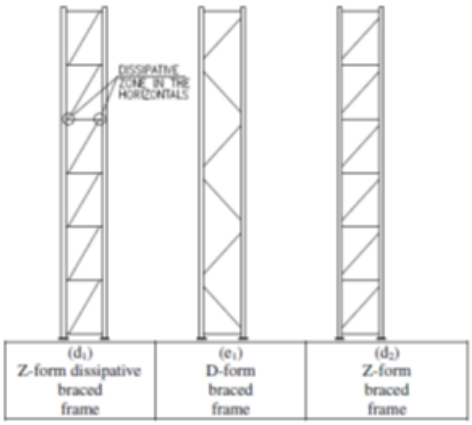

(d_1) Z-form dissipative braced frame	(e_1) D-form braced frame	(d_2) Z-form braced frame

Frame type	Structural type	Detailing rules for dissipative elements	MAXIMUM q factor	
			regular rack	not regular rack
	eccentric braced			

Figure 1.10. Bracing Configuration and Specified q Factor (EC3).

1.7. Comparative Analysis of Different Response Spectra's

A comparative analysis between the elastic response spectra defined by different national and international seismic codes is presented herein. The following standards are analyzed:

- Eurocode 8
- Turkish Seismic Code 2007,
- RMI 2008
- ASCE 7-2005

Seismic codes of different regions in the world have their own approach of performing design spectra's and these methods are updating based on the improvements of data collecting in ground motion and developing technologies. The conduction of all of them is almost the same in elastic spectra however when the elastic spectra is switching into design spectra different codes represents major huge distinctions. The same aspect is valid in forming design spectra of storage racking systems. The effects of ground types on the seismic response of the structures is so important, so considering different soil classifications in different codes, two types of poor and competent soil have been taken into account for comparing.

The site conditions have been classified into different categories in earthquake codes. These categories are named ground types, soil profile types, local site classes or subsoil classes. The Table 1.5 presents ground types and shear wave velocities given in the codes including TEC, UBC, IBC, EC8 and FEMA 368. As seen from this table, TEC gives more information about ground types depending on the topmost layer thickness of soil (h1). Four and six ground types are defined in TEC and US codes, respectively. It should be noted that in the 1998 edition of EC8 only three types of A, B and C were defined. However, five main ground types as to be A, B, C, D, E and two special ground types S1 and S2 have been described in the final version of EC8 (Dogangun, 2006).

Table 1.5. Comparison of Soil Classification in Different Specifications (Dogangun, 2006).

TEC			UBC,IBC and FEMA 368		EC8	
Ground types		Description	Ground types	Description	Ground types	Description
Z1	-	Massive volcanic rocks, unveathered sound metamorphic rocks, stiff cemeted sedimantary rocks V_s > 1000 m/s; Very dense sand, gravel V_s >700 m/s; Hard clay, sity clay V_s > 700 m/s	S^*_A S_B	Hard rock V_s >1500m/s		
	h_i^+ 15m	Soft volcanic rocks such tuff and agglomerate, weathered cemented sedimentary rocks with planes of discontinuity $V_s \approx$ 700-1000; Dense sand gravel $V_s \approx$ 400-700; Very stiff clay, silty clay $V_s \approx$ 300-700		Rock $V_s \approx$ 760 1500	A	Rock or rock-like geological formation including most 5m weaker material at the surfuce V_s >800 m/s
Z2	h_1 > 15m	Soft volcanic rocks such tuff and agglomerate, weathered cemented sedimentary rocks with planes of discontinuity $V_s \approx$ 700-1000; Dense sand gravel $V_s \approx$ 400-700; Very stiff clay, silty clay $V_s \approx$ 300-700	S_C	Very dense soil or rock $V_s \approx$ 360-760	B	Deposit of very dense sand or very stiff clay, at least serval tens of m in thicknesses, characterized by a gradual increase of mechanical properties with depth V_s 30 $\approx$ 360-800
	$h_1 \leq$ 15m	Highly weathered soft metamorphic rocks and cemented sedimentary rocks with planes of discontinuity $V_s \approx$ 400-700; Medium dense sand and gravel $V_s \approx$ 200-400; Stiff clay, silty clay $V_s \approx$ 200-300				
Z3	15m < $h_1 \leq$ 50m	Highly weathered soft metamorphic rocks and cemented sedimentary rocks with planes of discontinuity $V_s \approx$ 400-700; Medium dense sand and gravel $V_s \approx$ 200-400; Stiff clay, silty clay $V_s \approx$ 200-300	S_D	Stiff soil $V_{s,30}$ $Vs, 30 \approx$ 180-360	C	Deep deposits of dense or medium-dense sand, gravel or stiff clay with thickness from serval tens to many hundreds of m $V_s \approx$ 180-360
	h1$\leq$ 10m	Soft deep alluvial layers with high water table V_s < 200; Loose and V_s 200; Soft clay, silty clay V_s <200				
Z4	h_1 > 50m	Highly weathered soft metamorphic rocks and cemented sedimentary rocks with planes of discontinuity $V_s \approx$ 400-700; Medium dense sand and gravel $V_s \approx$ 200-400; Stiff clay, silty clay $V_s \approx$ 200-300	S_E	Soft soil V_s < 180	D	Depsits of loose-to-medium cohesionless soil (with or without some soft cohesive layers), or predominantly soft-to-firm cohesive soil. $V_{s,30}$ < 180
	h_1 > 10m	Soft, deep alluvial layers with high water table V_s <200; Loose sand V_s < 200; Soft clay, silty clay V_s < 200 In all seismic zones, soft, deep alluvial layers with high wated table V_s <200, loose sand V_s <200 and soft clay, silty clay V_s < 200 with water table less than clay V_s < 200 with water table less than 10m from the soil surface shall be investigated	SF	Soil requiring site specific evaluation it is more detailed defined in the IBC	E	A soil profile consisting of a surface alluvium layer with V_s,30 values of class C or D and thick-ness varying between about 5 and 20m, underalin by stiffer material with $V_{s,30}$ > 800 m/s
		and the results shall be documented to identify whether the liquefaction potential exists, by using appropriate analysitcal methods based on in-situ and laboratory tests.			S_1 S_2	Deposits consisting or containing a layer at least 10m thick of soft clays sits with high plasticity index (PI>40) and height water content, $V_{s,30}$< 100 m/s Deposits of liquefiable soils, of sentive clays, or any other soil profile not inclded in types A-E or S_1

where S_A, S_B, S_D, S_E and S_F given in the UBC are symbolized with A, B, C, D, E and F, respectively, in the IBC and FEMA 368 $^{+}h_1$ is the topmost layer thickness for subsoil.

The "Eurocode 8" (EC8) building code recommends the use of two design horizontal acceleration spectra, i.e. the Type 2 spectrum for regions where maximum magnitudes are not expected to exceed 5.5-6.0 (low to moderate seismicity) and the Type 1 spectrum for regions where maximum magnitudes are expected to exceed 5.5-6.0 (high seismicity).

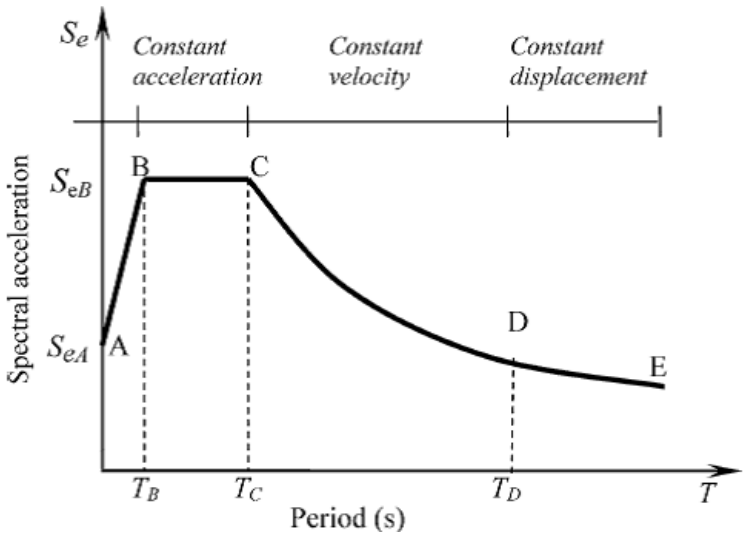

Figure 1.11. Typical form of Elastic Spectra (Dogangun 2006).

Atypical shape of horizontal elastic design spectrum can be drawn as seen in Figure 1.11 In this figure, T shows periods of structure, S_{eA} and S_{eB} show the ordinate values at points A and B of the elastic design spectra, T_B and T_C show the lower and the upper limits of the period of the constant spectral acceleration branch, and T_D shows the value defining the beginning of the constant displacement response range of the spectrum. There are some differences in spectral shapes recommended by the earthquake codes. The elastic spectra defined for equivalent competent soil classification in different codes including Turkish seismic code, "EC8" Type 2 and Type 1, "ASCE 7-05" and RMI are shown in the Figure 1.12. The peak spectra's at constant acceleration are aligned, however the interval of maximum accelerations are not the

same. The longest peak acceleration period occurs at "EC8" Type 1 and the shortest one at "EC8" Type 2. "ASCE 7-05" and RMI elastic spectra's are completely overlapped. It can be seen that TDY2007 elastic spectra and "ASCE7-05" are close to each other.

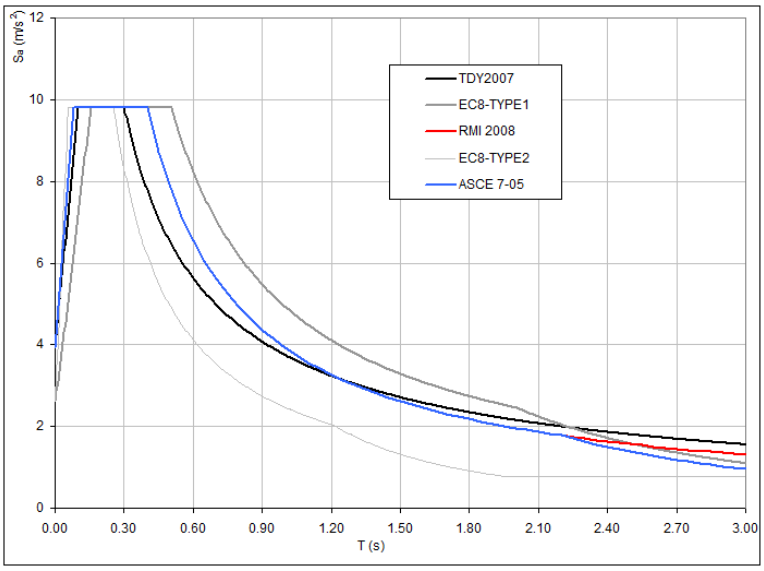

Figure 1.12. Elastic Spectra - Competent Soil (Hanoglu *et al.*, 2010).

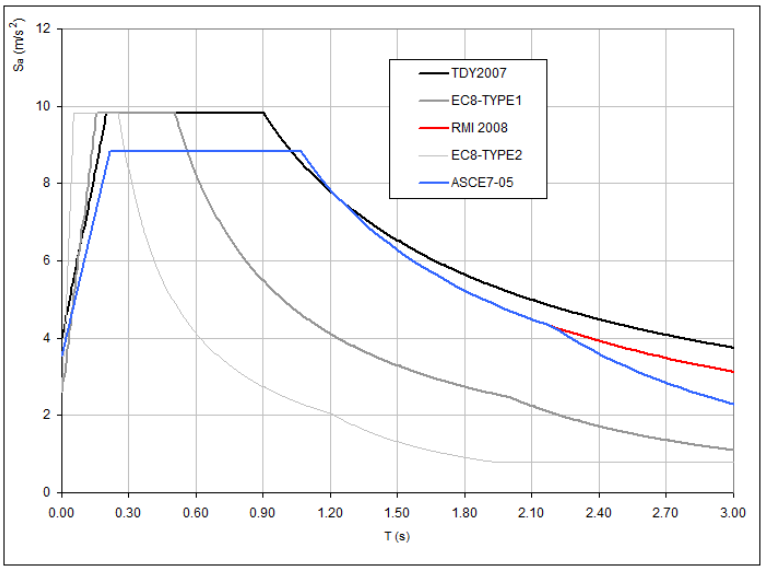

Figure 1.13. Elastic Spectra - Poor Soil (Hanoglu *et al.*, 2010).

The elastic spectra of ASCE 7-05 and RMI are superposed presented in Figure 1.13. The same scenario in competent soil is valid for poor soil too, TDY2007 spectra

is close into RMI except for maximum constant acceleration value. Type 2 EC8 owns the shortest constant acceleration period same as competent soil spectra. The interval of peak acceleration in Type 1 in contrast to competent soil is not the longest in poor soil.

Due to compatibility of ASCE 7-05 and RMI 2008, the spectra of RMI are going to be presented thereafter. In RMI response modification factor of racks is dependent on the direction; R values of 6 and 4 were assigned for storage racks in the down-aisle direction and the cross-aisle direction, respectively. Further, an importance factor of 1.5 was assigned for racks in areas accessible to the public. The R factor values of 6 and 4 were basically a translation of the UBC K values. Since RMI represents modification factors based on the direction of the racks, the following spectra's show design spectra along cross aisle and down aisle for poor and competent soils.

In EC8 for moment resisting frames the dissipative zones are located in the beams or in the beam-to-column connections, and in the bottom of the columns. A behaviour factor q=2 in general can be assumed for regular unbraced racks in down-aisle direction. However, based on the classification in the following comparison for poor and competent soil, and considering tension only bracing of the diagonals, the behavior factor q=1.5 is applicable for ductility class Low with no specific overstrength requirements for connections and the behavior factor q=4 is applicable for ductility class High and Medium, responsible for Type 2 and Type 1 of EC8.

In DBYYHY 2007 - Turkish seismic code, seismic coefficient factor is independent of direction. R=4 is the only coefficient considered for racks without any further requirement. In Figure 1.14, Figure 1.15, Figure 1.6 and Figure 1.17 design spectra of Type 1 Type 2 in EC8 and TDY07 and RMI are exhibited. Also minimum lateral force defined in RMI and EC8 are show with the red line for RMI and the black line for EC8. The most conservative coefficient is presented in Type 1 EC8 for both soil classifications along both directions. Along down aisle of the rack, RMI presents the highest seismic modification factor compared to other regulations. Along cross aisle direction and competent soil all standards approaches are almost same except Type 1

EC8.

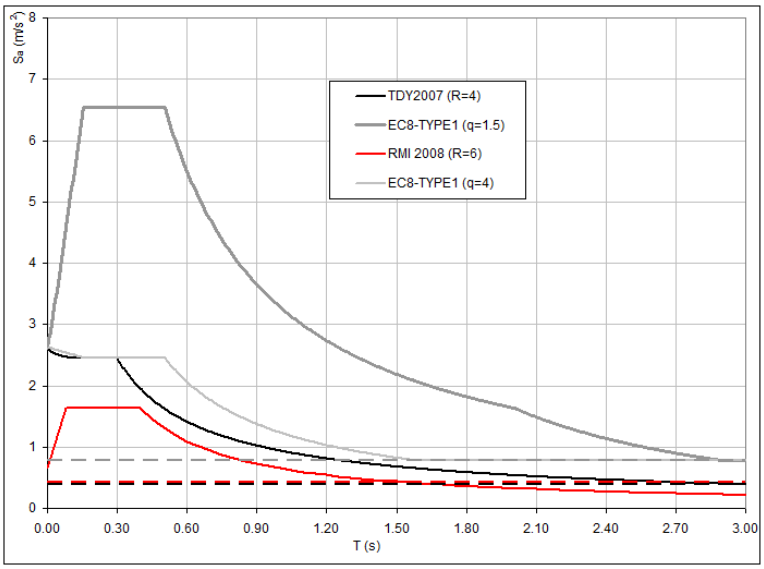

Figure 1.14. Comparing Design Spectra - Competent Soil - Down aisle (Hanoglu *et al.*, 2010).

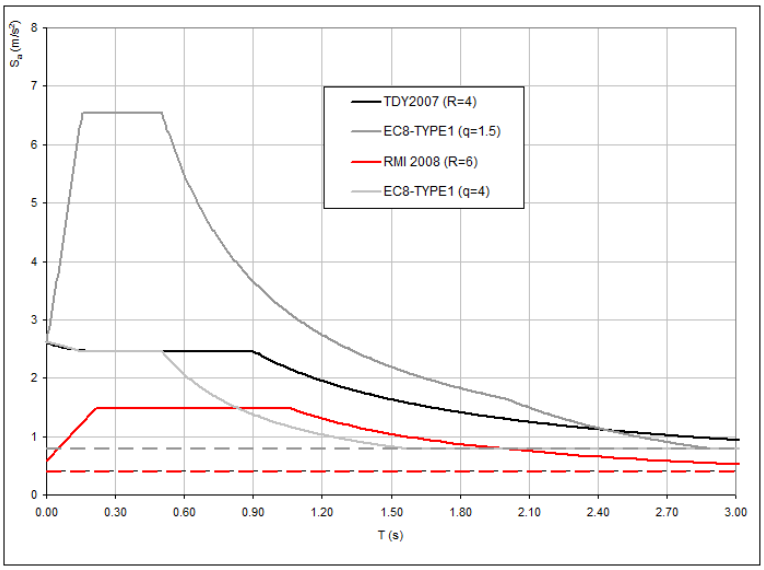

Figure 1.15. Comparing Design Spectra - Poor Soil - Down aisle (Hanoglu *et al.*, 2010).

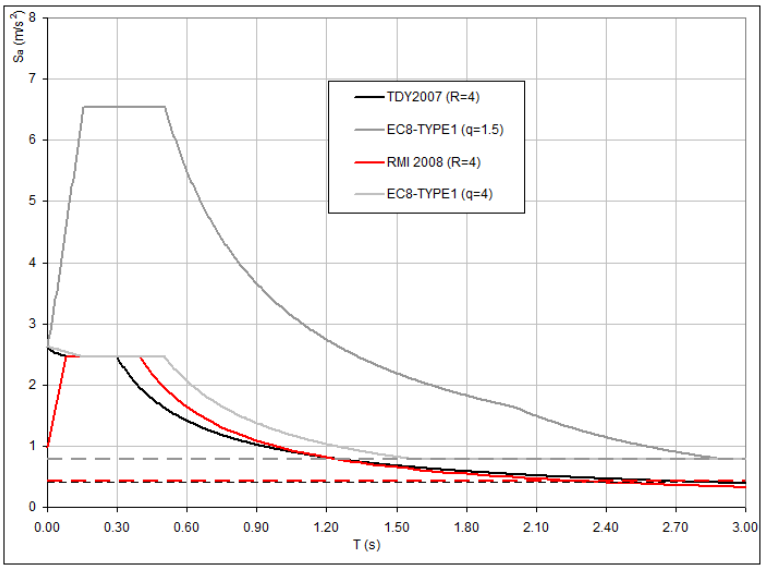

Figure 1.16. Comparing Design Spectra - Competent Soil - Cross aisle (Hanoglu *et al.*, 2010).

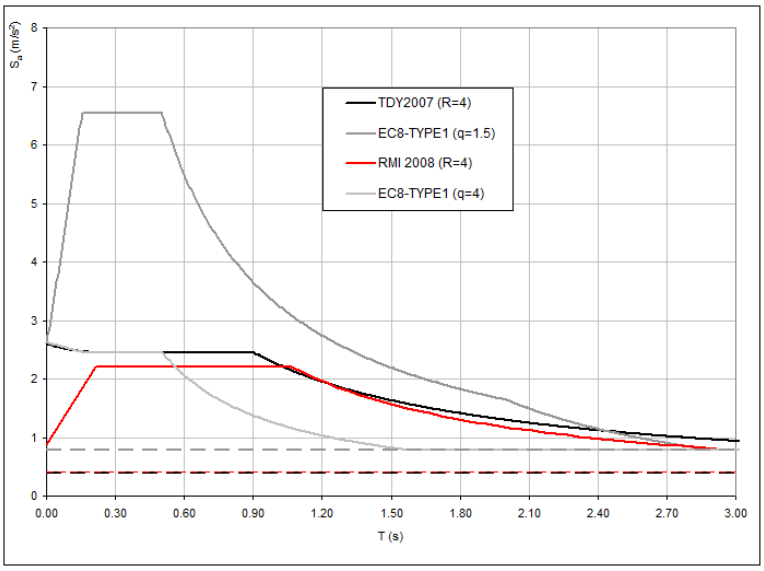

Figure 1.17. Comparing Design Spectra - Poor Soil - Cross aisle (Hanoglu *et al.*, 2010).

1.8. Global Analysis of Rack Systems

The design of the rack system is verified in two stages. The first is to determine the distribution of internal forces and displacements and the second is to check the individual elements of the structural system according to the strength of each element.

The actions or external loads might be as follow;

- Dead loads: weights of stored materials, the self weight of elements
- Live loads: loads from other equipment connected to the structure
- Wind loads
- Earthquake loads
- Vertical placement loads: loading method of the goods as manually or mechanically
- Horizontal placement loads: loading method of the goods as manually or mechanically
- Floor and Walkways loads
- Temperature loads
- Actions arised from imperfections

Pallet rack systems are usually fabricated from cold-formed sections and therefore, elastic methods are usually the most appropriate. However, nonlinear connection behavior may be incorporated in the analysis provided that the nonlinear characteristic used is based on test results which demonstrate adequate rotation capacity. The analysis of a rack system may be undertaken by considering first the down-aisle direction and then the cross-aisle direction. In order to design the uprights, the forces arising from these two analyses should be combined using the interaction formulas below;

1.8.1. Analysis of Braced and Unbraced Racks in the Down-Aisle Direction

The stability in the down-aisle direction shall be demonstrated by a rational analysis which takes account of the following factors;

- The destabilizing effect of axial compressive loads in the uprights (Second-order effects)
- The moment-rotation characteristics of the beam to upright connections
- The moment-rotation characteristics of the upright to floor connections
- The shear stiffness of the bracing system and its connection

- The moment-rotation characteristics of splices in the uprights
- Actions arising from down-aisle imperfections

The above items need to be determined by tests rather than mathematical models.

1.8.2. Pallet Beam-to-upright Connection Test in RMI 2008

The tests specified in this section have two objectives. One is to determine the moment capacity of the connection, the other is the determination of the joint spring constant F described below for use with the rational analysis approach. In a rigid frame analysis the members connected in a joint are assumed to maintain the angle between themselves while the frame deflected under applied loading. The joints between the upright columns and the pallet beam do not in general behave as rigid. This is primarily due to the distortion of the walls of the columns at the joint and to a lesser extent due to the distortion taking place at the connectors themselves. This peculiarity influences the overall behavior very significantly. The connection details vary widely. Thus, it is impossible to establish general procedures for computing joint stiffness and strength. It is therefore necessary to determine these characteristics by simple test.

The change in angle between the column and the connecting beam θ (in radius) can be idealized as follows:

$$\theta = M/F \tag{1.7}$$

where M is the moment at the joint between connecting members and F is the spring constant relating the moment to the rotation.

The Cantilever test provides a simple means of determining the connection moment capacity and rigidity. However, it has the disadvantage that the ratio of shear force to moment at the joint is not well represented. For typical rack connections this ratio is probably higher than it is in the cantilever test as spelled out in the Specification. In general a higher ratio would probably lead to a more rigid connection.

However, bending moment and shear force would interact and lower the ultimate load of the connection. This effect should be studied by reducing the length of the cantilever to the distance between the end of the beam and the expected location of the inflection point. This test is suitable for determining F for computing stresses due to vertical loads.

The relationship between the moment and the angular change at a joint is not linear. The following equation appears to be reasonable for determining a constant value of F to be used in a linear analysis.

$$F = \frac{(R.F.)}{\frac{\delta_{0.85}}{P_{0.85}L^2{}_b} - \frac{L_c}{16EI_c} - \frac{L_b}{3EI_b}} \tag{1.8}$$

where $P_{0.85}$ is 0.85 times the ultimate load and $\delta_{0.85}$ is the deflection of the free end of the cantilever at load $P_{0.85}$, L_c, L_b, I_c, I_b are the same lengths and moments of inertias of the columns and the beam, respectively. (R.F.) is a reduction factor to provide safety considering scatter of test results. Since a lower F means a higher design moment for the beam, an (R.F.)=2/3 should be taken in the design of the beam. However, in determining bending moments for the columns a higher F leads to a more conservative value of the bending moment. It is therefore recommended to take (R.F.) = 1.0 for this case.

It is suggested that the spring constant F be calculated on the basis of the average results on two tests of identical specimens provided that the deviation from the average results of two tests does not exceed 10%: if the deviation from the average exceeds 10%, then a third specimen is to be tested. The average of the two higher values is to be regarded as the result in the design of the columns.

2. EXPERIMENTAL PROGRAM

2.1. Background

In the event of earthquakes, rack structures are subjected to ground motions similar to motions experienced by host building. For seismic design criteria, most of the standards deal with the rack structures as building structures, and a few results are available about the structural performance governing the seismic behavior of racks, such as lateral resistance and stiffness, as well as energy dissipation. Structural behavior of the racks is further complicated because of the existence of the perforations on the upright and also semi-rigid behavior of the beam-to-upright connections. End connectors with taps are used to make beam-to-upright connection in storage racks. This is a boltless interlocked connection and its semi-rigid behavior is primarily due to the distortion of the upright at joint regions, tearing of the taps and upright perforation, and distortion of the beam end connector. Thus, it is important to have knowledge about the means for predicting the behavior of racks against earthquakes. Specifying the performance level of the rack structures can be apparently divided into two phases, member behavior and connection behavior, each one of them need a closer look. Beam-to-upright connection tests are usually conducted to determine the relationship of the moment at the joint and the change in angle between the upright and the connecting beam.

In the market, each rack manufacturer uses self-designed and in-house beam-to-upright connector to connect the horizontal and vertical members in the down-aisle direction. The end-connector usually is welded to each end of a shelf beam and locks into the slots in the face side of the upright. Some end-connectors are bolted to the upright, some have rivets that lock into perforations in the upright, and some have taps formed from the end-connector that are inserted into slots in the upright. Because of the variety in connection types, the RMI standard requires the determination of the strength and stiffness of each connection by testing. Once the testing is completed for one product line, the results may be used for all projects using that type of connection.

This rotational spring is then introduced between the end of the beam and the column and the structural analysis is performed (FEMA 460, 2005).

2.2. Structural Testing

Experimentation has a variety of objectives and utilizes different testing techniques, ranging from material testing, and field tests to dynamic testing, from prototype two dimensional into full scale three dimensional testing. Each of the testing has distinct advantages and disadvantages compared to each other. Selecting the most accurate testing technique is important for obtaining correct results. At this point, following standard guideline is an appropriate way for correct results. ATC-24 1992 and ECCS 1986 are two resources in US and Europe for testing procedure and for carrying out and interpreting tests. Many experiments on steel components and assemblies directed toward achieving a better understanding of the response of such components into seismic excitations. Most commonly, due to the nature of earthquakes, the experiments have to be cyclic for simulating the seismic effects, and performed with slow reversed cyclic load application.

Figure 2.1. Structural Testing Laboratory.

The lateral stiffness of storage rack systems in the down-aisle (moment-resisting frame) direction is greatly influenced by the distortions that occur at the beam-to-upright connections. For analytical modeling purposes, these distortions often are represented by simple rotational spring elements inserted between the beam ends and the upright center line. The rotational spring constant to be used in a numerical model can be obtained from moment-rotation relationships between a beam and an upright using the cantilever test method (RMI 2002).

2.2.1. Test Components

There are three main components in forming the joint which are beam with different sections as well as upright and the part attach the beam into upright, end connector. The main parameters in the research are the structural behavior of the joint including the moment-rotation relation of the connection, yield and ultimate moment capacity, energy dissipation through inelastic action in the joint and different buckling modes of the components. Section profiles have been selected after a survey from manufacturers in Turkey. The most used sections were selected for testing in this study. Selected sections for upright, pallet beam and end-connector are shown Figure 2.3, to, Figure 2.6. The main components of the test specimens are subassemblies as shown in Figure 2.6 and Figure 2.7. The selected components are the parts of the joint along the down-aisle direction of storage racks. Tee-joints are representative of outer joints in the real frame work shown in Figure 2.2. The height of column is chosen as it represents the distance between two stories. In rack structures the story height can be different so in analytical model it was attempted to analysis a rack structure with different story heights, so the upright might not be symmetrical with respect to connected beam. Considering the moment diagram of the pallet beam under lateral force and the deformability of the beam under gravity loads, the length of the beam is decided to be 900 mm.

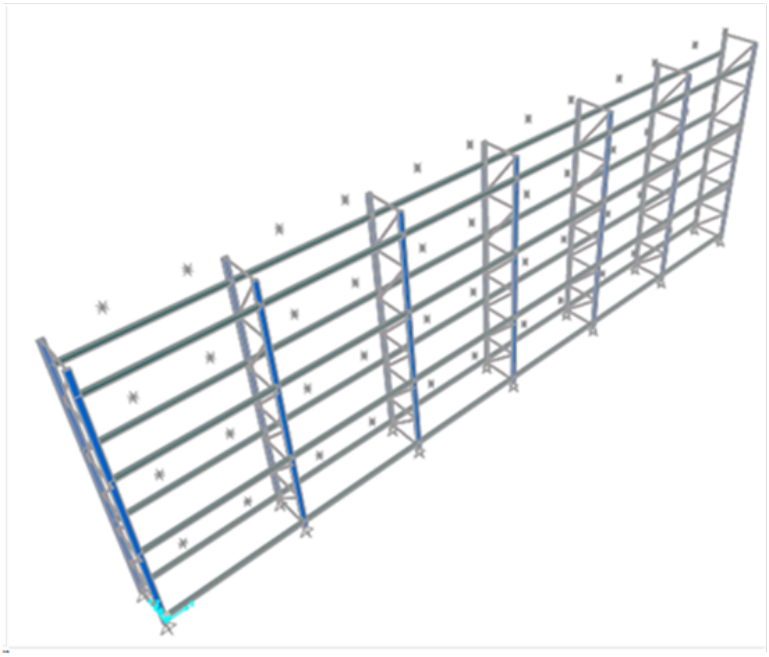

Figure 2.2. SAP2000 Model of Storage Rack.

In semi-rigid connections high rotation levels are expected, therefore the length of beam is chosen on the expected deformability of the connection. Bending in the beam is produced by displacement controlled point load applied at the end of the cantilever arm. Bending in the upright as a result of the loading on the beam will be produced by support reactions at the ends of the column. Since the objective of the study is to focus on the connection behavior, axial load simulating the gravity loads of the pallets is not applied on the upright. The beam is prevented to move in out-of-plane direction by lateral supports.

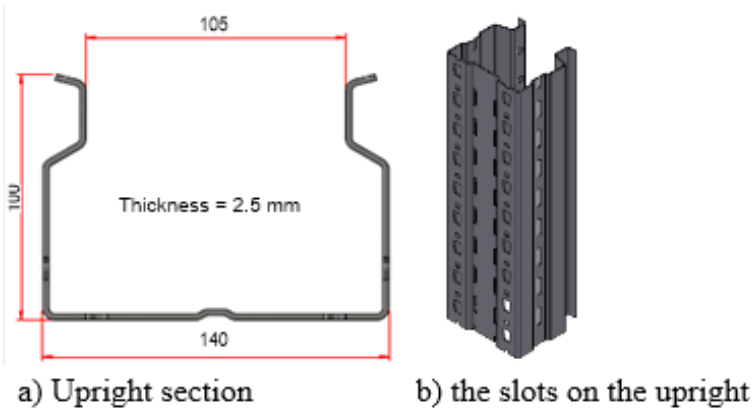

Figure 2.3. (a) Upright Section (b) The Slots on the Upright.

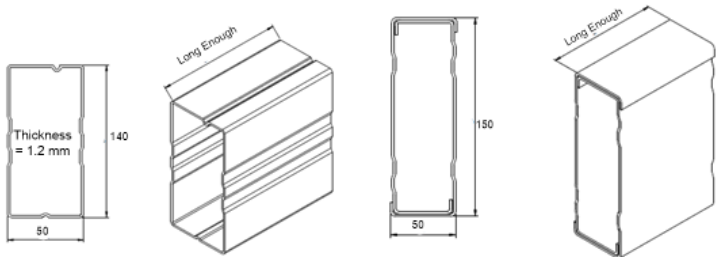

Figure 2.4. DD140 and DD150 Beam Cross Sections.

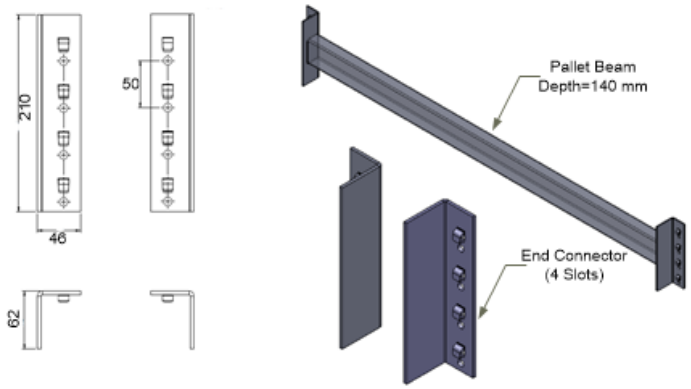

Figure 2.5. 4-Slots End-Connector.

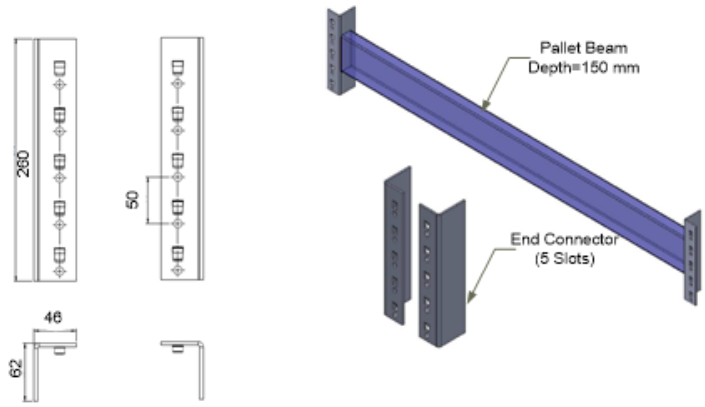

Figure 2.6. 5-Slots End-Connector.

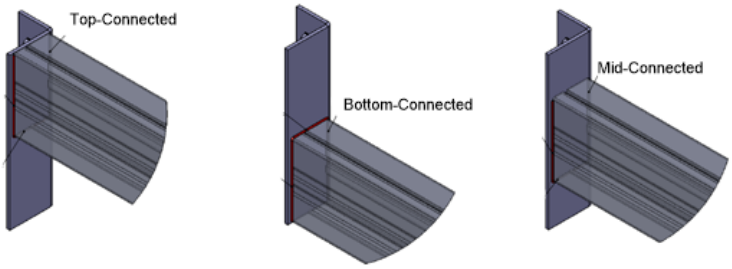

Figure 2.7. Unsymmetrical End Connector Connections to Pallet Beam.

It was highlighted that steel storage rack systems are framed structures constructed from cold-formed steel sections and for connecting the pallet beams into uprights hook-in end connectors are generally used. These mechanically connected assemblies are primarily boltless; however a bolt is mounted in the assembly to retain the end connector in-place. There are different types of beam end connectors with different geometries. In hook-in connections the pallet beam is welded into the end connector to be readily attached into the upright to form a joint. The specimen consists of an approximately 1050 mm long upright attached by end-connectors; each specimen is equipped with 5 inductive displacement transducers (LVDT).

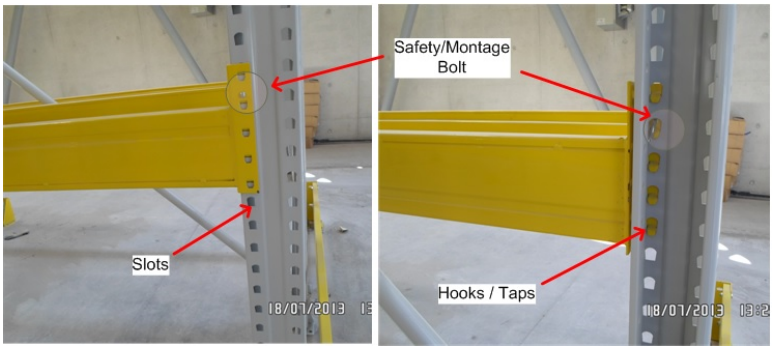

Figure 2.8. Main Components of End-Connector Joint.

Beside the scope of the study, the structural testing laboratory for evaluating the experiment was established in 2012. All equipment and measuring tools were installed and pilot tests were performed to calibrate the equipment. Much effort and work was made on the establishment of the structural laboratory and learning the operating of

the equipment for testing, meantime the testing approach for the connections of storage rack systems was studied.

2.2.2. Marking Definition and Abbreviations

The following definition was used to summarize test specimens in the structural laboratory;

- T end-connector is connected to beam from top,
- M end-connector is connected to beam from middle,
- B end-connector is connected to beam from bottom,
- P positive moment Clockwise,
- N negative moment - Counter clockwise.

2.2.3. Test Arrangement

The aim of cantilever test is to characterizing the behavior of beam-to-upright connection of rack structures, the stiffness and the bending strength of the beam end connector can be determined. Exactly the same section profiles used in industry were used in full scale tests. Special attention was paid to component and connection testing procedures presented in EN 15512 and ATC-24. The behavior of the upright and beam end-connector is important for the whole structure. The behavior is influenced by the following items;

- The type of the upright, thickness and the depth of the section
- The type of the beam, the position of the beam on the connector
- The weld connecting the beam into connector
- The bracket type, the number of holes and hooks
- The material properties

Section profiles have been selected after a survey from manufacturers and the most used sections were selected for testing in this study. The dimensions of the

specimens have been decided from the results of structural modeling of a real rack structure. Before launching main tests the following shall be determined;

(i) The Testing Procedure
(ii) The specimen geometry and the number of configurations to be studied
(iii) The measurements and the type of data to be collected
(iv) The number of cycles
(v) Deformation amplitudes
(vi) Sequences of cycles

1992 North-American ATC-24 "Applied Technology Council-24 Guidelines for Cyclic Seismic Testing of Components of Steel Structures" is used as testing procedure. The simulation of the connection behavior needs consideration of all important field conditions including initial and boundary conditions, field fabrications conditions, restraint conditions and loading conditions. The material properties must be apparent from the beginning through material testing. The most important prerequisite is analytical prediction of the anticipated response through precise structural modeling and careful planning of the loading and instrumentation program. The main parameters in cyclic testing which are performed to draw conclusions on the seismic performance of the connections are strength and stiffness characteristics and their history dependent variation like as cyclic hardening, softening , deterioration and failure modes. Different modes of buckling like as local and torsional and distortional modes, moment-rotation and load displacement of beam, end connector and upright serve the purpose of the study.

The test specimen is a set of components connected together to form the structural assembly. The specimen is composed of beam transverse, end-connector and upright to form an end-bay joint of rack system. The test specimen used in the study is generic test specimen according to ATC-24 classification of specimen types. Appropriate out-of-plane bracing and realistic end restraints have been provided to perform 2D joint. Gravity loads of the pallets have been ignored in 2D set-up; however an initial loading is applied which stands for the weight of pallets.

The main attempt in taking the samples is to fabricate the components of the specimen in a manner that simulates field and real conditions. The procedures of workmanship and quality control are audited in the QC department of the factory according to applicable standards. This applies particularly to welding and bolting. A prerequisite for testing is to predict the response of the test specimen as much as possible by analytical means. The yield and ultimate strengths and deformations of the test specimen are predicted analytically herein.

A HR 115x100x2.5 upright is connected to a relatively adequate stiff testing frame at two points with clear distance of h=1050mm, over this distance there is no contact between the upright and the stiff frame. A Beam section DD 140x50 is connected to upright by means of the end-connector L-formed 62x46x4.

Before applying cyclic tests on the beam-to-column joints, the component tests have to be done in order to determining the yield value of the joint. The first step of cyclic tests is done according to the yield value of the joint obtained from monotonic test. The behavior of components is strongly influenced by the unsymmetrical geometry of the profiles and the asymmetry caused by the inclined hooks, presence of the safety-bolt in the end-connector and slots in the profiles. The test set-up and measurement instrumentations used are shown in the set-up below;

2.2.4. Cantilever Test

This test is for determining the connection moment capacity. This test is also suitable for determining stiffness for computing stresses due to vertical loads.

All cantilever tests in this research were performed at structures laboratory in Research and Development department of ÜÇGE group in Bursa-Turkey. The tests are composed of two phases;

- Phase-I: Monotonic tests
- Phase-II: Cyclic tests. Cyclic testing procedure is dependent on monotonic test

results, since applied load at cyclic tests are estimated from proportion of yield value of the joint taken at monotonic tests.

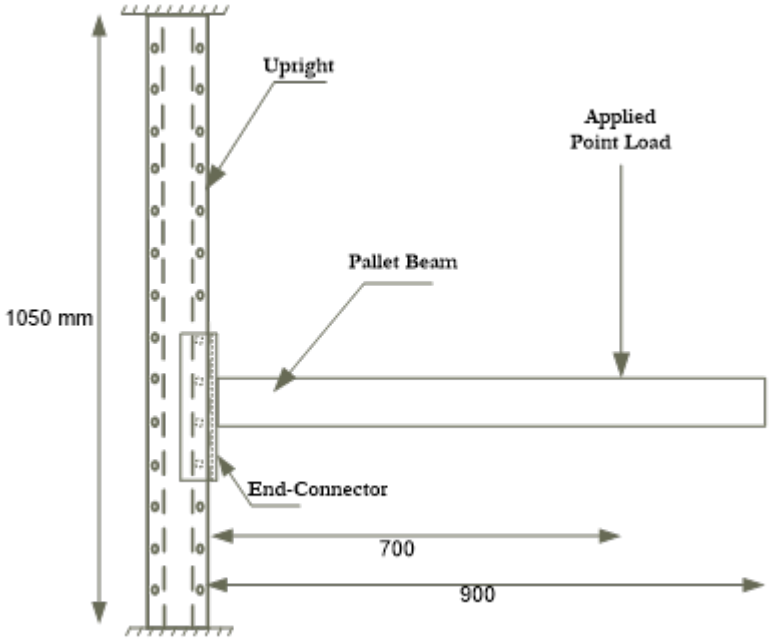

Figure 2.9. Cantilever Test Set-up.

Before applying cyclic tests on the beam-to-column joints, the component tests have to be done in order to determining the yield value of the joint. The first step of cyclic tests is done according to the yield value of the joint obtained from monotonic test. The behavior of components is strongly influenced by the unsymmetrical geometry of the profiles and the asymmetry caused by the inclined hooks, presence of the safety-bolt in the end-connector and slots in the profiles. The test set-up and measurement instrumentations used are shown in the set-up below;

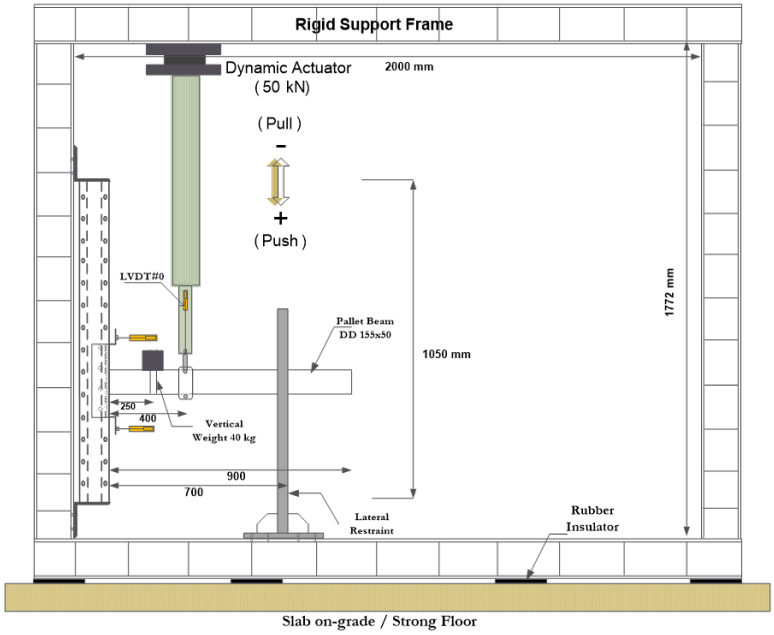

Figure 2.10. Test Setup.

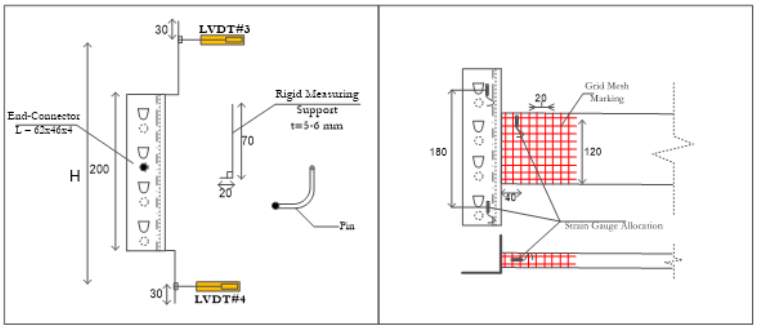

a) LVDT allocation b) Strain Gauge allocation

Figure 2.11. a) LVDT allocation, b) Strain Gauge allocation.

$$\varphi = \frac{F}{a} - (\frac{\delta_1 - \delta_2}{H}) \tag{2.1}$$

where F is the displacement applied by dynamic actuator, a is the lever arm for laod F, δ_1 is the deflection measured by LVDT $\neq 3$, δ_2 is the deflection measured by LVDT $\neq 4$, H is the destace between LVDTs.

The result from the cantilever test is normally used to design beams and con-

nections; the following is a review of cantilever test procedure in RMI 2008. In the cantilever test the constant connection stiffness S relating the moment to the rotation as;

$$S = \frac{M}{\theta} \tag{2.2}$$

Which is determined by using the known applied vertical load F and deflection of the free end of the cantilever as;

$$\delta = F{L_b}^2 \left(\frac{L_c}{16EI_c} + \frac{L_b}{3EI_b} + \frac{1}{S} \right) \tag{2.3}$$

Where E is the modulus of elasticity, L_b and L_c are the length of the beam and column segment, I_b and I_c are the moment of inertia of the beam and column segment, respectively. Solving the above equation for S;

$$S = \frac{1}{\left(\frac{\delta}{P{L_b}^2} - \frac{L_c}{16EI_c} - \frac{L_b}{3EI_b} \right)} \tag{2.4}$$

$$M = PL_b \tag{2.5}$$

S known and the rotation can be determined for each load step. Instantaneous stiffness ΔS can be found by connecting the resulting data points. The RMI specification recommends that the connection stiffness to be used in linear analyses can be given as the S determined from the equation above with F equal to 0.85 times the ultimate load and δ equal to the deflection at that point.

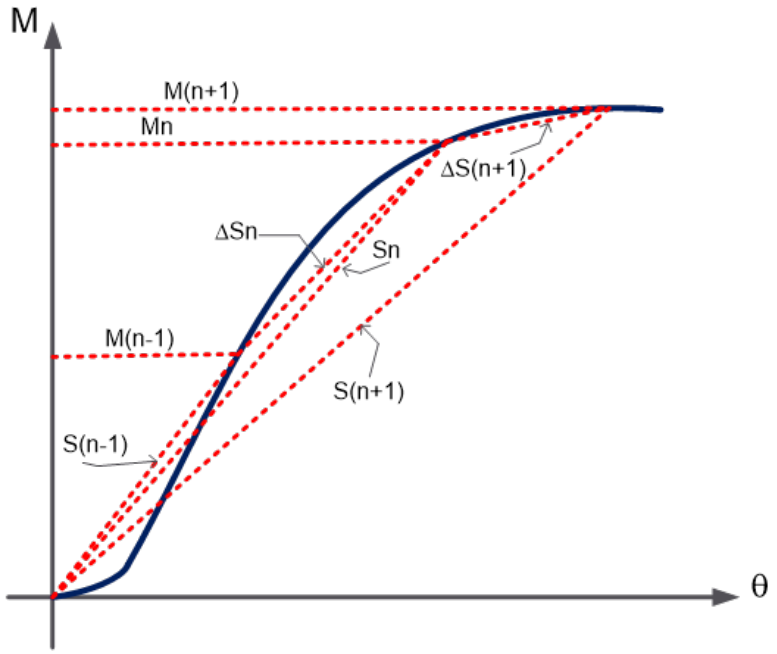

Figure 2.12. Beam to Upright Connection Stiffness.

2.2.5. Yield Parameters

Experiments must be performed by the control parameter for loading history, in this study the control parameter is deformation quantity at the point of the applied load. The force quantity that can be related best to the deformation control parameter at that point, is registered at each 1/8 seconds. Yield values are needed for test control and may be either determined experimentally from a monotonic test or predicted analytically. In both case, engineering judgment is required to determine the yield values an it is obvious that these values are for test control only and that different values may be more useful for test interpretation. The yield values to be used for test control should be associated with significant yielding in the critical region of the monotonic test specimen shown in Figure 2.9. The yield values of this study were taken from monotonic test result, the yield force Q_y and δ_y were taken from the procedure illustrated in Figure 2.13.

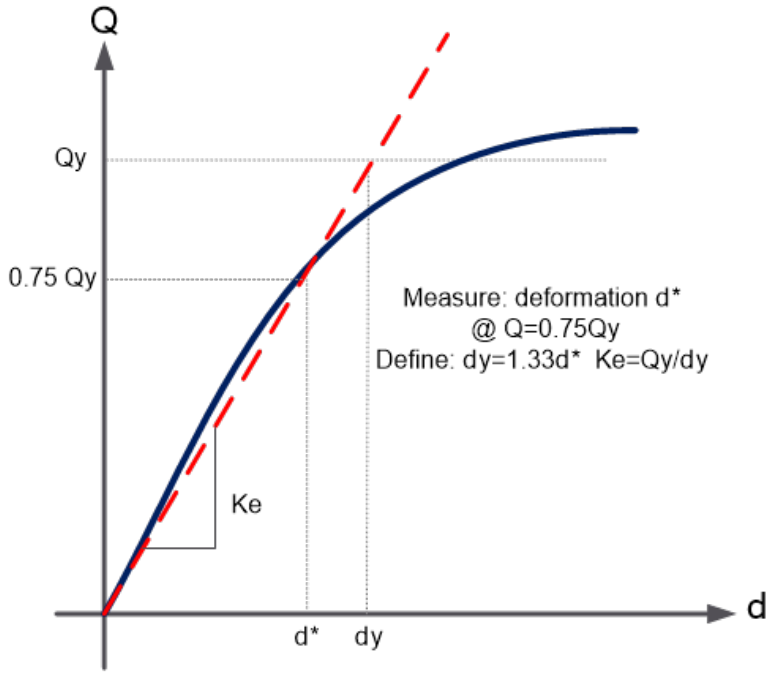

Figure 2.13. Determination of Yield Values and Elastic Stiffness.

The procedure requires force control loading performed by testing load cell to a level of 0.75 Q_y measurement of the corresponding control deformation δ^*, and prediction of δ_y and K_e as shown in Figure 2.13. The prerequisite of the test is measurement of material yield strength which is performed by tensile test.

2.2.6. Testing Program and Loading History

The necessity of a testing procedure is unquestionable, because the real cyclic behavior of structural element may differ by far from the ideal reference of the perfect elasto-plastic behavior. The testing procedure helps to verify the common design relation between a pseudo-static horizontal force and a specified ductility or displacement given by codes such as ATC-24 and ECCS. The procedures set forward the characteristics of the member or assembly. The complete definition of the test requires datas on the combination of seismic and static loads. The testing procedures addressed in ATC-24 and ECCS No.45 concern only with slow cyclic experimentation independent of time. Slow cyclic implies that load or deformation cycles are imposed on a test specimen in a gradual, controlled and predetermined manner. The dynamic effects as

well as vibrations effects are not categorized as slow cyclic testing. Cyclic test is one of the best approaches to provide knowledge on the behavior of the assemblies including data on strength and stiffness characteristics, deformation capacities, and energy absorption. The experiments of mechanical connection at rack structures shall be run with slow cyclic. Such tests are useful to provide basic information on connection behavior including data on strength and stiffness characteristics, deformation capacities, cyclic hardening of softening effects and deterioration behavior at large deformations. In general, the objective of the experiment is to acquire as much as of the above data as feasible since it is unlikely that all future uses of the experimental data can be foreseen at the time of testing. For testing procedure ATC-24 Guidelines for "Cyclic Seismic Testing of Components of Steel Structures" was used as illustrated in Figure 2.14.

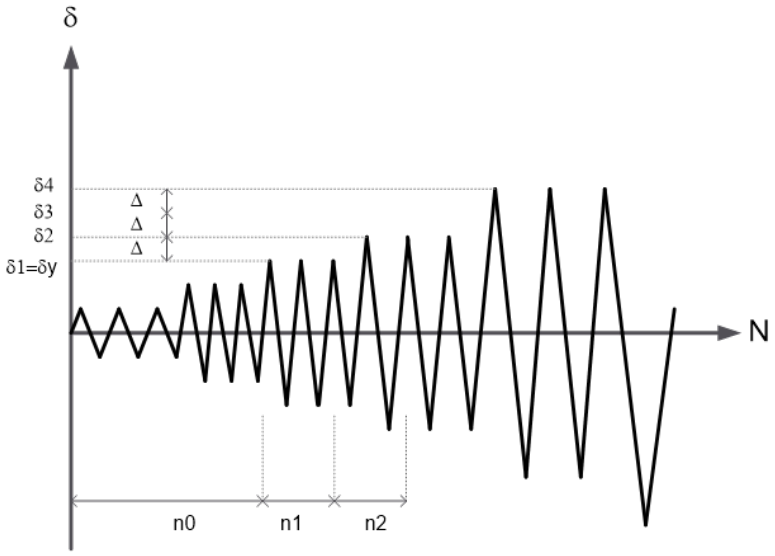

Figure 2.14. Slow Loading History in ATC-24.

The recommendation of ATC24 shown in Figure 2.14 is summarized as below;

- The number of cycles n0 with a peak deformation less than δ_y should be at least 6,
- The number of cycles n1 with peak deformation δ_1 equal to δ_y should be at least 3,
- The number of cycles n2 with peak deformation $\delta_2 = \delta_y + \Delta$ should be at least 3,
- The number of cycles n3 with peak deformation $\delta_3 = \delta_y + 2\Delta$ should be at least

3,

- The number of cycles n4 with peak deformation $\delta_4 = \delta_y + 3\Delta$ to $\delta_m = \delta_y + (\text{m-1})\Delta$ should be at least 2.

It is suggested to perform loading history with small cycles with force control, using a peak value of approximately 0.75 Q_y in elastic range. In all load steps with a peak deformation greater than δ_y the increment in peak deformation Δ should be a constant. This increment should be equal to δ_y.

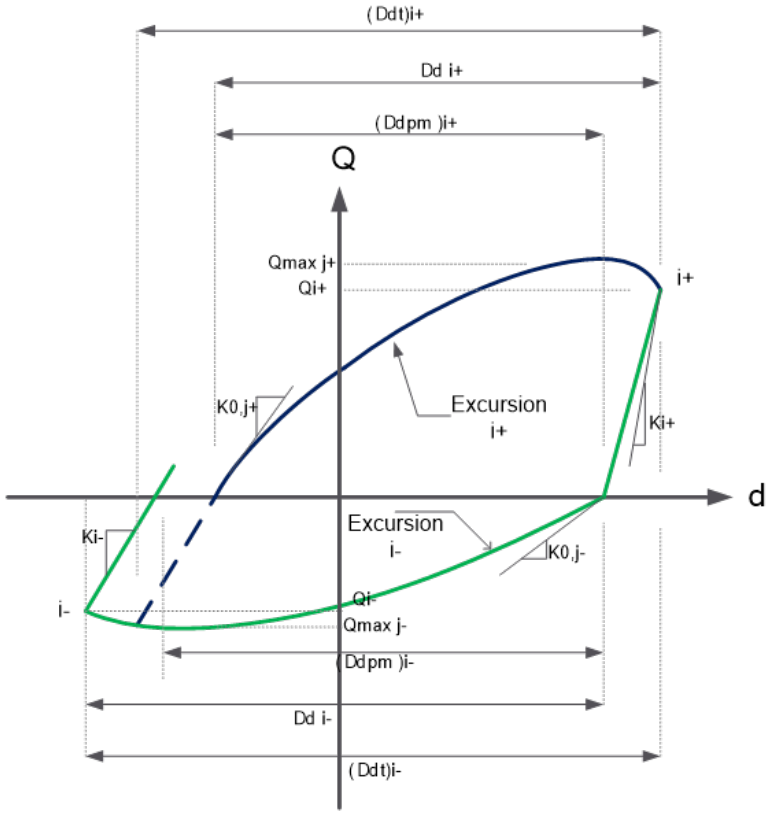

Figure 2.15. Parameters of Cyclic Tests.

The recommended loading (deformation) history to be applied consists of step-wise increasing deformation cycles (Multiple Step Test). In this history the cycles are symmetric in peak deformations. The history is divided into steps and the peak deformation of each step j is given as δ_j a predetermined value of the deformation control parameter.

- δ_j: the peak deformation in load step j
- n_j the number of cycles to be performed in load step j
- m: the total number of load steps to be performed with peak deformations equal to or exceeding the yield deformation
- Δ: the increment in peak deformation between two consecutive steps.

2.2.7. Material Testing

A series of tensile test have been done on the material used for cantilever test specimens. In order to figure out the stress-strain relationships, samples have been taken and coupon tests have been performed according to (ASTM E8 - 2013) for each section type, connecting elements in Structural Testing Laboratory of ÜÇGE Materials Laboratory. The upright type used in test has a nominal thickness of 2.5mm, the pallet beam has thickness of 1.2mm and the end-connector has thickness of 4.0 mm. the cross section of test component are shown in Figure 2.3 to Figure 2.6. The coupon samples were cut from flat lengths of steel sheet coils which were used to roll-form the upright and pallet beam. For each coil, two tensile tests were done using a gauge extensometer in order to measure the Young's modulus accurately. The coupons were tested in a 500 kN capacity testing machine with a strain rate of 2.80x10-4/s. Some photos taken during the coupon tests are given in Figure 2.16.

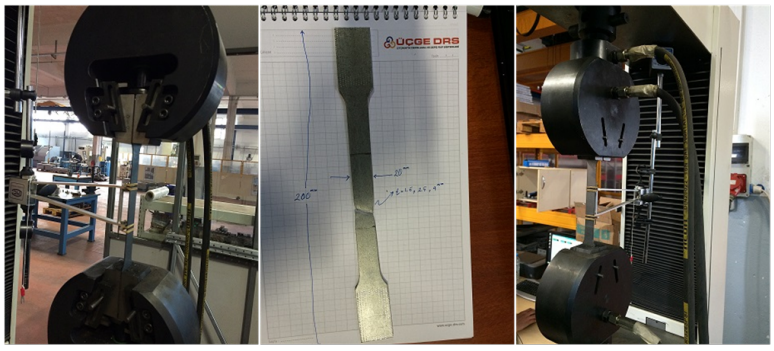

Figure 2.16. Coupon Test for Obtaining Yield Value of Material.

In large strain solutions, all stress-strain input and results will be in terms of true stress and true (or logarithmic) strain. For small-strain regions of response, true strain and engineering strain are essentially identical). To convert strain from small (engi-

neering) strain to logarithmic strain, ε_{ln}= ln (1 + ε_{eng}). To convert from engineering stress to true stress, σ_{true}= σ_{eng}(1 + eng). (This stress conversion is valid only for incompressible plasticity stress-strain data). The samples of tensile tests were taken from normal production of ÜÇGE manufacturing for the purpose of estimating the nominal yield stress. All processes of preparing the tensile tests were performed in accordance with the specified requirements in "ASTM E8-00 Standard Test Methods for Tension Testing of Metallic Material" (ASTM 2013). The dimensions of a typical tensile coupon are shown in Figure 2.17. Three tensile coupons were taken from each specimen, one from the upright, one from the pallet beam and one from the end-connector, average results are given in Table 2.1.

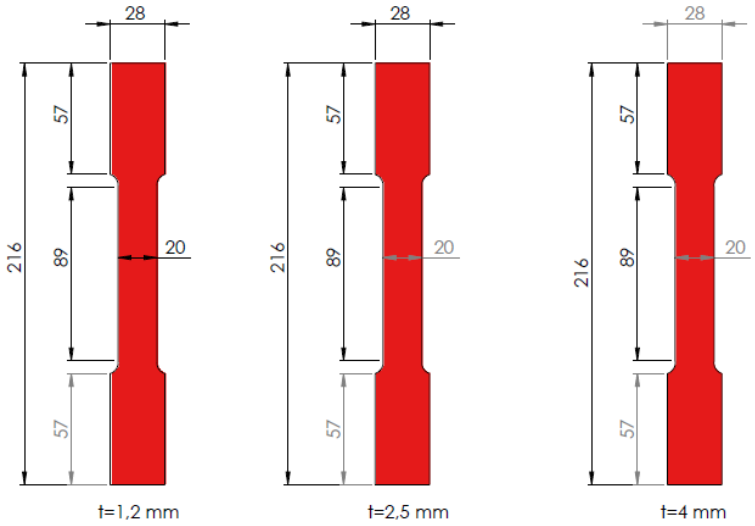

Figure 2.17. Dimensions of Tensile Coupon Test.

An automatic testing machine with a maximum capacity of 500 kN was used for the loading. An extensometer was employed to monitor the deformation. Strain gauges were installed on selected tensile coupons at the center, and on both sides, to verify the modulus of elasticity, E. Autographic diagram method for the materials exhibiting discontinuous yielding were employed as method for yield strength determination.

Table 2.1. True Stress and True Strain Results.

	4.0 mm (End-Connector)			2.5 mm (Upright)			1.2 mm (Pallet Beam)	
No	Strain (mm/mm)	Stress (N/mm^2)	No	Strain (mm/mm)	Stress (N/mm^2)	No	Strain (mm/mm)	Stress (N/mm^2)
1	0	0.00	1	0	0.00	1	0	0.00
2	0.000	182.46	2	0.00004	0.22	2	0.00001	1.00
3	0.002	345.22	3	0.00009	75.98	3	0.00020	34.42
4	0.005	347.24	4	0.00016	109.22	4	0.00200	406.63
5	0.007	358.12	5	0.00022	139.78	5	0.00358	412.25
6	0.011	390.70	6	0.00073	350.88	6	0.00623	418.46
7	0.014	402.50	7	0.00244	383.64	7	0.01175	428.00
8	0.018	421.00	8	0.01103	382.94	8	0.01503	432.42
9	0.022	437.00	9	0.01638	395.90	9	0.02025	438.08
10	0.027	451.22	10	0.01818	400.38	10	0.03050	445.88
11	0.032	461.90	11	0.02770	418.46	11	0.06128	453.88
12	0.042	475.72	12	0.03101	422.42	12	0.08235	452.00
13	0.090	497.50	13	0.04030	429.56	13	0.10085	447.00
14	0.126	479.04	14	0.07044	433.30	14	0.11406	435.00
15	0.136	470.00	15	0.08520	426.08	15	0.11946	425.13

The yield stress, f_y can vary greatly across the test series. The large variation in f_y complicates comparisons across the test database, but it is important to recognize this variation, as f_y for the test coupons of the upright varied from 330 to 505 MPa and for the end-connector from 210 to 480 MPa. Modulus of elasticity, E_s of 205 MPa is assumed for all of the members. This is supported by limited testing on 1.2 mm and 2.5 mm tensile specimens from the pallet beam and upright, which had an average E_s of 203 MPa.

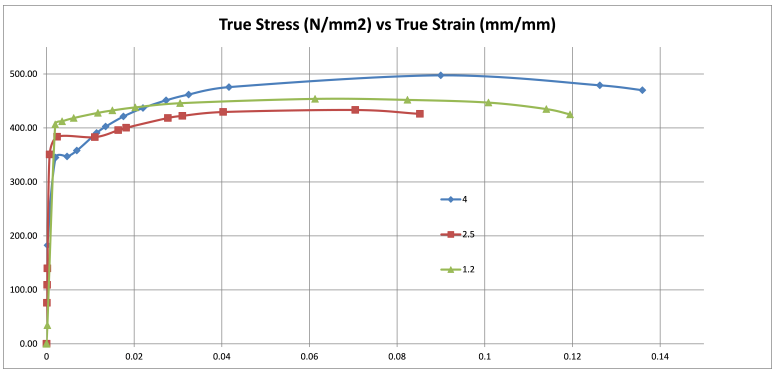

Figure 2.18. True Stress - True Strain Curves of Material.

2.2.8. Organization of the Experiments

Before setting up any analytical or experimental studies on the connection behavior the following questions were considered;

- Why do we deal with the structural behavior of rack systems? Why is the structural behavior of rack systems important?
- Why is the connection behavior of rack systems important?
- How do we perform a structural behavior of cold formed connections?
- What is the structural classification of rack systems and the element assemblies?
- Which parameters are we after?
- Is there similar studies and what makes this study unique?

And before launching main tests the following shall be determined;

(i) The Testing Procedure
(ii) The specimen geometry and the number of configurations to be studied
(iii) The measurements and the type of data to be collected
(iv) The number of cycles
(v) What deformation amplitudes
(vi) What sequences of cycles to evaluate seismic performance

1992 North-American ATC-24 Applied Technology Council-24 Guidelines For Cyclic Seismic Testing of Components of Steel Structures is used as testing procedure. The simulation of the connection behavior needs consideration of all important field conditions including initial and boundary conditions, field fabrications conditions, restraint conditions and loading conditions. The material properties must be apparent from the beginning through material testing. The most important prerequisite is analytical prediction of the anticipated response through precise structural modeling and careful planning of the loading and instrumentation program.

The main parameters in cyclic testing which are performed to draw conclusions on the seismic performance of the connections are strength and stiffness characteristics and their history dependent variation like as cyclic hardening, softening, deterioration and failure modes. Different modes of buckling like as local and torsional and distortional modes, moment-rotation and load displacement of beam, end connector and upright serve the purpose of the study which are the future works of experiments and are going to be studied by installing strain-gauges on the joint.

The test specimen is a set of components connected together to form the structural subassembly. The specimen is composed of beam transverse, end-connector and upright to form an end-bay joint of rack system. The test specimen used in the study is generic test specimen according to ATC-24 classification of specimen types. Appropriate out-of-plane bracing and realistic end restraints have been provided to perform 2D joint. Gravity loads of the pallets have been ignored in 2D set-up, however an initial loading is applied which stands for the weight of pallets.

The main attempt in constructing the samples is to fabricate the components of the specimen in a manner that simulates field and real conditions. The procedures of workmanship and quality control are audited in the QC department of the factory according to applicable standards. This applies particularly to welding and bolting. A prerequisite for testing is to predict the response of the test specimen as much as possible by analytical means. The yield and ultimate strengths and deformations of the test specimen were predicted analytically.

The cyclic load test in this study is performed as predetermined and planed loading history. In the elastic and inelastic range, the test is performed under deformation control. Since the loading history is dependent on the yield value of the specimen, this value is needed to control the test. This value can be determined experimentally from a monotonic load test either positive moment or negative moment.

3. CONNECTION TESTS

3.1. Beam-to-Upright Connections

Beam-to-Upright tests were performed with the aim of characterizing the behavior of joint along down-aisle direction of racks. To follow a correct and comfortable interpretation of full scale test as well as to suit and calibrate numerical models, component tests are essential. In former chapters it was highlighted that the behavior of beam-to-upright connections is significantly influenced by the following factors;

- Mechanical and material properties of thin walled section profiles of pallet beam and upright and the end-connector,
- The mechanical nature of the end-connector connection which is caused by the inclined hooks and the safety bolt.

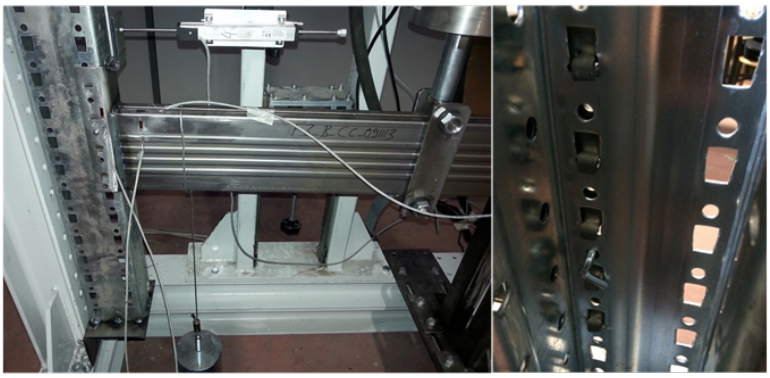

Figure 3.1. Typical Beam-to-Upright b) Inclined Hooks and Safety Bolt.

Based on testing procedure stated in RMI 2008 and ATC-24 the following tests were performed. This study focused on the beam-to-upright connection type shown in Figure 3.1. A L-shape bended end plate is welded to the pallet beam at both ends. Connection is settled by replacing the hooks in the perforation on the upright and by occasionally adding a safety bolt in installation phase. The beam-to-upright connection is apparently non-symmetric in both vertical and horizontal planes. In the vertical plane, non-symmetry is due non-symmetric connection between the end-

connector welded to the beam in the case of bottom and top connected types. Moreover, the weld is not continuously surrounded the cross section area of the boxed beam, the top flange or bottom flange of the beam is leaving un-weld after fabrication randomly which makes the specimen selection difficult. In the horizontal plane, non-symmetry is due to the shape of the end-connector that has inclined hooks on one side only, and is obtained by cold forming of a thin plate, bent in shape of an L. In the following section of the study, moment rotation curves of different types of beam-to-upright connections, and the failure modes of those under monotonic and cyclic loads are going to be assessed. Two different cross sections for pallet beams DD 140x50x1.2 and DD 150x50x1.2 were adopted. The upright cross section was remained the same for two different beams as HR 115x100x2.5. Accordingly, beam depth varied between 140 mm and 150 mm with two different welded end-connectors with depth of 210 mm and 245 mm respectively. The member geometrical properties are shown in Table 3.1 and Table 3.2.

Table 3.1. Geometrical Properties of Test Specimens of DD140.

L_b	500 mm	Length of beam
L_c	1050 mm	Length of column
L_{res}	750 mm	Length of out of plan restarined point
I_b	1661793 mm^4	Moment of inertia of the beam
I_c	1700250 mm^4	Moment of inertia of the column
E	210 Kn/mm^2	Modulus of elasticity
I_r	165	Arm of rotation in end-connector
d	140 mm	Depth of beam
h	210 mm	Depth of End-connector

Table 3.2. Geometrical Properties of Test Specimens of DD150.

L_b	500 mm	Length of beam
L_c	1050 mm	Length of column
L_{res}	750 mm	Length of out of plan restarined point
I_b	2492690 mm^4	Moment of inertia of the beam
I_c	2501467 mm^4	Moment of inertia of the column
E	210 Kn/mm^2	Modulus of elasticity
I_r	183	Arm of rotation in end-connector
d	150 mm	Depth of beam
h	245 mm	Depth of End-connector

The material used for beams and upright is various 345 MPa, 383 MPa and 406 MPa yield strength respectively for end-connector, upright and beam. Table 3.4 identifies two different types of beams as DD140 and DD150 and two different types of applied load as monotonic and cyclic, and three types of connection into end-connector as top, bottom and middle welded beam into end-connector. For 18 different test configurations, overall 50 tests carried out on beam-to-upright specimens. Monotonic tests were performed under both clockwise and counter-clockwise moments as shown in Table 3.4.

Table 3.3. Monotonic Tests Carried Out on Beam-to-Upright Connections.

Test Type	Joint Type	Description	No. of Specimen
Monotonic	TP 140	Pallet Beam Depth = 140 mm End-Connector = Top Applied Load = Downward	3
	TP 150	Pallet Beam Depth = 150 mm End-Connector = Top Applied Load = Downward	2
	MP 140	Pallet Beam Depth = 140 mm End-Connector = Middle Applied Load = Downward	3
	MP 150	Pallet Beam Depth = 150 mm End-Connector = Middle Applied Load = Downward	3
	BP 140	Pallet Beam Depth = 140 mm End-Connector = Bottom Applied Load = Downward	3
	BP 150	Pallet Beam Depth = 150 mm End-Connector = Bottom Applied Load = Downward	3
	TN 140	Pallet Beam Depth = 140 mm End-Connector = Top Applied Load = Upward	3
	TN 150	Pallet Beam Depth = 150 mm End-Connector = Top Applied Load = upward	2
	MN 140	Pallet Beam Depth = 140 mm End-Connector = Middle Applied Load = upward	3
	MN 150	Pallet Beam Depth = 150 mm End-Connector = Middle Applied Load = Upward	3
	BN 140	Pallet Beam Depth = 140 mm End-Connector = Bottom Applied Load = Upward	3
	BN 150	Pallet Beam Depth = 150 mm End-Connector = Bottom Applied Load = Upward	3

Table 3.4. Cyclic Tests Carried Out on Beam-to-Upright Connections.

Test Type	Joint Type	Description	No. of Specimen
Cyclic	TC 140	Pallet Beam Depth = 140 mm End-Connector = Top Applied Load = Cyclic	3
	TC 150	Pallet Beam Depth = 150 mm End-Connector = Top Applied Load = Cyclic	2
	MC 140	Pallet Beam Depth = 140 mm End-Connector = Middle Applied Load = Cyclic	3
	MC 150	Pallet Beam Depth = 150 mm End-Connector = Middle Applied Load = Cyclic	3
	BC 140	Pallet Beam Depth = 140 mm End-Connector = Bottom Applied Load = Cyclic	2
	BC 150	Pallet Beam Depth = 150 mm End-Connector = Bottom Applied Load = Cyclic	3

The cyclic testing procedure proposed by ATC-24 was used for simulating seismic behavior of beam-to-upright joints. Sufficient number of strain gauges was also stick on the predicted sensitive surfaces as shown in Figure 3.2.

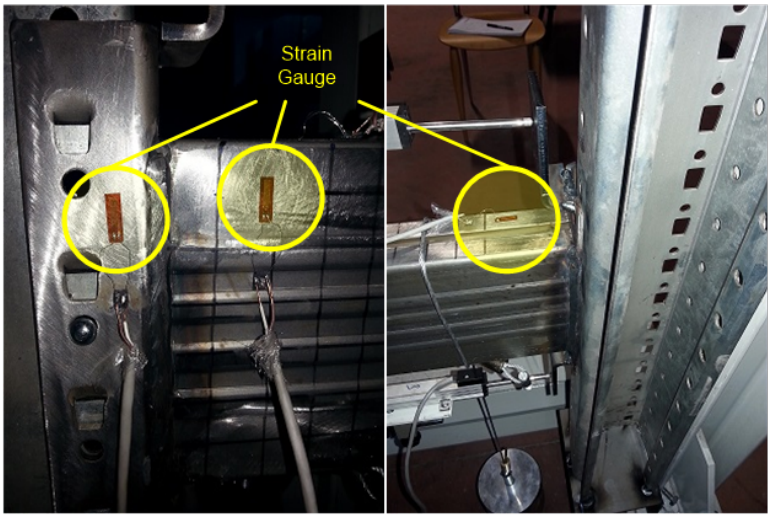

Figure 3.2. Arrangement of Strain Gauges.

3.2. Monotonic Test Results

3.2.1. Force-Displacement Responses

Experimental parameters obtained from monotonic test are yield strength; yield deformation, ultimate strength as well as ultimate displacement, initial elastic stiffness and also energy absorption and failure modes of in the joint region. The derivation of these parameters can be conventionally defined according to ATC-24 as shown in Figure 3.13. The monotonic tests listed in Table 3.5 were carried out on beam-to-upright connections with DD140 and DD150 beams.

It should be noted that in all specimen the safety bolt was used in middle slot of the end-connector to retain the beam. During the pilot tests, it was observed that without safety bolt almost all the specimens slip particularly during upward loading. Originally, during the site installation of storage racks, safety bolt is used as montage bolt to keep in place the installed pallet beams after a sudden impact like crashing the fork of the forklift which cause the collapse of the beam and the pallet. Therefore, in all specimens the safety bolt was used and the behavior of the bolt was registered. The safety bolt was not crashed or yielded during tests, thus it was noted to be modeled as rigid element in finite element models.

Table 3.5. Monotonic Test on Beam-to-Upright Connection with DD140 and DD150.

Loading		Joint Type	Q_y (kN)	δy (mm)	K_e (kN/mm)	Q_{ult} (kN9
Downward	(Clockwise)	TP 140	3.99	15.96	0.25	6.98
		TP 150	4.09	14.6	0.28	5.79
		MP 140	5.31	25.27	0.21	5.85
		MP 150	6.54	25.64	0.26	7.81
		BP 140	4.98	23.94	0.21	6.77
		BP 150	6.34	29.94	0.27	8.48
Upward	(Counter-Clockwise)	TN 140	5.19	17.29	0.3	8.63
		TN 150	5.84	16.2	0.33	8.91
		MN 140	4.98	21.92	0.16	5.8
		MN 150	7.02	31.92	0.22	10.11
		BN 140	4.27	29.26	0.15	5.89
		BN 150	6	20	0.3	7.32

Table 3.5 shows the values of yield strength and ultimate strength measured for each test. The yield strength values are high for DD150 tests relative for DD140 tests. The number of inclined hooks is 5 for DD150 tests and 4 for DD140 tests, and strictly the height of end-connector for DD150 is larger than DD140 end-connectors. Therefore, the higher end-connector and deeper pallet beam can cause higher yield strength and ultimate strength. The same evaluation cannot be stated for yield displacement of tests, however end-connector height and depth of the beam might be one of the factors affecting the yield displacement, so interpreting yield displacement needs more parameters than the available values in Table 3.5. Initial stiffness is also influenced by the height of end-connector and pallet beam depth, as shown in Table 3.5 DD150 test specimens are stiffer than DD140.

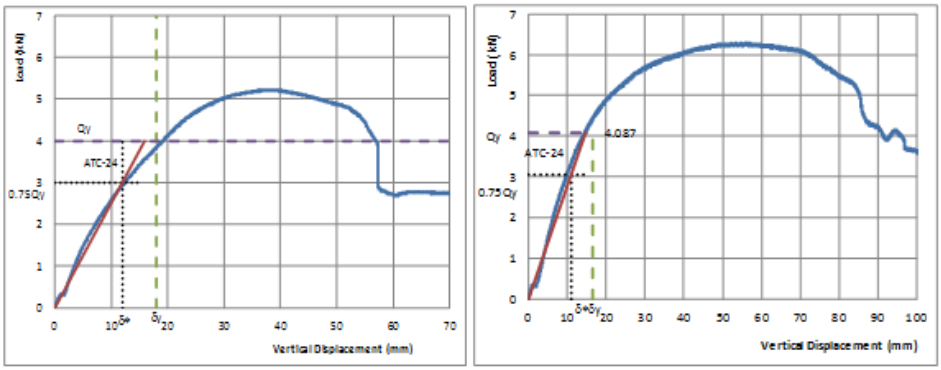

Figure 3.3. Force Displacement Curve for TP140 and TP150.

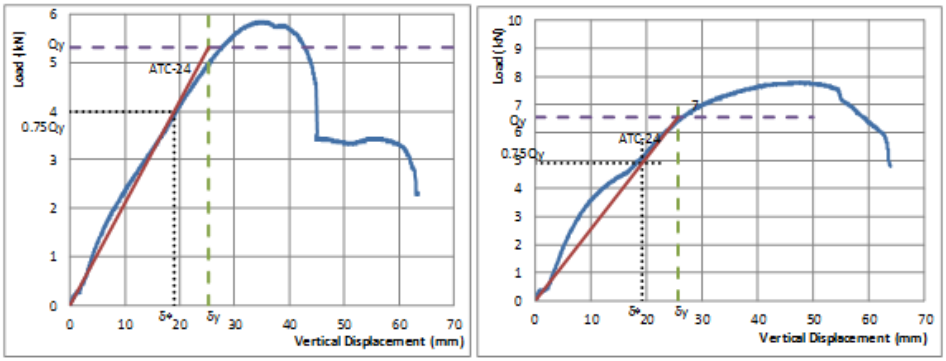

Figure 3.4. Force Displacement Curve for MP140 and MP150.

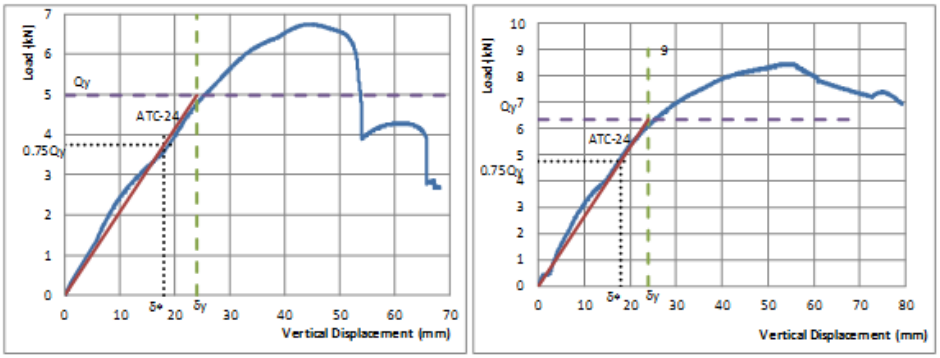

Figure 3.5. Force Displacement Curve for BP140 and BP150.

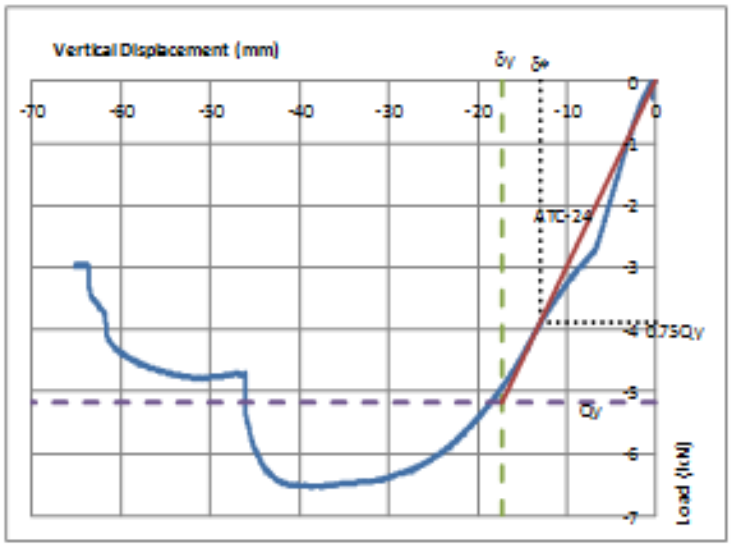

Figure 3.6. Force Displacement Curve for TN140.

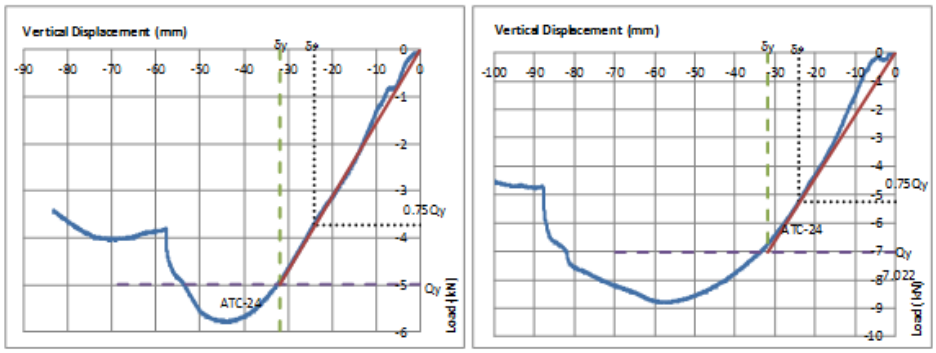

Figure 3.7. Force Displacement Curve for MN140 and MN150.

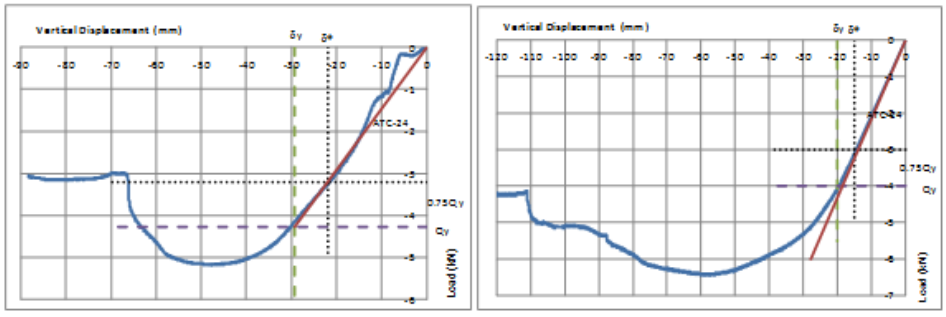

Figure 3.8. Force Displacement Curve for BN140 and BN150.

3.2.2. Moment-Rotation Results

The monotonic tests listed in Table 3.6 were carried out on beam-to-upright connections specified in Table 3.4. Cantilever tests were performed along downward and upward directions respectively for clockwise and counter-clockwise bending moment applied by load cell. Table 3.6 reports nominal values measured from moment-rotation curves according into the procedures of ATC-24. The values are un-factored measured as the average of the number of tests performed as shown in Table 3.4. At least two and at last three tests were repeated for each specimen excluding pilot tests. Observations made during testing of the specimens were noted associating with apparent damage level like as hook tearing, distortion of end-connector and distortion of pallet beam. All qualitative information during and after test were summarized and provided below to illustrate the overall specimen behavior.

For each specimen the ductility level is specified in Table 3.6. It is observed that all test specimens embrace a level of ductility despite the fact of looseness in such connection which cause the slip of joint and the contact positions of hook and perforation change due to that. If the problem of looseness is eliminated, the level of ductility would be higher than the existing state. In fact, looseness, ductility and stability are three different cases influenced each other in storage racks. The looseness is a stability issue, in other words it is a mode of mechanism in joint region. Minimum ductility is observed at MN140 as 1.323 and the maximum at TP150 as 2.662. as expected scenario, the highest ductility is in DD150 series with 150mm beam depth, therefore, beam depth directly influenced the ductility.

Table 3.6. Monotonic Test Results Obtained from Moment-Rotation Curves.

Loading		Joint Type	M_y (kN.m)	Φ_y (m.rad)	S_i (kN.m/rad)	M_u (kN.m)	Φ_u (m.rad)	μ
Downward	(Clockwise)	TP 140	2.354	41.66	56.51	1.616	76.88	1.845
		TP 150	2.827	41.93	67.43	3.142	11.6	2.662
		MP 140	1.972	50.94	51.63	2.922	71.23	1.398
		MP 150	3.506	53.3	65.78	3.896	95.55	1.793
		BP 140	3.042	60.75	50.08	3.381	88.8	1.462
		BP 150	3.816	58.02	65.76	4.24	108.2	1.865
Upward	(Counter-Clockwise)	TN 140	2.94	39.8	73.81	3.27	77.2	1.940
		TN 150	3.06	40.02	76.49	3.38	79.52	1.987
		MN 140	2.61	66.8	39.01	2.90	88.4	1.323
		MN 150	3.97	73.1	54.3	4.41	114	1.560
		BN 140	2.34	64.2	36.39	2.59	96.5	1.503
		BN 150	2.90	58.2	49.86	3.23	115	1.976

A graphical comparison between the yield and ultimate strength, yield rotation and initial rotational stiffness is exhibited in Figure 3.9: Moment-Rotation results comparison to summarize moment-rotation curves.

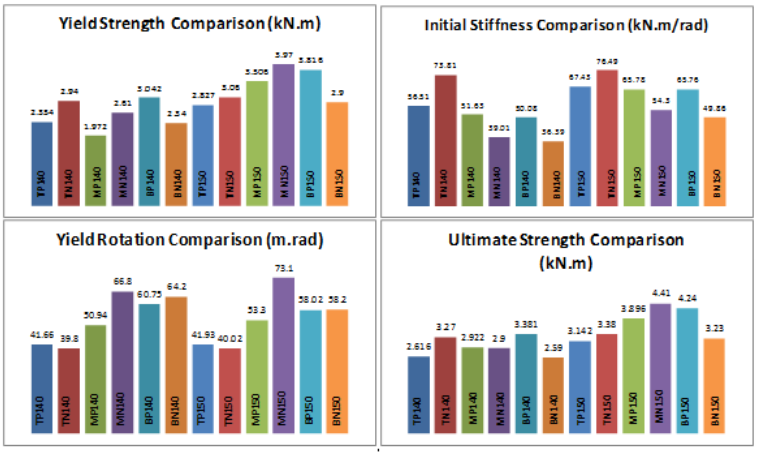

Figure 3.9. Moment-Rotation Results Comparison.

Table 3.7 reports the difference ratio between downward (positive) and counter-

clockwise (negative) loading of the test specimens. Considering yield strength, T and M joints have higher yield strength in upward loading than downward loading. Along upward direction loading, the hooks start yielding after direct contact, the contact mode type is completely frictional contact between the hooks edge sides and upright perforations. Thus, almost all hooks - 4 hooks in DD140 and 5 in DD150 - start rotate in T and M joint contrary to B joints. Hooks start yielding after full contact at edges and increase the resistance of whole joint, in other word, hooks contributes to joint stiffness. At both B140 and B150 joint upward loading yield strength is about 30% lower than downward loading. Since, at B connected joint the pallet beam is welded into bottom side of end-connector when the load cell pull the specimen the lowest hook start moving slowly toward the beam, after hitting the edge of upright perforation, the hook yields and start tearing. During the test, it was observed that the second lowest hook also start yielding when the lowest one fully collapse. The highest difference between positive and negative loading of joints is in B150 with -32% and the lowest difference at T150 with 8% considering yield strength values. Yield strength comparison between the specimens is a good tool to understand the behavior of joint; the joint must have not only high strength at both direction but also symmetrical performance at both upward and downward direction. In this respect, M150 exhibits the most appropriate joint compared with other joints. Since the difference between up and down loading is about 12% - acceptable for being counted as symmetrical joint and has yield strength of 3.97 kN.m upward and 3.506 kN.m downward. Obviously, the yield strength alone cannot create a scale of reference for comparing the joints; other parameters influence the overall performance. Initial rotational stiffness is another important parameter taken from moment-rotation curves. M and B joint have larger initial stiffness in upward than downward direction; however the contrary is valid for T joints at both DD140 and DD150. The highest rotational stiffness is observed in T joints in upward loading, with 76.49 and 73.81 kN.m/rad respectively for beam 150 mm and 140 mm in depth. The largest difference in rotational stiffness between upward and downward loading is seen at B140 joint and B150 joint with -38% and -32% difference. Another important parameter taken from moment-rotation curve is ultimate strength. The difference between upward and downward loading in the case of ultimate strength is not as much as yield strength and initial stiffness cases.

Table 3.7. Differences Between Downward and Upward of Joint Specimens.

Joint	Yield Strenght	Rotational Stiffness	Ultimate Strenght
T140	20%	23%	20%
M140	24%	-32%	-1%
B140	-30%	-38%	-31%
T150	8%	12%	7%
M150	12%	-21%	12%
B150	-32%	-32%	-31%

For each specimen the rotational stiffness has been calculated according to 1.8.2 Section. The method specified in RMI 2008. For the purpose of comparison, the red line which shows the calculated rotational stiffness specified by RMI 2008 is exhibited in all moment-rotation curves. The Table 3.8 is the summary of all calculations of 1.8.2 Section.

Table 3.8. Rotational Stiffness Calculated According to RMI.

Joint	P_{ult} (kN)	$P_{0.85}$ (kN)	δ_{ult} (mm)	$\delta_{0.85}$ (mm)	R.F.$_{beam}$	R.F.$_{upright}$	F
BP140	6.76	5.75	44.4	37.74	1.00	1.00	92811
BN140	5.19	4.41	48.24	41.00	1.00	1.00	63994
MP140	5.84	4.97	35.61	30.27	1.00	1.00	100670
MN140	5.85	4.97	35.61	30.27	1.00	1.00	100670
TP140	5.23	4.45	38.44	32.67	1.00	1.00	82232
TN140	6.23	5.55	38.63	32.83	1.00	1.00	104070
BP150	8.48	7.21	54.1	45.99	0.85	1.00	79139
BN150	6.45	5.48	57.59	49.95	0.85	1.00	55674
MP150	7.79	6.62	47.78	40.61	1.00	1.00	97097
MN150	7.99	6.78	47.88	41.02	1.00	1.00	353299
TP150	6.28	5.34	55.79	47.42	1.00	1.00	65866
TN150	7.54	6.41	62.08	52.77	1.00	1.00	86975

3.2.3. T140 Moment-Rotation Curves

A comparison was made between yield strength, ultimate strength, initial rotational stiffness and yield rotation of all specimens. The results are shown in Figure 3.10

Comparing TP140 with TN140, DD140 top connected beam into end-connector downward and upward loaded, this type of joint has about 20% larger yield strength along upward than downward direction. Considering gravity direction along downward, the T140 joint might behave better in seismic rather than gravity conditions. However, since seismic forces are reversed cyclic, this outcome should be approved by further cyclic tests in next section.

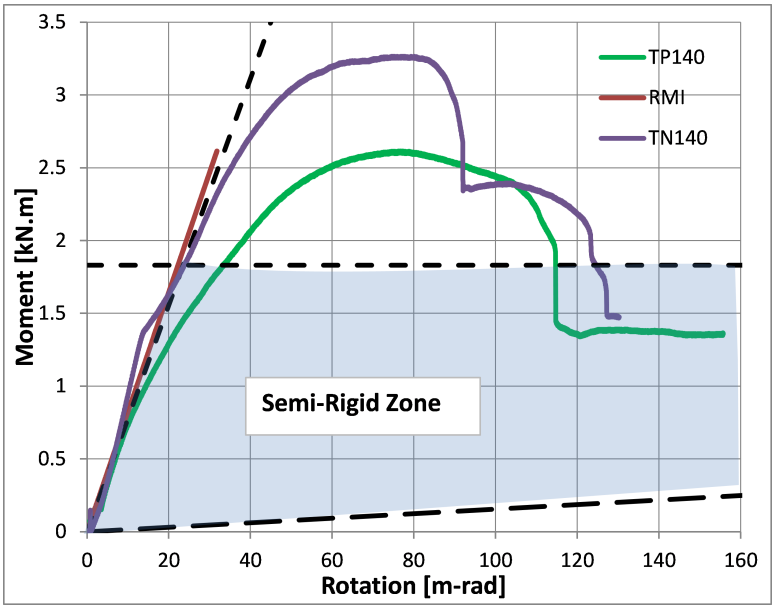

Figure 3.10. Comparison of the Moment-Rotation Curves for TP140/TN140.

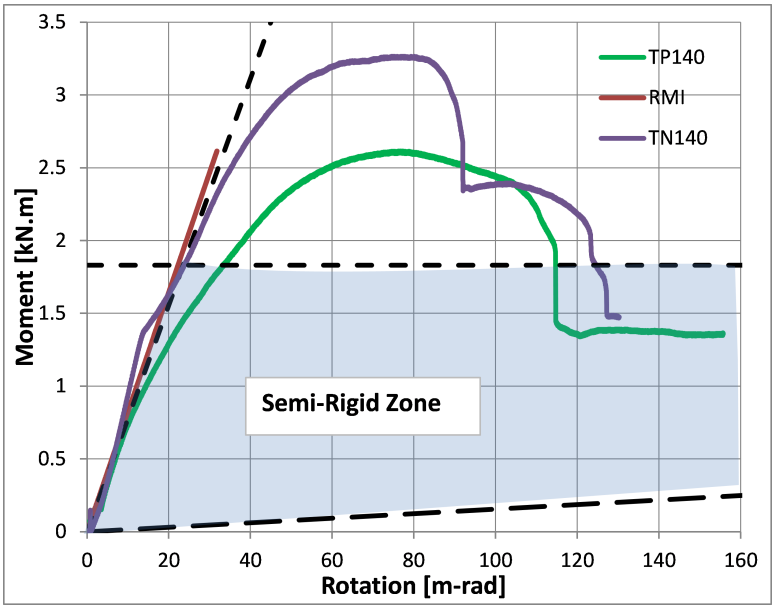

Figure 3.11. Failure Modes in Monotonic Tests on TP140 Specimens.

Figure 3.12. Failure Modes in Monotonic Tests on TN140 Specimens.

Figure 3.10 compares the moment-rotation curves for both clockwise (positive) and counter-clockwise (negative) bending, in the case of top connected end-connector into DD140 beam, TP140 and TN140. It can be noticed that the specimens under negative bending show larger ultimate strength than the specimens under positive bending moments, and also the same difference can be seen in the case of yield strength, but the initial stiffness of both positive and negative bending is almost the same. In the case of ductility, it can be stated that both specimens behave ductile at equivalent levels. In RMI 2008 the approximate analytical rotational stiffness used for the design of this joint is shown in red in the Figure 3.10 which is similar with experimental results.

3.2.4. M140 Moment-Rotation Curves

Figure 3.13 compares the moment-rotation curves for both positive and negative bending, in the case of middle connected 140 mm beam into 4 hooks end-connector. It can be noticed that the specimens show similar yield and ultimate strength and even similar level of ductility under positive and negative bending, but larger initial elastic stiffness in positive loading than the specimens under negative bending. This similarity can be explained observing the following Figure 3.15, presenting typical failure modes observed during the monotonic tests.

Both specimens remain in semi-rigid zone classification specified in “Eurocode 3”. The dashed lines according to Eurocode 3 provide the designers with two diagrams which enable the classification of joints according to their stiffness and strength (Jaspart

1999) The lower boundary distinguishes fully pinned area than semi-rigid area. the horizontal dashed line - the moment that corresponds to the yield plateau is termed design resistance. It may be understood as the pseudo-plastic moment resistance of the joint.

Strain-hardening effects and possible membrane effects are neglected herein, that explains the straight horizontal dashed line. The elastic rotational stiffness considered in RMI 2008 is higher than negative and positive loaded specimens' stiffness. The red line show un-factored design curve considered for M140 joint in RMI 2008. Generally, the approach introduced in RMI 2008 recommends using 0.85 factor to reduce the applied load by load cell. Failure of both specimens subjected to positive and negative bending was due to large deformations in the beam end-connector, respectively resulting in the top and bottom hooks coming out of the perforations in the upright.

At both test specimens the safety bolt installed in the middle slot of the end-connector took the end-connector in place and prevent sliding the joint and replacing it, in other word it retained the neutral axis of the joint until the failure mode. The safety bolt occasionally was controlled to see any tension or compression; it started carrying the shear and tension after deforming the end-connector and tearing the hooks as shown in Figure 3.15.

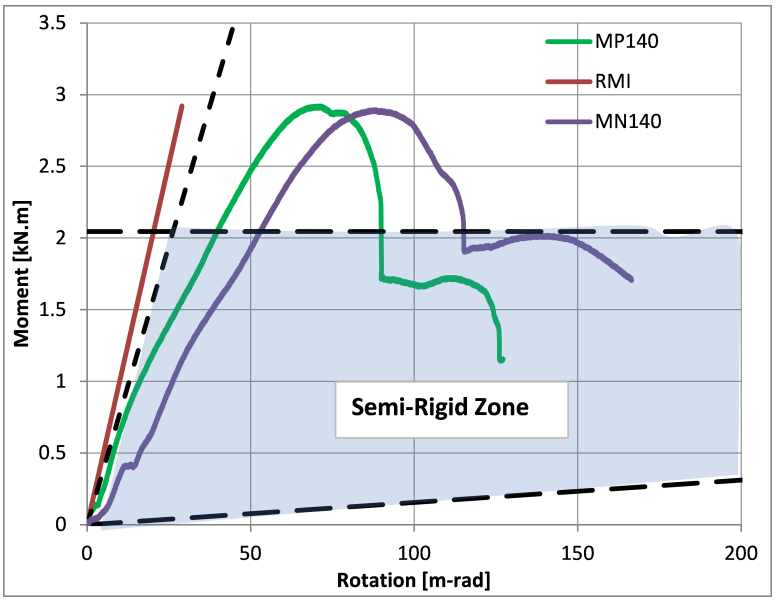

Figure 3.13. Comparison of the Moment-Rotation Curves for MP140/MN140.

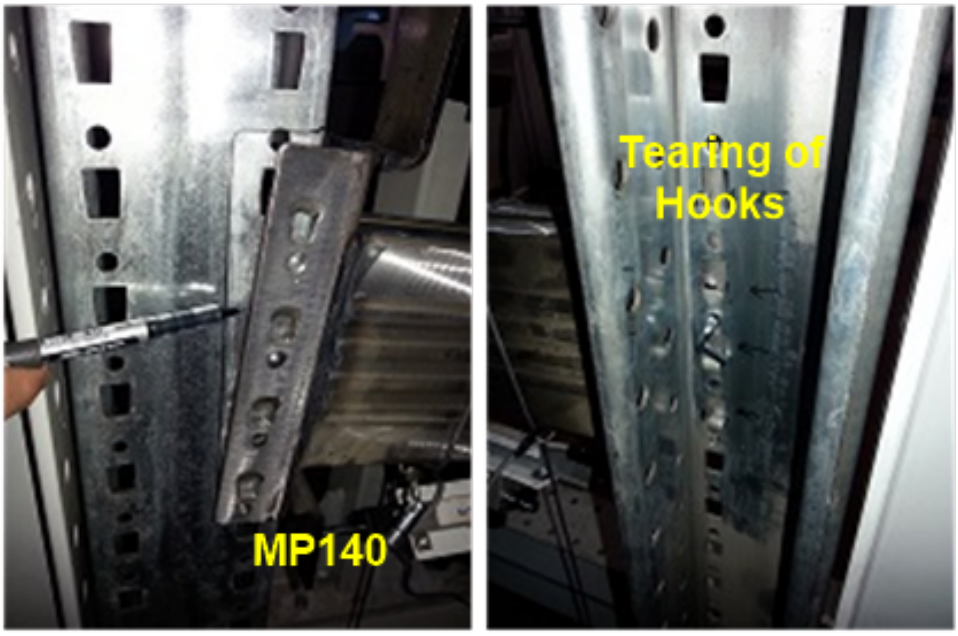

Figure 3.14. Failure Modes in Monotonic Tests on MP140 Specimens.

Figure 3.15. Failure Modes in Monotonic Tests on MN140 Specimens.

3.2.5. B140 Moment-Rotation Curves

Figure 3.16 presents moment-rotation curve comparison for BP140 and BN140. Large difference between specimens under positive and negative bending is noticed. Yield strength under positive bending is approximately 30% larger, initial stiffness about 38% and the ultimate strength about 32% larger than negative bending. However, the ductility ratio is similar at both loading, which is about 1.5. The large difference can be explained by the geometrical position of the beam with respect to

end-connector. The pallet beam is welded into the bottom of the end-connector, and while applying positive bending the bottom of the end-connector undergoes compression and the top in tension. Bottom of the end-connector is more rigid than the top due to presence of the beam behind the end-connector. The bottom of the end-connector contact the flange of the upright just after getting loaded and the rigidity increases. The effect of the top hooks should not be ignored, but frictional contact between the interior surface of the end-connector and the outer surface of the upright is the most important reason for increasing rigidity. The failure mode of B140 specimens subjected to positive and negative bending was distortion of end-connector and tearing of hooks up to crashing level.

Typical failure modes observed during the monotonic tests are presented in Figure 3.17. No failure was observed at safety bolt, and the connection behavior was not influenced by bolt deformation. At both specimens, joint strain hardening was observed; it can be explained by correlation of hooks and end-connector. Shortly after applying load, the hooks at top and bottom respectively under positive and negative bending, started replacing horizontally toward beam and getting in direct contact with side edge of the upright perforations. They started yielding resulted in rotation around their axes. Hooks failed completely and crashed out of the joint system and just after that the end-connector fully pushed the upright toward the axis of the upright. This contact in between the end-connector and the upright caused a jump in the moment-rotation curve which can be explained in terms of strain hardening of the joint. The performance of the B140 joint is not symmetrical at both directions. Join is affected by positive and negative bending under seismic forces, thus a desirable performance under seismic forces is the one that act at both directions. B140 behaved unsymmetrical and might not be a correct choice for seismic design.

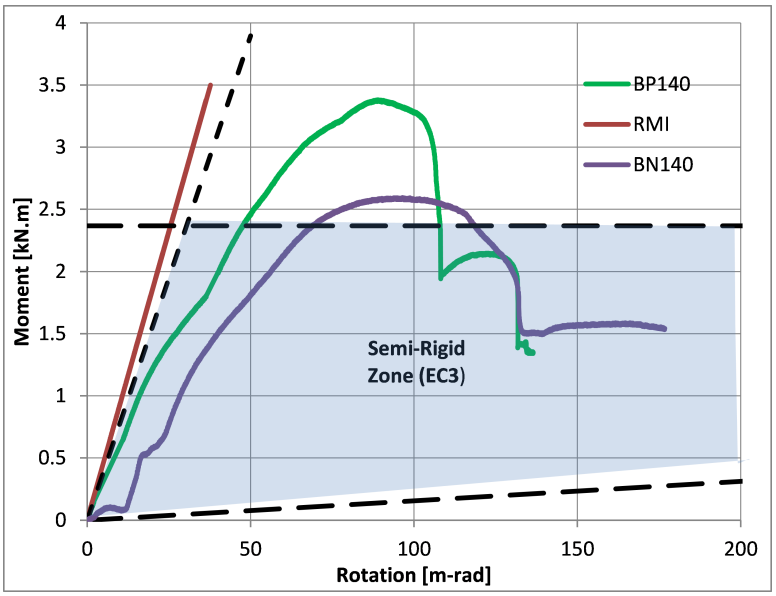

Figure 3.16. Comparison of the Moment-Rotation Curves for BP140/BN140.

Figure 3.17. Failure Modes in Monotonic Tests on BP140 Specimens.

Figure 3.18. Failure Modes in Monotonic Tests on BN140 Specimens.

3.2.6. T150 Moment-Rotation Curves

The monotonic test result of TP150 specimen is shown in Figure 3.19. The initial rotational stiffness of the specimen fulfill with the constant value obtained by RMI 2008 analytical method. As it can be seen from the curve, the relationship between the moment and the angular change at a joint is not linear. The proposed approach in RMI 2008 defined in 2.2.4. appears to be reasonable for determining a constant value of rotational stiffness appropriate for the design. The ductile behavior of TP150 is quite higher than TP140 because of deeper pallet beam and five hooked end-connector instead of four hooked one. The position of the safety bolt did not change during the test and it did not affect the overall joint performance. The failure mode of TP150 specimen subjected to positive bending was the local distortion of the bottom flange and the web of the pallet beam as shown in Figure 3.20. Two the highest inclined hooks distorted due to tearing and completely fallen down during the test.

Upper hooks of the end-connector started punching through the hole of the upright; the presence of the safety bolt retrains the deformation of the upper part of the end-connector. Hence, only the highest two hooks could come out of the perforation and fallen down. After crashing the hooks, the end-connector distorted and took the shape as shown in the figure. The bottom of the beam applied compression into the upright flange which caused minor fracture and major buckling at bottom flange of the beam. In fact, that increased the rigidity of the joint and the ductility level was raised up at the system. The joint can be classified near close as fully rigid because the rotational stiffness is quite high.

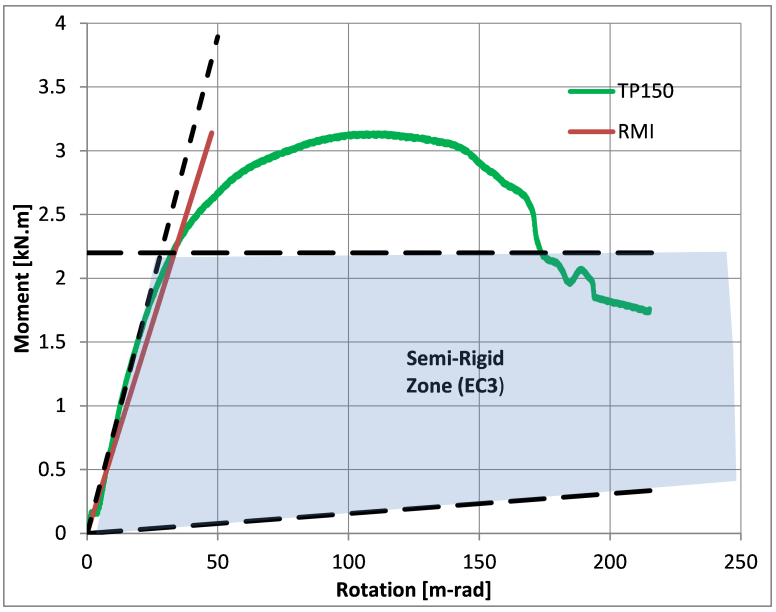

Figure 3.19. Moment-Rotation Curve for TP150.

Figure 3.20. Failure Modes in Monotonic Tests on TP140 Specimens - Back Face.

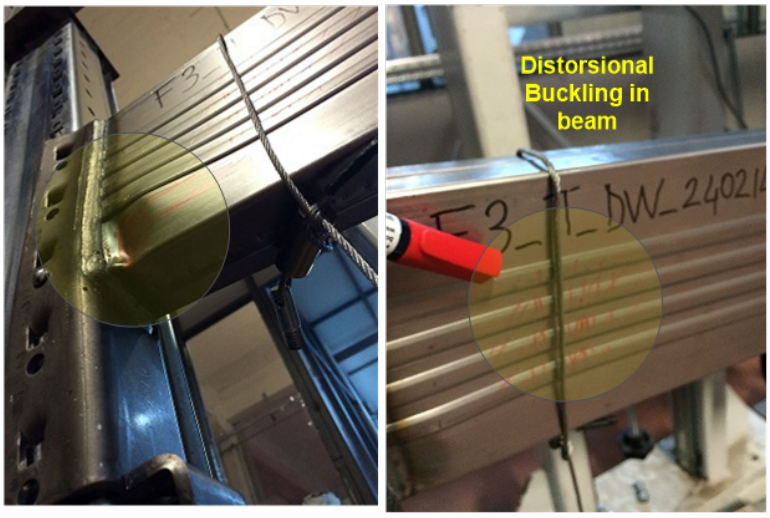

Figure 3.21. Failure Modes in Monotonic Tests on TP140 Specimens - Front Face.

3.2.7. M150 Moment-Rotation Curves

Figure 3.2 presents moment-rotation curve comparison for MP150 and MN150. Specimen under negative bending shows about 12% larger yield strength and about 7% larger ultimate strength, but lower initial elastic rotational stiffness than the specimen under positive bending moment. The specimen also shows larger ultimate rotation under negative bending than the positive one. In the case of ductility level, the specimen under positive bending behave more ductile that the negative specimen. Since the ductility level is the ratio of ultimate rotation into the yield rotation of the joint, the yield rotation of the specimen under negative bending is higher than the positive one and the same is valid in the case of ultimate rotation, however the proportion is larger under positive bending. the initial stiffness of the specimen under positive bending is about 12% larger than the negative bending.

The joint remained at semi-rigid region at both bending directions. Failure of both specimens subjected to negative and positive bending was due to large deformation in the end-connector, respectively resulting in the top and bottom hooks pulling out of the perforations in the upright. Under negative bending the safety bolt is in tension and tending to coming out of the slot as shown in Figure 3.23. The safety bolt resisted escaping the end-connector under negative bending. End-connector is distorted at top and bottom respectively under positive and negative bending. in M150 joint local buckling of the pallet beam was also observed, the flange of 1.2mm thick beam was yield and distorted. The collapse mechanism is governed by the failure of the hooks in the lower part of the end-connector; on the contrary, it was governed by distortion of the top flange of the beam and also tearing of the top hooks. Larger strength at negative bending than positive bending can be explained by the existing of the safety bolt and performing as a part of the joint.

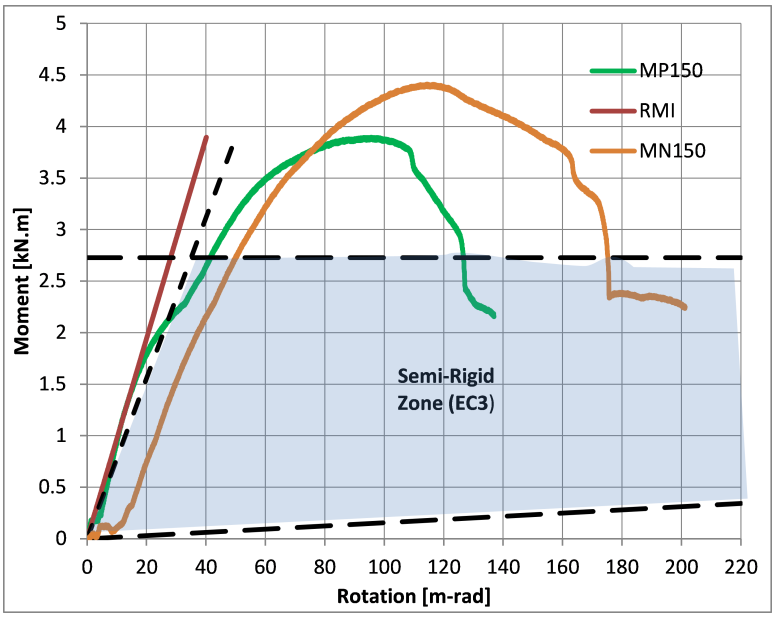

Figure 3.22. Comparison of the Moment-Rotation Curves for MP150/MN150.

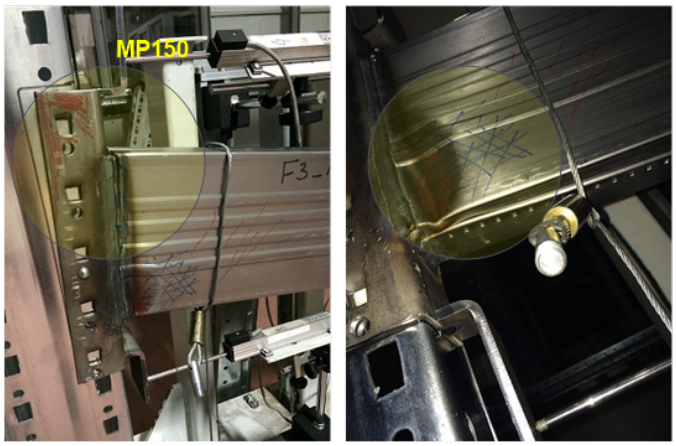

Figure 3.23. Failure Modes in Monotonic Tests on MP150 Specimens.

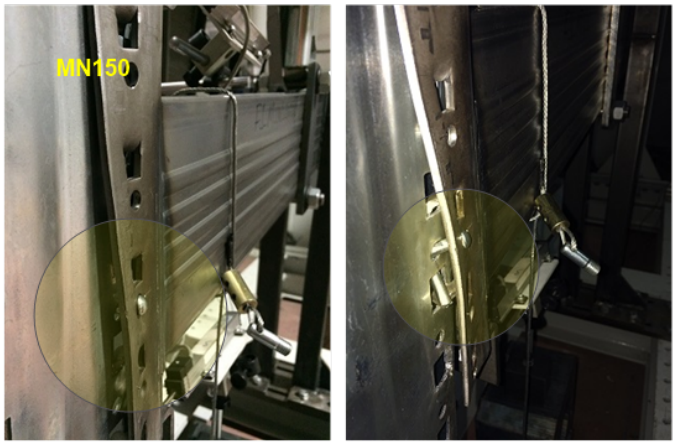

Figure 3.24. Failure Modes in Monotonic Tests on MN150 Specimens.

3.2.8. B150 Moment-Rotation Curves

Figure 3.25 exhibits moment-rotation curves for BP150 and BN150, bottom connected 150mm beam into end-connector under positive and negative bending moments. All yield strength, initial stiffness, and ultimate strength values under negative bending are approximately 31% lower than positive bending specimen. The ductility levels are similar about 1.9 at both cases. 32% difference in between positive and negative directions can be explained observing the following Figure 3.26 presenting typical failure modes observed during the monotonic tests. The failure mode of BN150 specimen subjected to negative bending was the tearing of the bottom hooks and coming out of the hole. The hooks started approaching toward the edge of the upright perforation and getting in full contact with that surface. The lowest hooks rotated around and cracks took placed. It was come out despite existing the safety bolt. During the test, the safety bolt was occasionally controlled; it was in full tension while the lowest hook crashed due to the cracks. The safety bolt did not collapse however changed the performance of the joint since it contributed to overall strength and stiffness.

The end-connector was completely distorted and failed as shown in Figure 3.26. In BN150 the upright was not distorted and remained almost fully straight during the tests. However, the straight position of the upright changed and bended at BP150 specimen subjected to positive bending. The failure mechanism in the case of BP150 was governed by global distortional buckling of the upright at joint region, local distortional buckling in the web of the beam, distortion of the end-connector and also tearing of the top hooks sequentially. Safety bolt played no crucial role in the failure mode of the joint because no tension or shear was on the bolt.

BP150 can be classified as a good example of the joint since almost all parts forming the joint contributes to joint strength and stiffness. A full bonded compression-only contact took place in between the bottom of the end-connector and flange of the upright which increased the rigidity of the joint. Contrary to BP150, the performance of BN150 was not governed by all parts of the joint. Unsymmetrical behavior was observed under positive and negative bending moments. The joint would not be a

correct selection for seismic design.

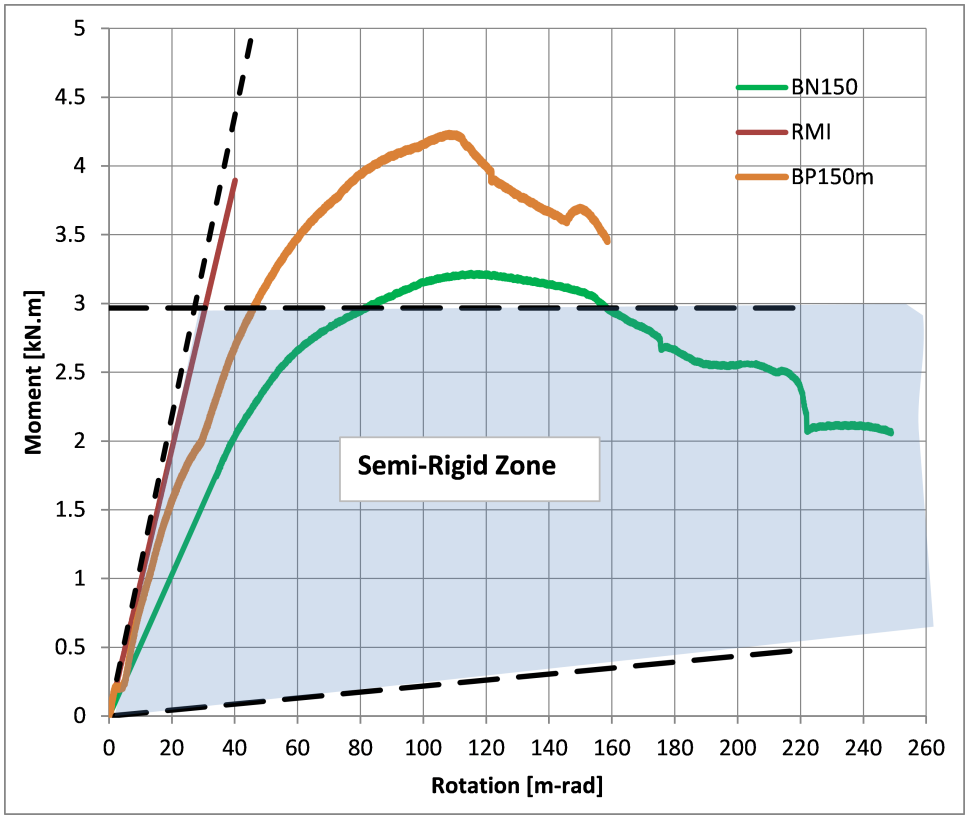

Figure 3.25. Comparison of the Moment-Rotation Curves for BP150/BN150.

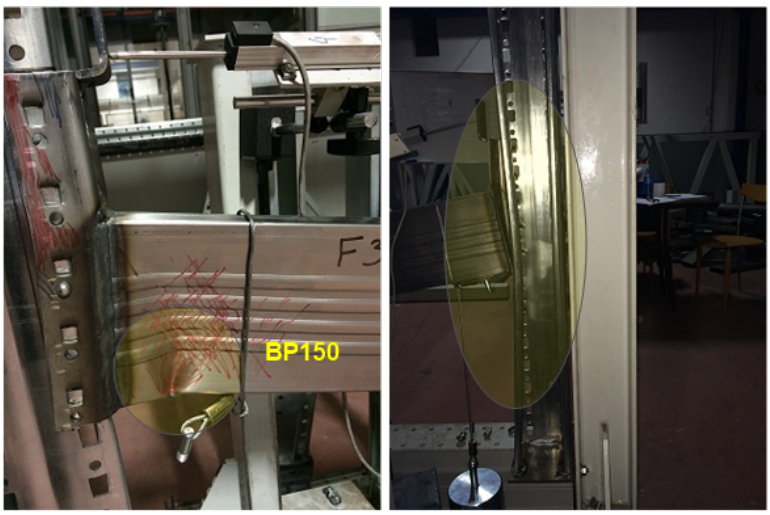

Figure 3.26. Failure Modes in Monotonic Tests on BP150 Specimens.

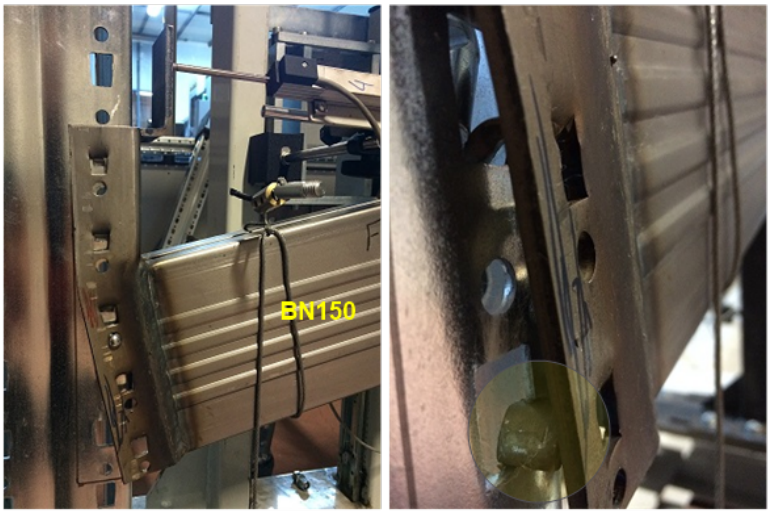

Figure 3.27. Failure Modes in Monotonic Tests on BN150 Specimens.

3.3. Reversed Cyclic Test Results

All the specimens tested by monotonic procedures were subjected to a symmetrical reversed cyclic displacement history. Cyclic tests were performed as displacement-controlled by using the yield displacement information taken by monotonic tests. Since monotonic tests were applied under positive and negative bending directions thereby two different yield displacement were obtained. Therefore, the lowest yield displacement was used in applying reversed cyclic tests and displacement history was expressed in terms of imposed displacement ductility evaluated in monotonic test. All tests were performed with reference to recommendations proposed by ATC-24 (1992). Loading cycles were repeated at least three cycles for every displacement within elastic and inelastic range. The cyclic effect was applied by the load cell at the end of the cantilever beam by pull and push forces started by low amplitude toward large ones. Load was applied step-wise, gradually and controlled. The seismic behavior of beam-to-upright connections is not similar to that of semi-rigid steel connection because the joint rotates only in steel tests however it translate in vertical direction in addition to rotation. The quantity of vertical displacement and slackness of the connection is shown in Figure 3.29. The joint during the slackness owns no stiffness and generally occurs during interchanging the positive bending into negative. Between hook and the upright minor gaps occur and the interlock position is not valid during this position. The safety bolt

immobilizes end-connector and prevents further distraction.

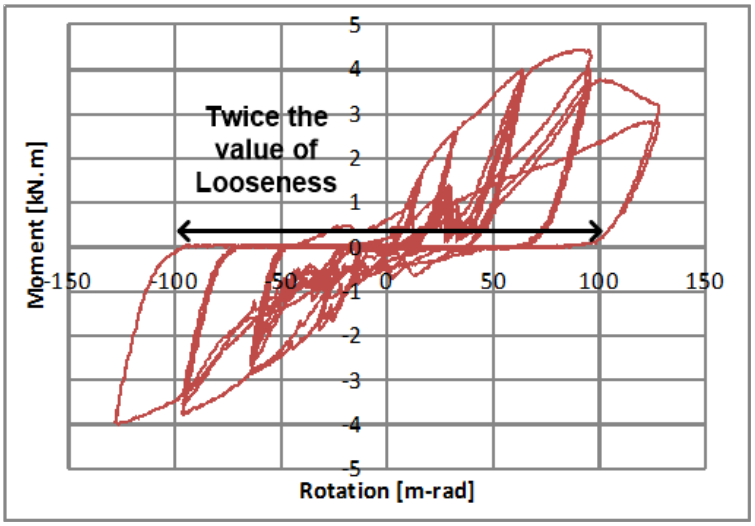

Figure 3.28. Twice the Value of Looseness Occurred in Reversed Cyclic Tests.

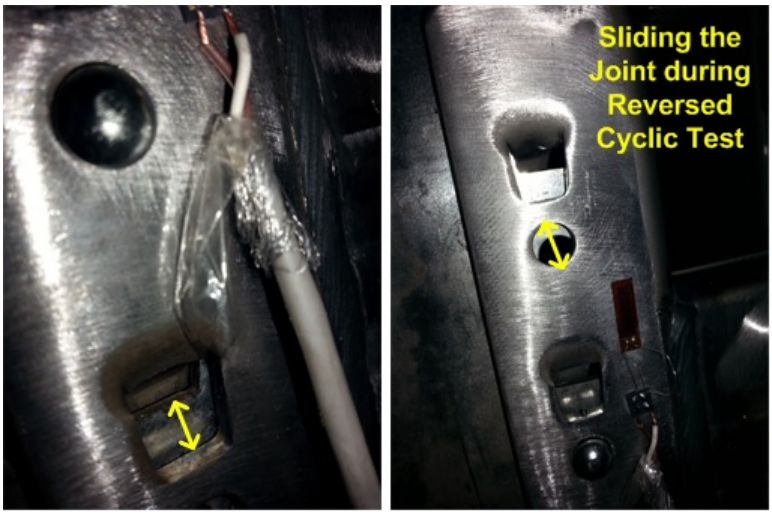

Figure 3.29. Sliding and Looseness of Joint During Test.

3.3.1. T140 and B140 Reversed Cyclic Tests

Figure 3.30 presents the hysteresis loops for specimen TC140. The initial rotational stiffness does not match under negative bending moment with the one obtained in TCN140. The initial stiffness carried out in reversed cyclic test is clearly lower about 30% than monotonic test. In the beginning it was correlated to the test set-up, however after repeating three times, it was understood that in all cyclic tests the initial stiffness

under negative bending is lower than monotonic results. In BC140 and MC140 this difference was not that much. It can be explained by completely non symmetric configuration of T140 joint and the start phase of reversed cyclic test in TC140. The test was performed by 8mm displacement downward as target point, when the specimen reached -8mm the next target point was +8mm upward. The interchanging point from downward to upward moment was not remain at start position due to the sliding in joint which caused minor gaps in between hooks and upright. The gap might reduce the initial stiffness. Apart from initial stiffness, other parameters like yield strength and ultimate strength fulfill with monotonic results. The ductility level under positive bending in cyclic test is 22% lower than in monotonic test. The reduction in rotational capacity might be due to progressive collapse in cyclic test. The hooks were crashed from both edge sides in cyclic test, but only one side adjacent to upright hole in monotonic test. In other words, the collapse occurred in negative bending governed the overall collapse of the joint, thus the specimen could not reach the ultimate rotation of positive monotonic test and failed. The performance ofTC140 and BC140 were close and the approach was same since they were mirror connection from the middle of end-connector.

Figure 3.31 shows the hysteresis loops in terms of moment-rotation, for the cyclic test performed on beam-to-upright connection with 140mm beam and bottom welded into end-connector (B140). The cyclic test shows practically the same initial rotational stiffness for both positive and negative monotonic bending. The strength of the joint dropped through the loops of the hysteresis, in other words strength deterioration took place for rotations larger than 50 m-rad in the case of positive bending. The same deterioration is observed under negative bending for rotations larger than 75 m-rad. Hysteresis loops are unsymmetrical that might be result from unsymmetrical connection detailing, bottom connected beam to end-connector. Load carrying capacities - ultimate strength - excessively differ 30% from positive to negative bending. Total number of cycles is 10 for BC140, the last cycles was recorded at fully collapse position. The observed collapse mechanisms were the same as in monotonic tests. In all reversed cyclic tests performed according to ATC-24, each cycle was repeated for three times. At least 2 different cycles were applied before yield displacement cycle. In the first

round of every cycle a significant amount of the energy was deteriorated and energy was released, in sequence the second and third loops of a cycle a gradually deterioration of the energy dissipation capacity was observed. In other word, the second and third loops of that cycle did not have any influence on the joint and no energy was released because the joint rotated free on that cycles. The first distortion at cyclic loading occurred at top hooks. Similar to positive bending of monotonic test, top hooks replaced toward the edge of the perforation of upright, interlocked completely and retained in place, and then cracks took place on the surfaces of the hooks in further cycles which result in falling down of the hooks. All cyclic tests were started by applying load downward - positive bending. From the beginning of BC140 test, slackness and looseness occurred in the joint; therefore, stiffness degradation could not be determined precisely. Since, the joint encountered new resistance coming from a different part of the joint at each new cycle. For instance, in the beginning hooks made the stiffness contribution to the joint and distorted, then the end-connector contacted into the upright and even punched through. At reversal cycles, the end-connector touched the upright push it and then moved away, which caused a significant gap as shown in Figure 3.33: Failure modes of BC140. An important result carried out from reversed cyclic test was the sequential strength and stiffness contribution of different parts in the joint. Despite the fact that the same sequential collapse occurred in monotonic tests, it was much more obvious in cyclic tests. In addition, the looseness failure could not be observed in monotonic tests as detailed as cyclic tests.

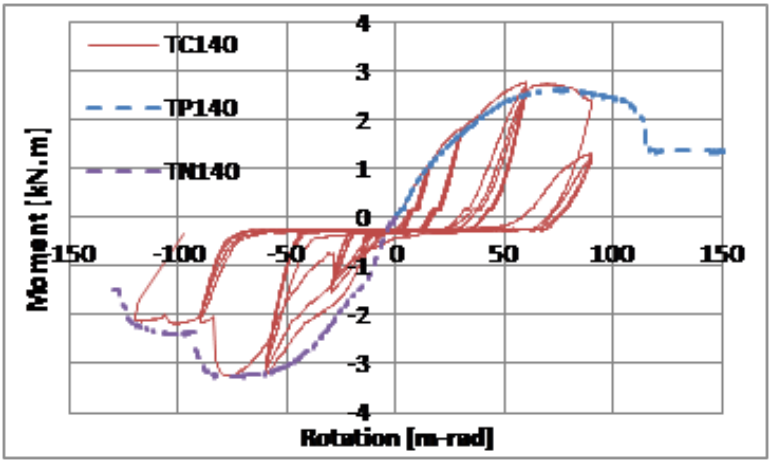

Figure 3.30. Comparison of Monotonic and Cyclic Moment-Rotation Curves for T140 Beam.

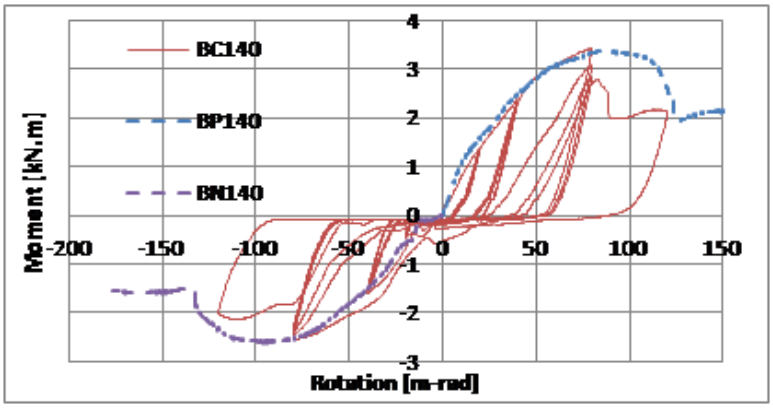

Figure 3.31. Comparison of Monotonic and Cyclic Moment-Rotation Curves for B140 Beam.

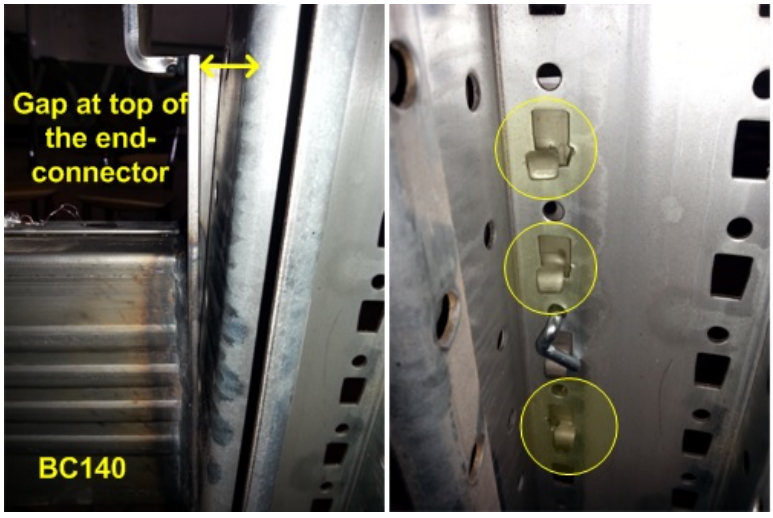

Figure 3.32. Failure Modes of BC140 - Gap at Top of the End-Connector.

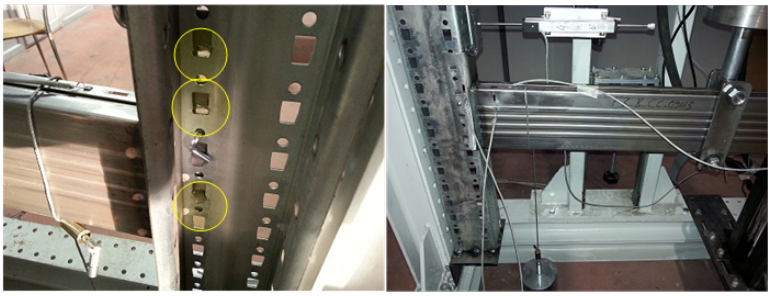

Figure 3.33. Failure Modes of BC140 - Tearing at Tabs.

Effect of beam middle connected to end-connector on hysteresis is presented in Figure 3.35. Monotonic test results under positive and negative bending are also shown

to make comparison. The yield displacement used for composing displacement history was the minimum value of yield displacements calculated in positive and negative monotonic tests, which was 40 mm. 8 full cycle and a half cycle took place for MC140 specimen, after 8th cycle the specimen failed and the measurement devices were out of the record. Collapse of the connection was attained approximately under the first cycle of cycles just after yield displacement. Hysteresis loops almost symmetric for MC140, with similar maximum value of positive and negative moments and their corresponding rotations. Initial rotational stiffness is lower than the one obtained in monotonic test in both directions. The level of ductility is almost the same under positive bending but much lower in negative direction. In overall, the response of the MC140 specimen is nearly symmetric; little non symmetry is due to the reaction of inclined hooks under downward and upward moments, which can be explained by gravity effect on the connection. It must be noted that during the reversed cyclic test of MC140 the beam reclined toward adjacent out-of-plane restraint device just after reaching the yield displacement as shown in Figure 3.37. The out-of-plane movement of the beam is a matter of stability, since the beam did have adequate rigidity to remain straight in plane and also no rigidity was available in the joint for transferring the load into the upright. The cyclic test was started by applying load downward up to 5 mm displacement as the first target point. The test procedure was displacement-controlled so all target displacements for each cycle were calculated considering monotonic results. Slackness failure was also observed in MC140, contrary to BC140 and TC140 the looseness was lower in MC140 witch might be because of symmetric configuration of MC140. The performance of inclined hooks was not different, translating toward upright edge perforation, crashing and tearing up and finally falling down. The top first and the second hooks were completely crashed and fallen under positive bending and the bottom first hook fallen down in negative bending moment of reversal loading. All failure modes were observed and noted thanks to slow displacement-controlled, the speed of all cyclic tests was adjusted to 0.0833 mm/s.

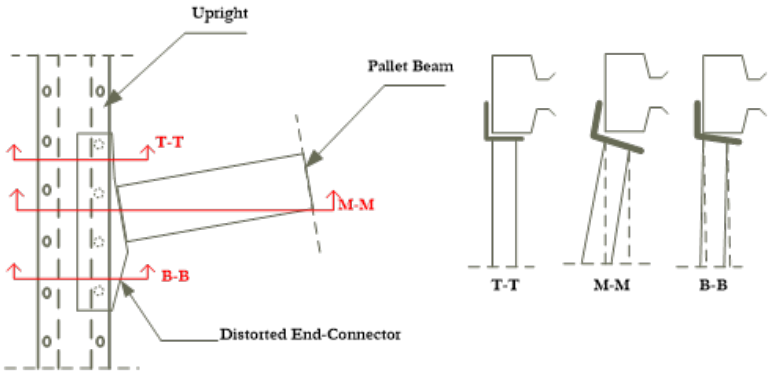

Figure 3.34. Schematic of Connection Kinematics and Out-of-Plane Failure.

The failure modes of MC140 joint were essentially because of weak performance of hooks and result of that on end-connector distortion. The safety bolt was not in tension and did not influence joint performance. Basically, the reason why cracks form on hooks could be observed and clearly understood in MC140. The out-of-plane instability of the beam was a result of insufficient joint rigidity for keeping the beam in plane as shown in Figure 3.34. The joint might be assumed symmetric along vertical direction, however it is fully non symmetric along horizontal plane. Non symmetrical configuration of joint caused asymmetrical internal force distribution in joint especially along horizontal plane. In addition to non-symmetric configuration, sliding along horizontal and mostly along vertical direction caused looseness in joint which made the joint from a steady static position into non-controlled dynamic position. Replacement caused many contacts in between the surfaces. Various types of contacts took place like as compression-only bonded, frictional and frictionless.

It was noticed that the crack on 2.5mm thick hooks started from the edge side, the surface in contact with the upright. However, the bottom surface which was also in contact with upright, affected by shear and compression forces. The crack on steel elements mostly forms because of tension forces. However, in this case the side of the hole is punching through the curved part of the hook. For example, when a nail is punched in a soft element, the crash occurs in contact region. The same can be explained herein, with a minor difference. Fixed part in this action is side of the hole and the moving part is hook. The friction on the surfaces of the hook caused

accumulating the energy on those parts. Tearing and crashing mechanisms of the fallen down hook were analyzed in laboratory and also by numerical finite element methods in next chapter.

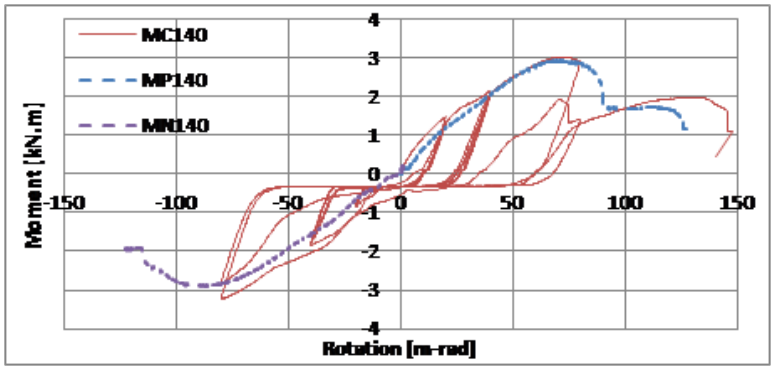

Figure 3.35. Comparison of Monotonic and Cyclic Moment-Rotation Curves for M140 Beam.

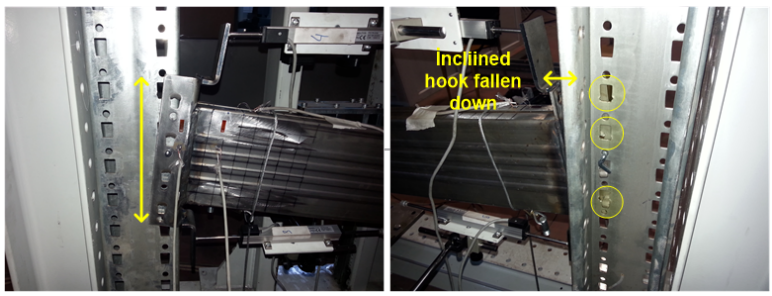

Figure 3.36. Collapse Modes in MC140 - Distorted End-Connector.

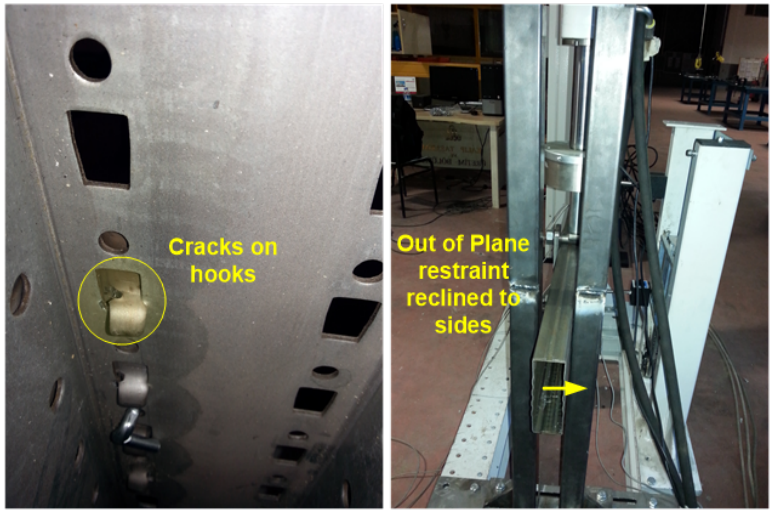

Figure 3.37. Collapse Modes in MC140 - Cracks in Tabs.

3.3.2. T150 and B150 Reversed Cyclic Tests

In the second series of cyclic tests, the number of inclined hooks was increase from four to five thereby the depth of end-connector increased from 210mm into 240mm. the depth of pallet beam raised up from 140mm into 150mm. Apart from these major modifications, all remaining parts were similar to DD140 tests.

Figure 3.38 presents the hysteresis loops in terms of moment-rotation, for the cyclic tests performed on beam-to-upright connections specimens with B150. Figure 3.39 also presents the hysteresis behavior of T150. Non symmetric behavior is noticed at both tests. The rotational capacity under positive bending is about two and half times that under negative bending in the case of B150 and this is about one and half times in the case of T150. The ductility levels differ for the cases. The ductility level under positive bending in monotonic test and cyclic test of B150 and T150 are approximately overlapped. However, there is great difference under negative bending in B150 test. The web of pallet beam was distorted when the specimen reached third cycle of yield displacement. The buckling in beam caused instability of the joint and the stiffness reduced. The ultimate strength was also affected because of instability in the web. Thus, the specimen could not carry any additional forces. This might be a explanation of high difference in ductility level between monotonic and cyclic tests of BC150.

The range of looseness of T150 and B150 are lower than that in D140 tests. Since, DD150 tests have high stiffness and strength due to higher number of inclined hooks and deeper pallet beam and end-connector.

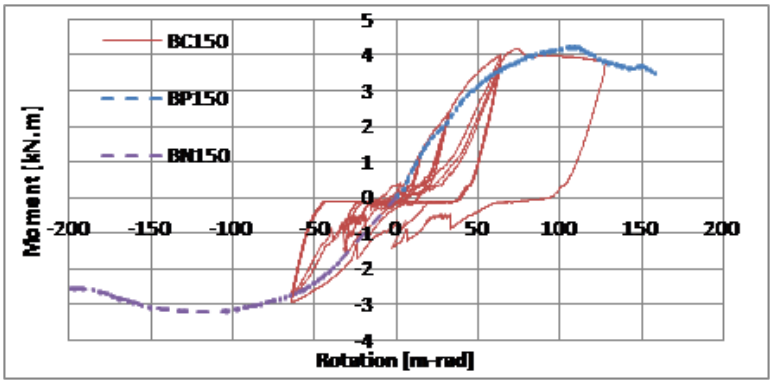

Figure 3.38. Comparison of Monotonic and Cyclic Moment-Rotation Curves for B150 Beam.

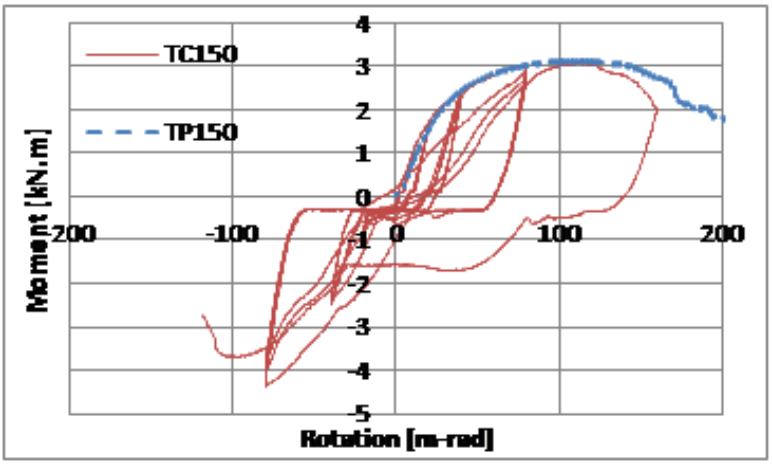

Figure 3.39. Comparison of Monotonic and Cyclic Moment-Rotation Curves for T150 Beam.

Before starting tests, the shade lines of the end-connector were drawn. During the test the replacement of the end-connector was controlled by LVDT's and visualize by shade lines. At both BC150 and TC150, the end-connectors replace horizontally and vertically. The safety factor prevented larger replacement which resulted in tension forces in the bolt. The stress magnitude was measured by strain-gauge devices at critical regions to be used in numerical analysis.

The failure mode of BC150 was similar to failure modes occurred on monotonic tests. Top hooks was collapse due to propagation crack mechanisms on the side and bottom surfaces of hook, precisely in the surfaces in direct contact with the sides

of perforation in the upright. The sharp sides of the perforations punched through the hook and penetrated through. As it was stated in previous section, the reason of crashing out of the hooks might not be tension forces but also penetration of the sharp sides. In addition to tearing of the hooks, distortional buckling of pallet beam was also observed in BC150 tests. This was occurred simultaneously to distortion of end-connector. The end-connector was fully deformed and resulted in out-of-plane instability in joint and beam.

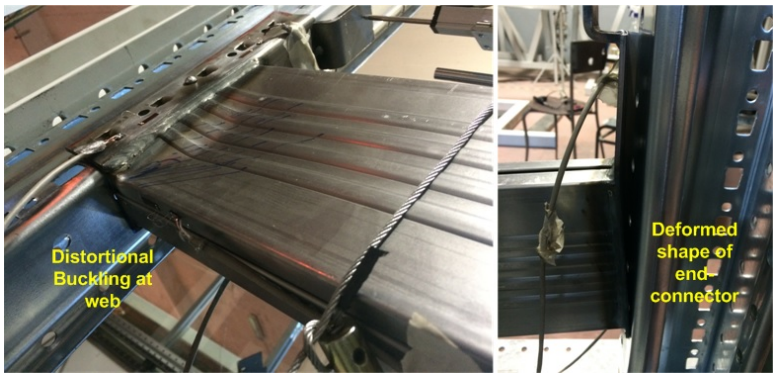

Figure 3.40. Collapse Modes in BC150.

Collapse mechanism in TC150 case was due to deformation of the end-connector, to punching of the safety bolt through outside and deformation of the hook at the top and at the bottom as shown in Figure 3.41. The second and the fourth hooks were partially deformed and the middle hook remained undeformed. Assuming the neutral axis of the beam as the neutral axis of the joint which is not symmetric, under positive and negative bending moments, top and bottom of the neutral axis imposed to reversal compression and tension stresses. When the top is in tension a gap formed in top and the hooks yields sequentially mostly started from the top. On the contrary, the bottom of the joint imposed to compression and the interior surface of the end-connector in full frictional contact with the exterior surface of the upright. The influence of hooks at the case of compression is minor to overall joint stiffness. However, shifting from compression state into tension state caused cracks and tearing of the hooks. This reversal behavior continued until fully collapse of the top and the bottom hooks as shown in Figure 3.41. The top hook came out of the perforation and completely rotated and distorted but not fallen down. The end-connector was also

fully collapsed when the test reached the ultimate rotational capacity under positive bending and resulted in higher ductility level than negative bending.

Figure 3.41. Collapse Modes in TC150.

3.3.3. M150 Reversed Cyclic Tests

Effect of DD150 beam middle connected to end-connector on hysteresis form is presented in Figure 3.42. Monotonic test results under positive and negative bending are also shown to make comparison. The yield displacement used for composing displacement history was the minimum value of yield displacements calculated in positive and negative monotonic tests, which was 40 mm. 14 full cycle and a half cycle took place for MC150 specimen, after 12th cycle the specimen failed and the measurement devices were out of the record. Hysteresis loops were almost symmetric for MC150,

with similar maximum value of positive and negative moments and their corresponding rotations. Initial rotational stiffness is lower than the one obtained in monotonic test in negative direction. The level of ductility is almost the same under positive bending but much lower in negative direction. In overall, the response of the MC150 specimen is nearly symmetric. MC150 was the only test that fracture failure was occurred. In addition to tearing of hooks, distortional buckling of end-connector and pallet beam, fracture of top flange was a new mechanism encountered in reversed cyclic tests. Considering the weld application on the end-connector, the top flange was not welded into the end-connector. Making weld at top flange might result in better performance and the fracture might be diminished from failure modes of the joint. This type of mechanism was not observed in monotonic tests. The influence of safety bolt was crucial at MC150. An important outcome can be carried out from MC150, deeper beam and deeper end-connector increased joint rigidity and the ultimate collapse mode was shifted from joint region toward beam region. This can be interpreted by weak beam and strong column essential to compose the plastic hinge on beam. So far, the plastic hinge allocation was generally at joint area instead being in beam.

The secondary elements of the end-connector as a primary element are inclined hooks and the safety bolt, it was observed from tests as shown in Figure 3.43, that end-connector was not deformed as much as end-connectors of former tests. However, the hooks yielded and even rotated, and also the safety bolt came out of the original plane. The contribution of the secondary elements caused high stiffness and strength of end-connector as a whole. Concurrently, the end-connector is the major part of the joint. The performance of the end-connector governed the overall performance. High performance and contribution of hooks and safety bolt caused low deformation in end-connector and obligated the energy accumulation toward the beam. Thus, the hinge took place in the beam which is a desirable performance for design. MC150 exhibited symmetric behavior and at the same time the configuration is almost symmetric, the hinge allocation was also a desirable factor, the monotonic curves overlapped with reversed cyclic hysteresis, all these results can be counted as advantage for MC150. In elastic design MC150 might be a convenient joint for resisting against gravity and seismic forces.

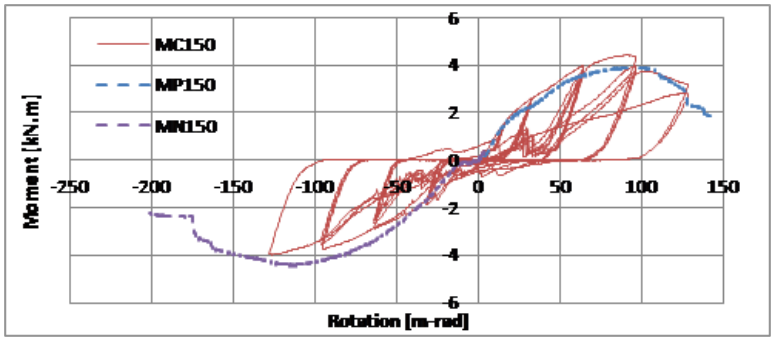

Figure 3.42. Comparison of Monotonic and Cyclic Moment-Rotation Curves for M150 Beam.

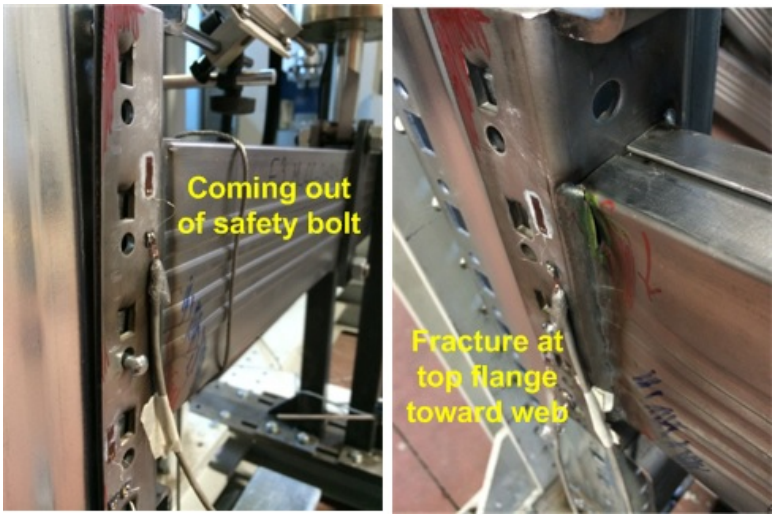

Figure 3.43. Collapse Modes in MC150.

4. ANSYS MODEL OF BEAM-TO-UPRIGHT CONNECTION

Structural analysis is the most common application of the finite element method. The primary unknowns (nodal degrees of freedom) calculated in a structural analysis are displacements. Other quantities, such as strains, stresses, and reaction forces, are then derived from the nodal displacements. A three-dimensional finite element model of the full-scale specimen was created to simulate the test set-up shown in the figure Figure 4.1. The static step-wise loading analysis independent of time can be performed for this model. The finite element model was developed using the commercial finite element software "ANSYS". The preliminary model to be used in "ANSYS" was developed in "SOLIDWORKS" software and plug into "ANSYS" for analysis. There are a few investigations on semi-rigid connections both theoretically and experimentally, theoretical studies have used simplified yield-line mechanisms or finite element techniques. Almost whole relevant studies have been concerned with bolted connections. There are a few studies on boltless connections reported in the literature, even no FE model on this type of connection.

The end boundary conditions at the two ends of upright are fully restrained and the pallet beam is out-of-plane restrained at the near end far from the upright. Nonlinear structural behavior arises from a number of causes, which can be grouped into three principal categories explained in following sections.

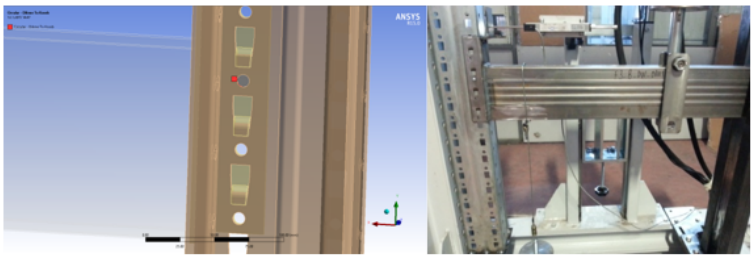

Figure 4.1. Finite Element Model Developed in ANSYS.

4.1. Background

In the past, researchers have investigated various different types of connectors used in rack structures. Baldassino and Bernuzzi (2000) have given the influence of beam-to-upright joint modeling on the overall frame response in their numerical study. Bernuzzi, and Castiglioni (2001) carried out some experiments on the behavior of flexible connections, when subjected to cyclic reversal loading and investigated the effect of joint performance on the overall frame response. Bajora and Talikoti (2006) carried out double cantilever tests and compared the results with nonlinear finite element analysis. This paper claims far superior result in double cantilever tests than conventional single cantilever tests, because flexibility of the connector was close to the full scale frame test in double cantilever test.

4.1.1. Changing Status

Many common structural features exhibit nonlinear behavior that is status-dependent. For example, a tension-only cable is either slack or taut; a roller support is either in contact or not in contact. Status changes might be directly related to load or they might be determined by some external cause. Situations in which contact occurs are common to many different nonlinear applications. Contact creates a distinctive and important subset to the category of changing-status nonlinearities.

4.1.2. Geometric Nonlinearities

If a structure experiences large deformations, its changing geometric configuration can cause the structure to respond nonlinearly. An example would be the fishing rod. Geometric nonlinearity is characterized by “large” displacements and/or rotations.

4.1.3. Material Nonlinearities

Nonlinear stress-strain relationships are a common cause of nonlinear structural behavior. Many factors can influence a material’s stress-strain properties, including

load history, environmental conditions, and the amount of time that a load is applied.

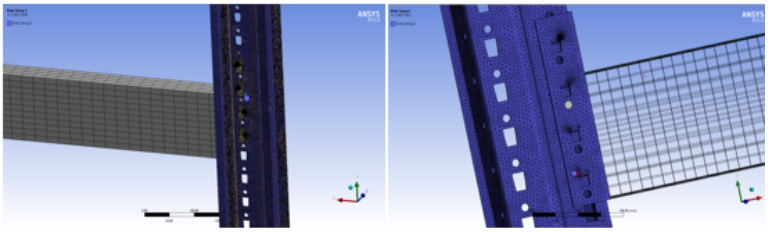

Figure 4.2. Finite Element Model - Mesh Elements.

"ANSYS" employs the "Newton-Raphson" approach to solve nonlinear problems. In this approach, the load is subdivided into a series of load increments. The load increments can be applied over several load steps. Before each solution, the "Newton-Raphson" method evaluates the out-of-balance load vector, which is the difference between the restoring forces and the applied loads. The program then performs a linear solution, using the out-of-balance loads and checks for convergence. If convergence criteria are not satisfied, the out-of-balance load vector is re-evaluated, the stiffness matrix is updated, and a new solution is obtained. This iterative procedure continues until the problem converges. If convergence cannot be achieved, then the program attempts to solve with a smaller load increment (ANSYS 2012).

The arc-length method causes the "Newton-Raphson" equilibrium iterations to converge along an arc, thereby often preventing divergence, even when the slope of the load vs. deflection curve becomes zero or negative.

4.1.4. Substeps

When using multiple substeps, to achieve a balance between accuracy and economy: more substeps usually result in better accuracy, but at a cost of increased run times. Automatic time stepping adjusts the time step size as needed, gaining a better balance between accuracy and economy.

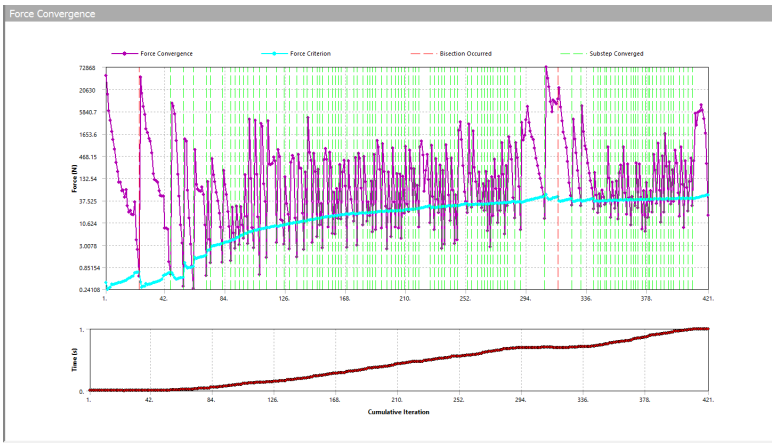

Figure 4.3. Convergence Result for Beam-to-Upright Connection.

In large displacements, the loads applied to the system maintain constant direction no matter how the structure deflects. In other cases, forces will change direction, "following" the elements as they undergo large rotations. Surface loads always act normal to the deflected element surface, and can be used to model following forces.

4.1.5. Stress-Strain

In large strain solutions, all stress-strain input and results will be in terms of true stress and true or logarithmic strain. For small-strain regions of response, true strain and engineering strain are essentially identical. To convert strain from small or engineering strain to logarithmic strain, ln= ln $(1 + \varepsilon_{eng})$. To convert from engineering stress to true stress, σ_{true}= $\sigma_{eng}(1 + \varepsilon_{eng})$ were used.

The samples of tensile tests were taken from normal production of manufacturer for the purpose of estimating the nominal yield stress. All processes of preparing the tensile tests were performed in accordance with the specified requirements in "ASTM E8 Standard Test Methods for Tension Testing of Metallic Materia" (ASTM 2000).

4.1.6. Finite Element Simulation of the Cantilever Test

An automatic testing machine with a maximum capacity of 50 kN was used for the loading. An extensometer was employed to monitor the deformation. Strain gauges were installed on selected tensile coupons at the center, and on both sides, to verify the modulus of elasticity, E. Autographic diagram method for the materials exhibiting discontinuous yielding were employed as method for yield strength determination. The yield stress - f_y -can vary greatly across the test series. The large variation in f_y complicates comparisons across the test database, but it is important to recognize this variation, as f_y for the test coupons of the upright varied from 330 to 505 MPa and for the end-connector from 210 to 480 MPa. E of 205 MPa is assumed for all of the members. This is supported by limited testing on 1.2 mm and 2.5 mm tensile specimens from the pallet beam and upright, which had an average E of 203 MPa.

Plasticity is a non-conservative, path-dependent phenomenon. In other words, the sequence in which loads are applied and in which plastic responses occur affects the final solution results. If plastic response is anticipated in the analysis, loads shall be applied as a series of small incremental load steps or time steps, so that the model follows the load-response path as closely as possible. One of the main challenges in modeling the response of this type of connection is the presence of various types of contacts in between the surfaces. In experimental phase of the study it was observed the moment-rotation behavior of connections was dominated either by flexure in the beams or by tearing of taps of the end-connector. FE models presented herein incorporate geometrical nonlinearities and multilinear isotropic material nonlinearity properties obtained from tensile coupon tests.

The geometry, boundary conditions, restrained supports and loading in FE model were developed to the cantilever experiments as much close as possible using advanced contact properties of ANSYS software. Since the cold formed sections are very thin elements and exposed to local buckling, for accurate modeling both shell element and solid element were investigated and compared. Due to complex contact surfaces in between end-connector and upright and the curved shape of taps and geometrical

difficulties all members were modeled using Solid element in ANSYS, however this type of modeling is equivalent to long running time. Contact problems are highly nonlinear and require significant computer resources to solve. It is important to understand the physics of the problem and take the time to set up a model to run as efficiently as possible. Contact problems present two significant difficulties. First, the regions of contact are unknown until running the problem. Depending on the loads, material, boundary conditions, and other factors, surfaces can come into and go out of contact with each other in a largely unpredictable and abrupt manner. Second, most contact problems need to account for friction. There are several friction laws and models to choose from, and all are nonlinear. Frictional response can be chaotic, making solution convergence difficult.

The pallet beam is welded into the end-connector, the connection in between these two members was assumed as totally bonded since beam stand completely rigid into end-connector with no relevant rotation to end-connector. The contact between the end-connector's inside surface and uprights' outside surface is frictional contact surfaces. To simulate the interaction between the taps and upright, frictional and frictionless surface to surface and edge to surface contact algorithms were used. The converged model contained approximately 400,000 elements and one and half day run-time.

The experimental works showed that the behavior of the connection was primarily governed by the rotation of the end-connector and the ultimate phase is occurred after yielding the taps. The failure mechanism is tearing the tabs through the upright. Therefore, the tabs of the end-connector govern the extent of the rotation. The pallet beam was subjected to a point load 500mm from the upright face. When the load started to apply the gap in between the end-connector and the upright and gap in between the sides of tabs and slots were closed. This action caused the frictional contact in between the end-connector and upright face to become active in the FE model. The bottom of tabs was also in contact with the slots edge. The rest of the contacts were initially not active. As the load is increased the connector distorts and eventually the face of the connector comes into contact with the upright and the other

contacts were involved in the analysis. Due to existence of minor gaps between contact surfaces, the pinball property with various radius of pinball was used in between the surfaces. Pinball radius is an imaginary radius to make fine mesh at such regions.

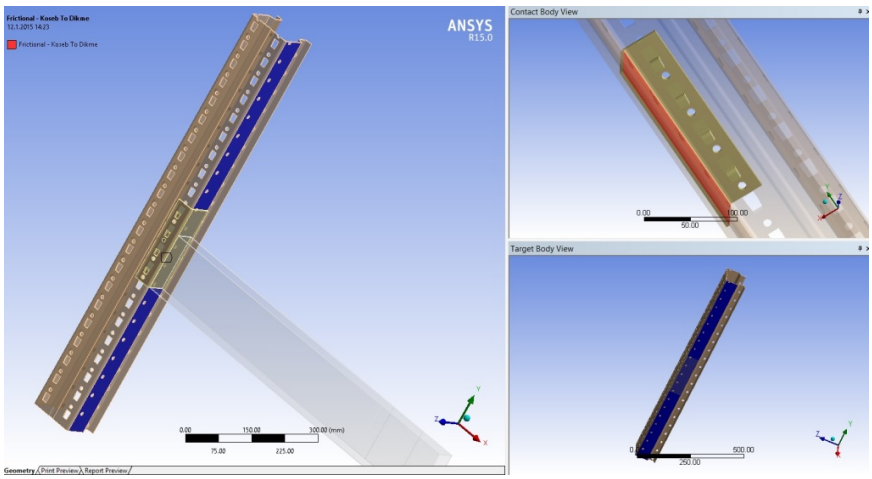

Figure 4.4. Frictional Contact Between Interior Face of End-Connector and Exterior Face of Upright.

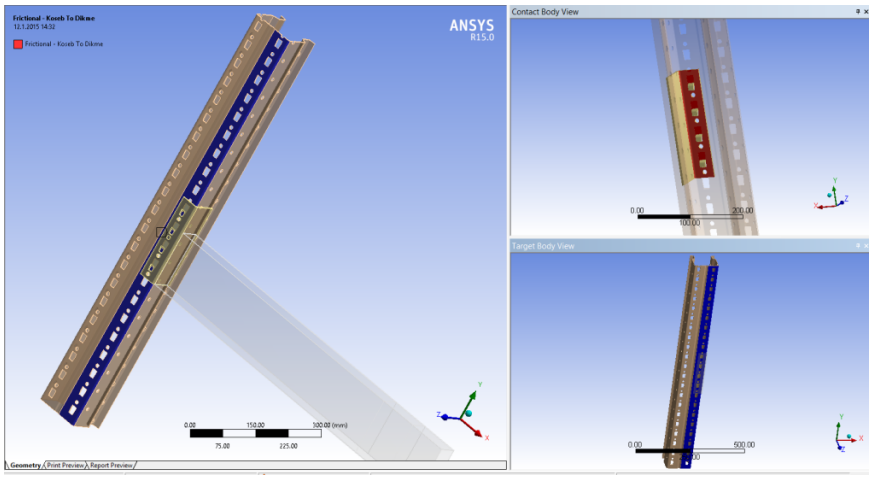

Figure 4.5. Frictional Contact Between Interior Face of End-Connector and Exterior Face of Upright.

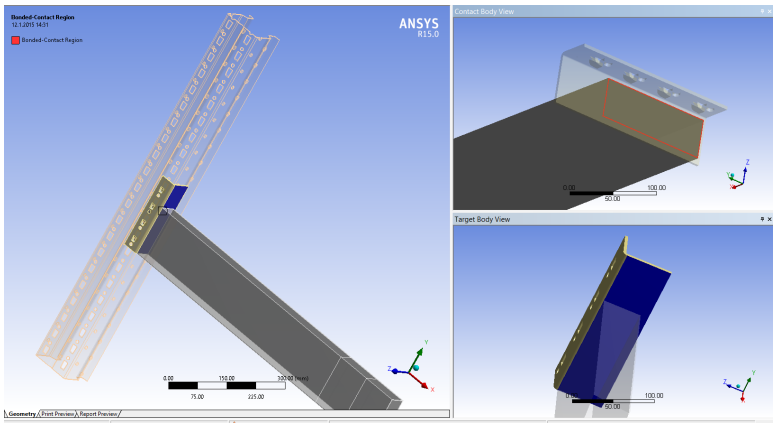

Figure 4.6. Bonded Contact Between Cross Sectional Face of Beam and End-Connector.

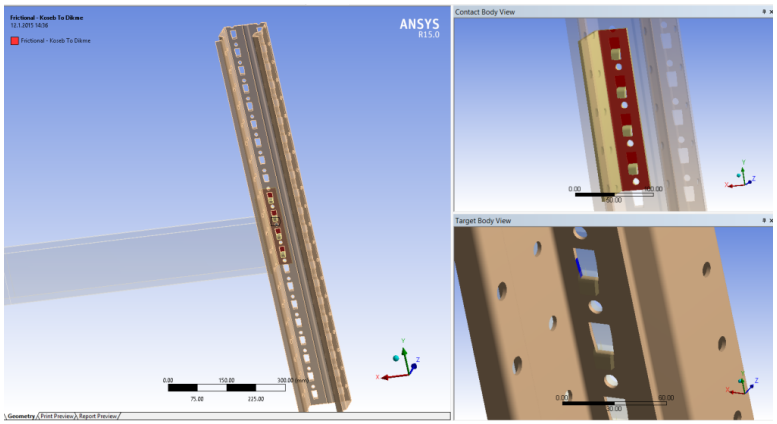

Figure 4.7. Frictional Contact Between Interior Face of End-Connector and Side Edge of Upright at Right Side of the first Tap.

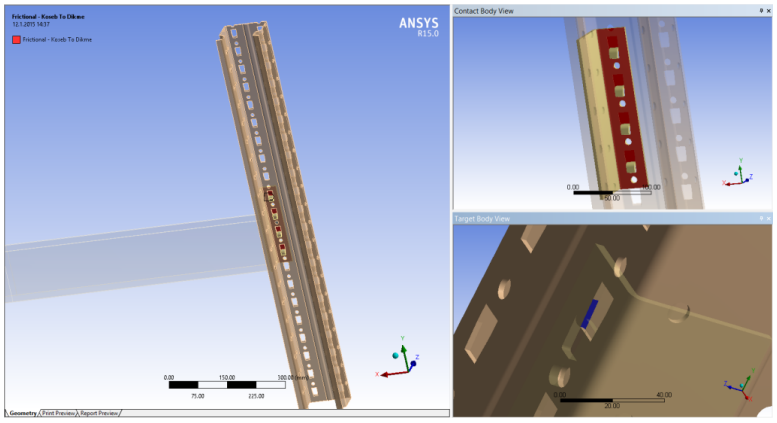

Figure 4.8. Frictional Contact Between Interior Face of End-Connector and Side Edge of Upright at Left Side of the first Tap.

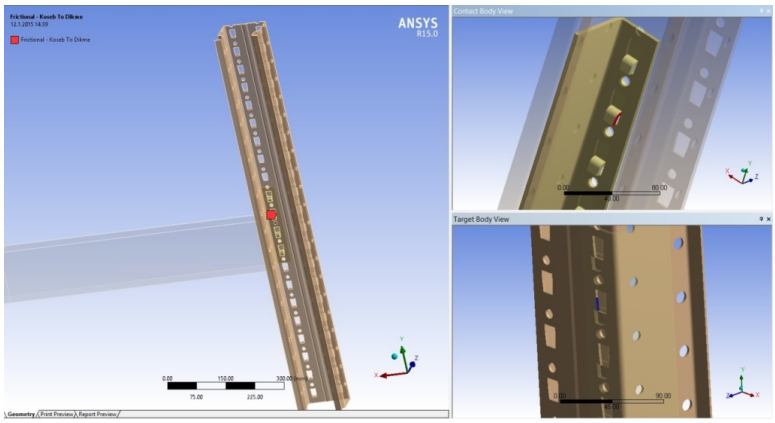

Figure 4.9. Frictional Contact Between Right Edge Side of the first Tap and Associated Edge of the Slot in Upright.

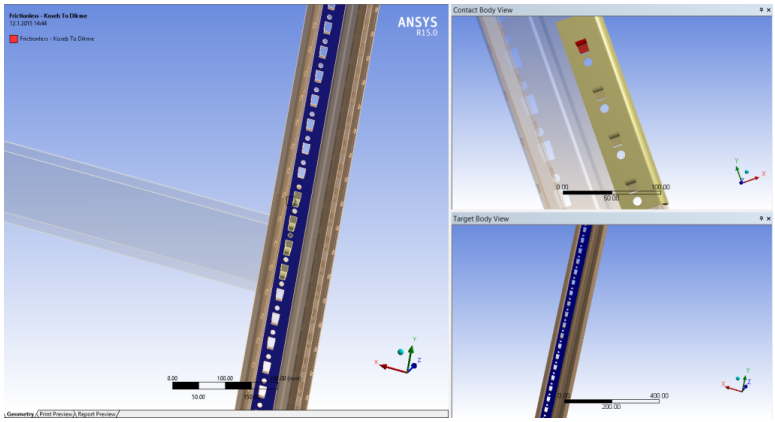

Figure 4.10. Frictional Contact Between Bottom Face of the first Tap and Associated Interior Surface in Upright.

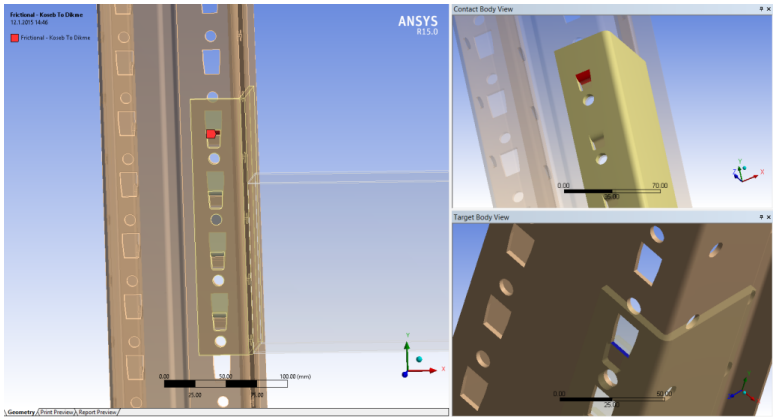

Figure 4.11. Frictional Contact Between Bottom Face of the first Tap and Support Edge Surface of Upright.

4.2. Analysis Results of ANSYS Software

Von mises stress theory is widely used by designers as a tool to present their results. This theory is more realistic and accurate into normal stress theory. Normal stress theory is used for interpreting tensile test results. Yield stress and ultimate stress level results in normal stress theory are the results derived from unidirectional loading on specimen. However, Von mises is used in determining whether an isotropic and ductile material will yield when subjected to a complex loading condition different than unidirectional loading. This is accomplished by calculating the von Mises stress and comparing it to the material's yield stress, which constitutes the "Von Mises Yield Criterion". The objective is to develop a yield criterion for ductile metals that works for any complex 3-D loading condition, regardless of the mix of normal and shear stresses.

The Von Mises stress does this by degrading the complex stress state down into a single scalar number that is compared to a metal's yield strength, also a single scalar numerical value determined from a uniaxial tension test on the material in a lab. The developed model for finite element analysis is a boltless semi-rigid connection. A plastic nonlinear three-dimensional analysis of the connector was made and the results are shown herein. The effects of different boundary conditions were investigated and compared with experimental results to be considered the optimal boundary condition in finite element analysis. The contacts are important in defining the hypothesis of the joint in the finite element model. The first definition is angled end-plate connector welded to end of the pallet beam. The weld is groove type all around the beam webs and top flange. The weld was defined as bonded contact.

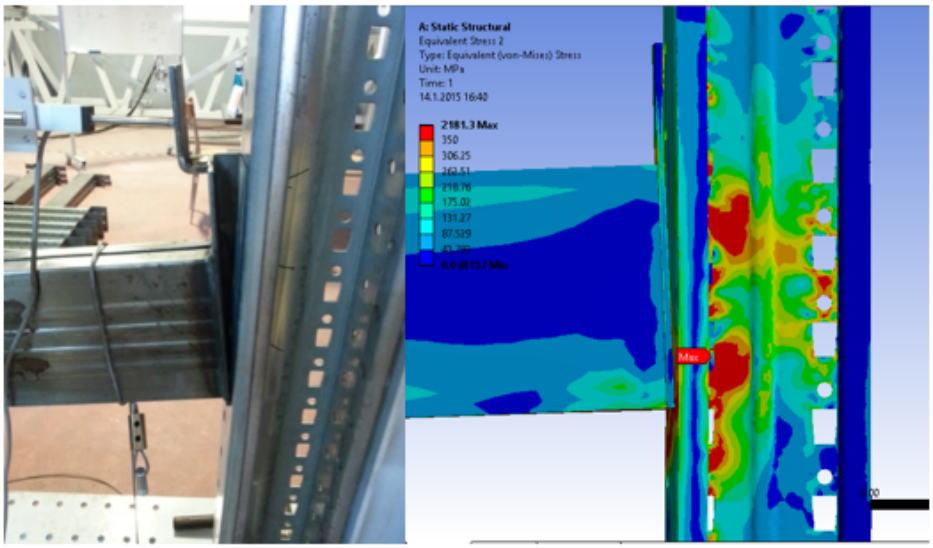

Figure 4.12. Comparison Between Experimental and Numerical Results.

Contacts in between the end-connector and upright emerged from the interlocking of taps into perforation of upright. The interlocking arrangements are in the form of a series of tabs and perform the same function as those of bolts in semi-rigid structural joints (Markazi *et al.*, 2001). The pallet beam and upright of the model are produced from roll-formed steel 1.2mm and 2.5 mm thick and the end-connector is manufactured from steel plate 4mm thick. The gap between the end-connector's interior surface and the upright's flange outer face was ignored in finite element model. Three-dimensional finite element model of the connection was developed using the SOLIDWORKS program. The developed model was plug into ANSYS software and geometrical enhancements were applied in design modeler. The boundary conditions at the ends of upright are fully restrained and the beam is restrained along z-axis, out of plane direction. Mesh refinement and manual mesh enhancement were performed on the model particularly into the curved tap surfaces.

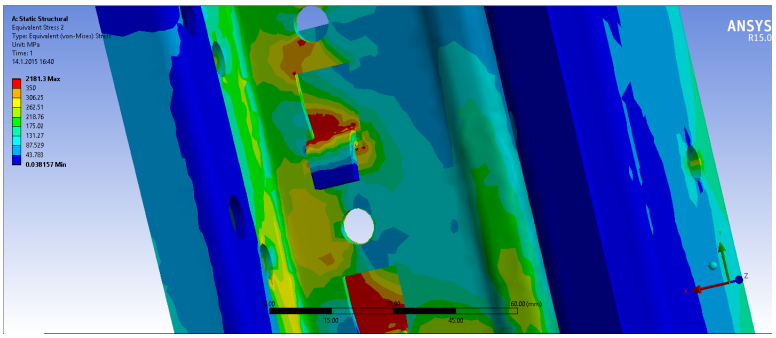

Figure 4.13. Finite Element Simulation of the Cantilever Test: Von Mises Stress at Ultimate Load.

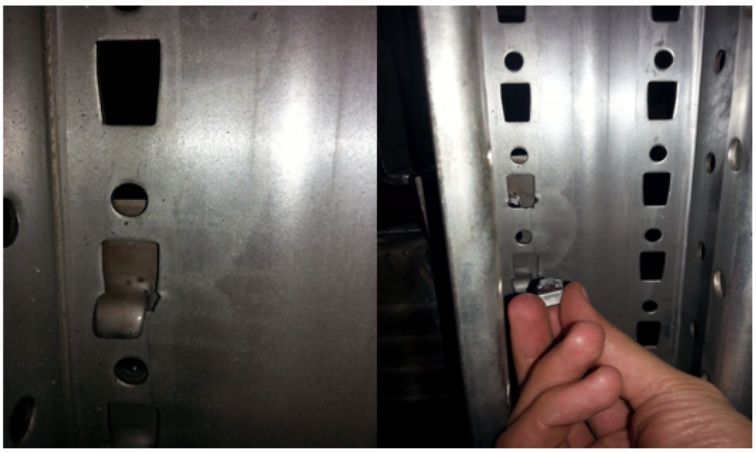

Figure 4.14. Tearing of Tabs in Test.

Appendix B presents Von-mises stress distribution on different face of the joint region step-by-step. Since the testing procedure was displacement-controlled, the target displacement was applied independent of time started from 0 to 1 second. In other words, all target displacement was given in a normalized interval. For comparing the results, force-displacement curves at the end of the cantilever beam were used as shown in Figure 4.15. The highest yield strength of the specimens was recorded as 350 MPa and this value was used as upper limit. The red regions show the surfaces which the Von-mises criterion is overstepped. Generally, the local failures occurred before reaching yield displacement, which was approved by experimental tests. The overlapped curves of numerical and experimental results in terms of initial stiffness, ultimate strength are agreed; however the ductility level and rotational capacities are different.

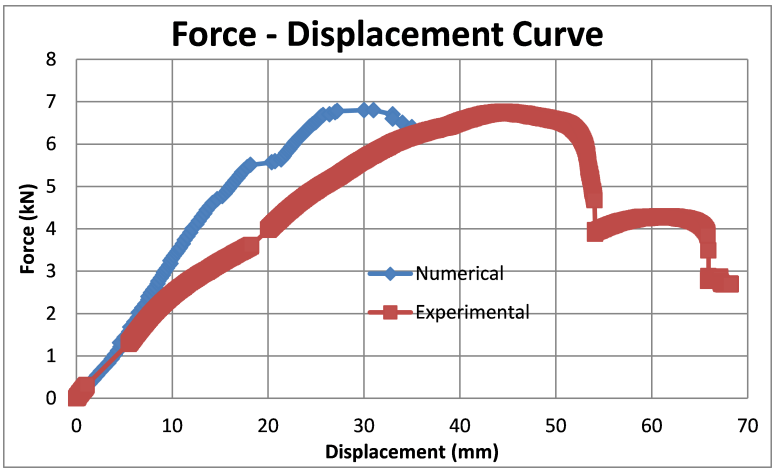

Figure 4.15. Comparison Between Experimental and Numerical Results.

5. CONCLUSIONS

In this dissertation, a selected beam-to-upright connection of a rack structure was studied. Investigations were based on testing and ANSYS modeling of beam-to-upright connection specimens. After determining tensile parameters of the 1.2mm, 2.5mm and 4.0mm thickness of the elements, the set-up required for monotonic tests was scheduled as push or pull actions of load cell. Laboratory tests were performed in two separate phases where first the yield displacement and yield strength properties were investigated by monotonic tests, and following these tests, reversed cyclic tests were conducted. Two test series with three different connections were examined where the difference was in configuration of beam connected to the end-connector as connected from top, bottom and middle. The difference in between the test series was in the depth and the number of inclined hooks and also the depth of the beam. Within the scope defined, monotonic tests on each specimen were conducted upward and downward as step-wise loading and gradually increased loading. The tests were executed in increasing the order of configuration and complexity at least three times for each specimen, and the results were graphically presented. Despite difficulties in installing a permanent set-up caused by slippage of the connection, results of each pilot test were incorporated to the failure load prediction of the final tests. The data taken from the pilot tests were calibrated with the results of a second laboratory then the final test set-up was decided. Data collected upon completion of the first and second phases of laboratory work, provided reliable information on the behavior of beam-to-upright connections considered in this study. The major parameters of the study were the information obtained from moment-rotation curves, primarily yield and ultimate moment capacities, rotational stiffness and the ductility level of end-connector connections.

5.1. Results

Generally the first cycles in reversed cyclic tests were stable and regular characterized by a progressive and regular deterioration of stiffness; both push and pull in the first cycle in elastic range were close to the responses obtained by monotonic tests.

Beams did not exhibit ductile behavior in DD140 test series; however end-connector implied ductility which compensated the non-ductile behavior of the beams. The ductility contribution of beams in DD150 test series, caused hinge allocation on the beam instead of end-connector. DD150 specimens embraced higher rotational stiffness than DD140 specimens and the ductility level was significantly higher. After first cycle of the yield displacement, the form of the hysteresis loops changed greatly owing to the influence of the residual deformations of the end-connector, resulting in deterioration in end-connector. Residual deformations in the tabs were observed in correspondence with the zero load level. Increasing with the number of executed cycles, at both edge sides of the tap in the vicinity of the slots, cracks appeared and stiffness deterioration occurred.

The cyclic response, contrary to the first cycle, was different from the cycles associated with joints for traditional steel framed buildings, which are generally characterized by stable behavior. The most important reason for the difference was slippage and gaps between the contact surfaces. Moreover, non-symmetric configuration which caused non symmetric hysteresis is another important reason. No brittle failure due to a sudden collapse of joint components was observed in any specimen except the rupture of hooks and fallen down of the taps.

The failure mode of DD140, four tapped end-connector consisted of tearing at bottom and top taps, and large deformation of the end-connector. The safety bolt contributed to joint stiffness very little at T140 and B140 specimens. The collapse mechanism of DD150 specimens was mostly due to tearing of the taps while beam was distorted at regions close to end-connector. The connection behavior of all tests was not influenced by safety bolt in elastic region. After yielding in the joint, the safety bolt caused an effect similar to strain hardening at ultimate phase. Increasing the number of tap from four into five and deeper beam caused higher initial stiffness, ultimate strength and ductility. All test specimens can be considered as semi-rigid connection according to Eurocode 3. The initial stiffness of monotonic tests was approximately equivalent to analytical stiffness calculated by RMI 2008.

Experimental test results show significant looseness in interlocked hook connections. Slackness and slippage in the connection are major disadvantages for accurate measuring and determining test set-up, concurrently induced earlier failure of the connection than expected. Therefore, looseness and slippage must be considered in the design phase of storage rack systems.

The beam-to-upright connection initial stiffness and ultimate strength obtained from the finite element cantilever test simulation agrees well with the test results. The failure modes captured in FE model was almost similar to the failure mode observed in the test. The rotational capacity of the FE model was about 20% different than the rotational capacity of the test, so the ductility levels did not comply. Improvement in the finite element result can be made by using more developed computer to reduce the run-time and by considering fracture mechanics to model the crack and tearing of the taps. Full agreement and overlap between experimental and numerical results need more detailed model which can be run by super computers to reduce the run time.

5.2. Evaluation and Comments on Future Works

This research provides test results and their interpretation of the cyclic behavior of two beam-to-upright connections with beam 140 mm and 150 mm depth respectively with four slots end-connector and five slots end-connector. Moment-rotation curves of four and five slots beam-to-upright have shown semi-rigid behavior in accordance with the classification specified in Eurocode 3. Furthermore, typical beam-to-upright connections with five slots have been shown to behave as more rigid than four slots end-connector connections.

Parametric studies of the research have demonstrated that the contribution of the end-connector depth and the number of inclined hooks might be beneficial in terms of rotational stiffness and ultimate strength of the tested connection. Concurrently to the number of slots and beam depth, the position of beam welded into end-connector (top, bottom and middle connected) have been influenced the parameters of the test like as rotational stiffness, strength, ductility and energy absorption. Particularly, beam-

to-upright connections in negative loading did not behave as predicted by RMI 2008, the rotational stiffness values of the specimens were beneath the RMI 2008 predictions due to looseness failure. By means of hysteresis loops evaluated from moment-rotation curves, monotonic and cyclic test results indicated the need for including looseness effect in connection analysis.

There remain a few areas in which further studies could provide verification of presented results as well as additional data for a more comprehensive investigation. The main areas include experimental works on the type and size of end-connectors, parametric study on different type of end-connector configurations like as using bolted connections and even interlocked connection type in which the looseness failure is inhibited in negative direction of loading. In the area of experimental work, additional data could be provided through enhancement of interlocked beam-to-upright connection types.

Five slots and pim-bolted beam-to-upright connection tests not conducted in this program include tests with deep end-connector, bolts instead of pim bolt, extended tap details, end-connectors with more than one vertical row of bolts, and fully extended plate instead of L-shape end-connectors, could be used for the development of models of moment-rotation and application to analytical and parametric studies.

The experimental data used in the current study was obtained from the cantilever test which is commonly used to design beams and beam-to-upright connections in rack structures. The beam-to-upright connection stiffness obtained from the portal test for side-sway analysis of frames could be conducted in future research to evaluate the frame stability, also base connection tests need to be performed to assess the base stiffness contribution to the structural behavior of the system. Furthermore, with reference to analytical models, the model presented in this study was limited to moment-rotation curves applicable to pushover or nonlinear static analyses. Therefore, seismic modification factors could be predicted using nonlinear static analyses in future studies. Future work in this area could include the development of simplified cyclic, degrading moment-rotation models for the purpose of nonlinear analyses. With the

knowledge on the cyclic behavior of the beam-to-upright connections, the moment-rotation results could be useful in the evaluation of the existing and new rack structures.

Further nonlinear FE models like as top and middle beam connected into end-connector and even loading in negative direction would demonstrate whether or not the model and the contact assumptions presented in this study remain applicable. FE models would include the effect of the pim-bolt located at top or bottom instead of the middle of the end-connector.

5.3. Discussion

The root cause of the structural analyses in engineering is to solve a design problem and understand the behavior of the structure. The problems resulting from earthquakes threaten human life and make damage in terms of economy and life safety. Despite the recent developments in structural engineering, earthquake damage remains a major problem for storage rack systems. It is because this type of structures is not even accepted as a structure. Most of the manufacturers of storage racks are unfortunately amateur about the behavior of rack structures. Even manufacturers who claim that they produce advanced and safe product may not be familiar with engineering aspects and code compliance design, and can have difficulties in doing analysis and design. Therefore, satisfactory realization of the problem is a must. Major obstacles to the life safety in earthquake-prone areas are the lack of enforcement of appropriate design codes and the lack of education in seismic design. While it is not possible to account for and prevent all sources of risk to human safety, engineers can play an important role in fulfilling the objective of reduction of seismic risk. In order to avoid design mistakes, standards are base solution. Design code and standards which helps to fulfill the design objectives.

To build a steel building, the design and analysis is done by engineers, the next stage is to build it by an approved contractor with required permit, and all process is inspected by an audit. The lack of standards for storage structures makes it simple for everyone to enter this market without adequate knowledge and without professional

competence. Therefore, non-standard and poor designs made for high profit must be avoided. Briefly, the approach toward the design of rack systems is not apparently equivalent to other structural systems because of the lack of standards and inadequate care by the responsible authorities. For the sake of profits and business, many manufacturers further decrease the self-weight of rack structures and make them as light as possible; therefore they can compete more favorably in the market with others but with safety problem. The major reason for this situation is the absence of structural engineers and relevant authorities in the market.

Apart from earthquakes, fire, impact and overloading are the reasons for catastrophic consequences for improperly designed and incorrectly implemented storage rack structures. Therefore, design philosophy for storage rack systems and the approach into this type of structures should be changed toward more engineered concept. A design for earthquakes must go beyond improving the seismic resistance of structures and connections and enforce the seismic design codes. The efforts should be concentrated, the objectives should be well defined and the outcomes should be the product of a group of knowledgeable people from backgrounds covering all related fields from sciences to engineering.

APPENDIX A: STEP-BY-STEP EVALUATION OF REVERSED HYSTERESIS

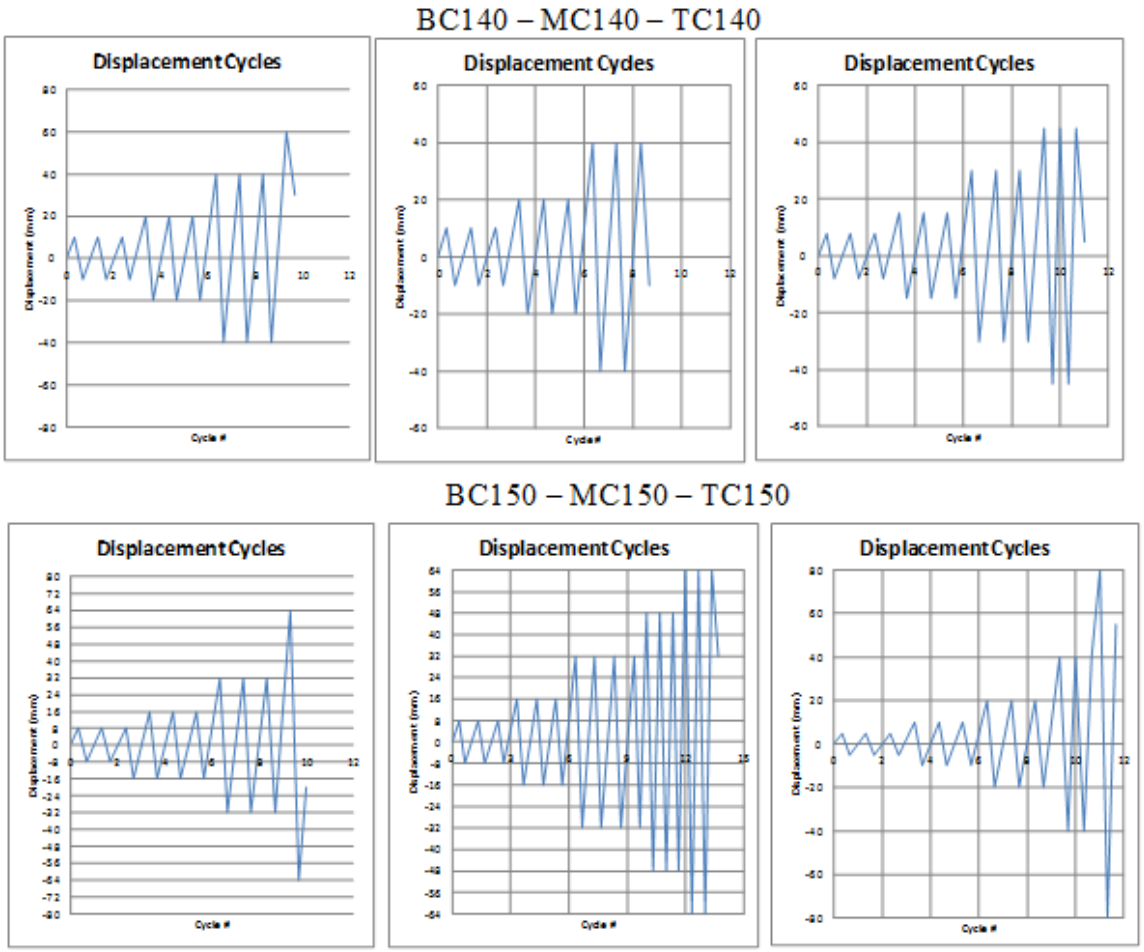

Figure A.1. Step by Step BC140 - MC140 - TC140 and BC150 - MC150 - TC150.

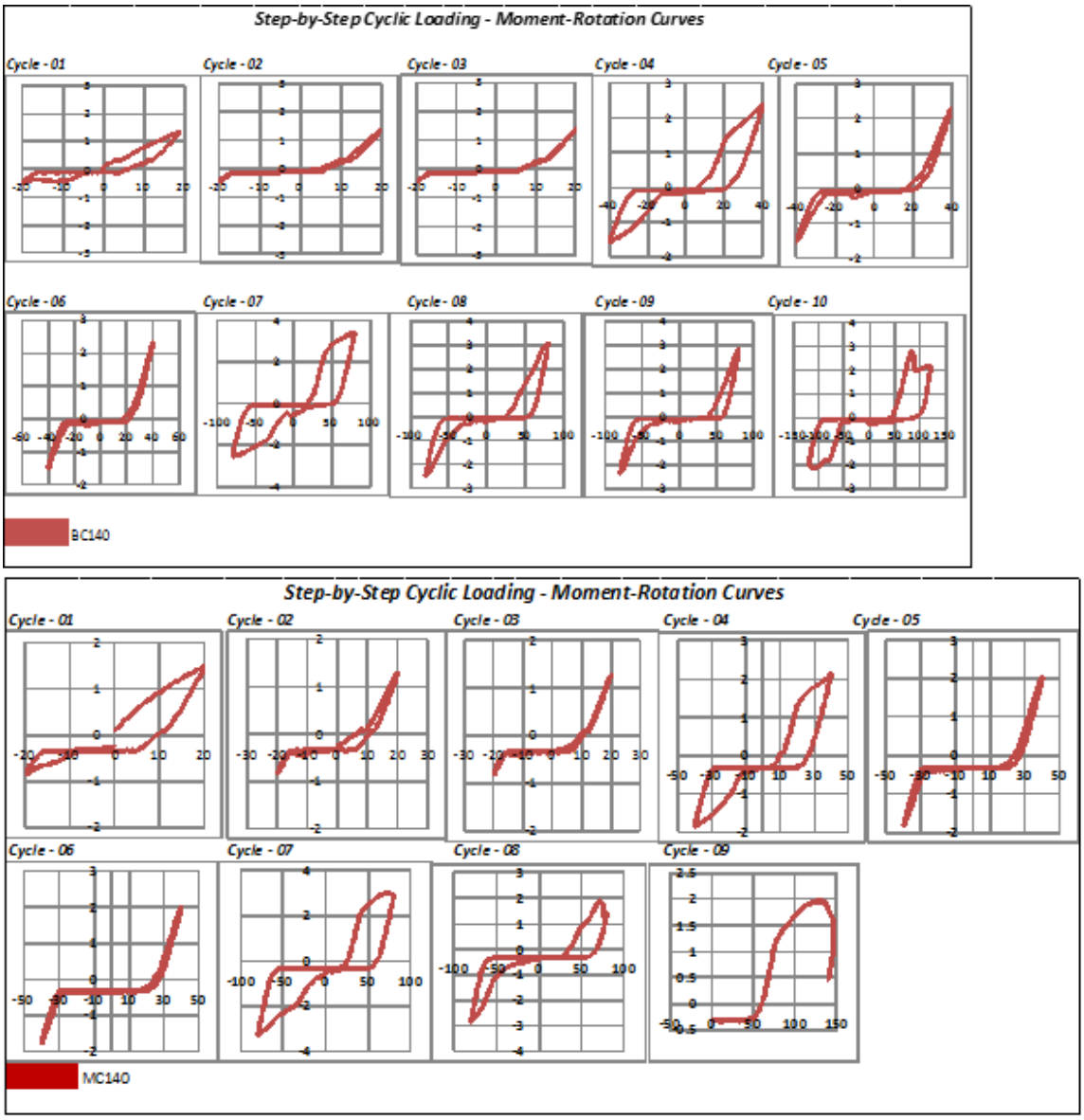

Figure A.2. Step by Step Cyclic Loading Moment Rotation Curves 1.

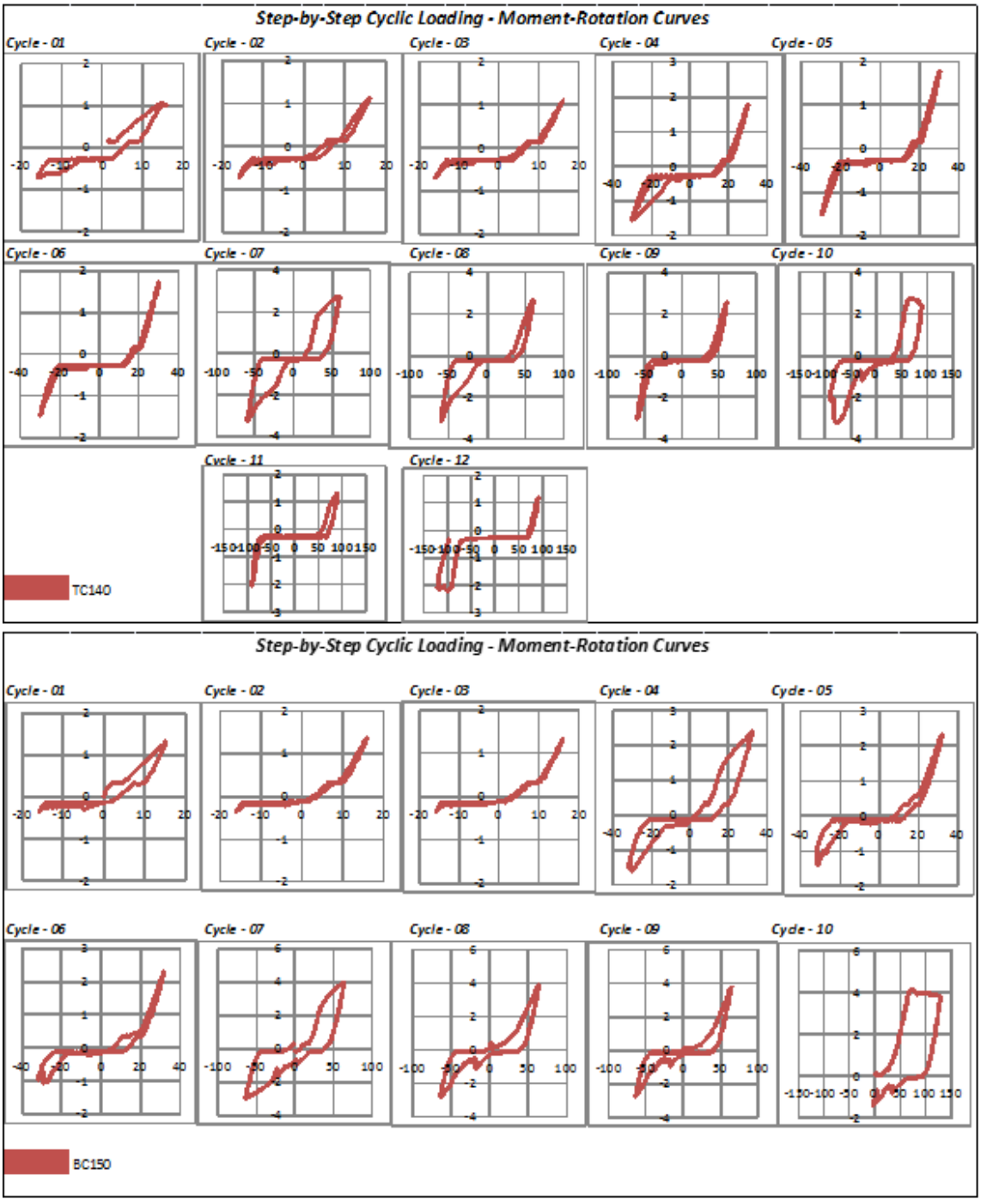

Figure A.3. Step by Step Cyclic Loading Moment Rotation Curves 2.

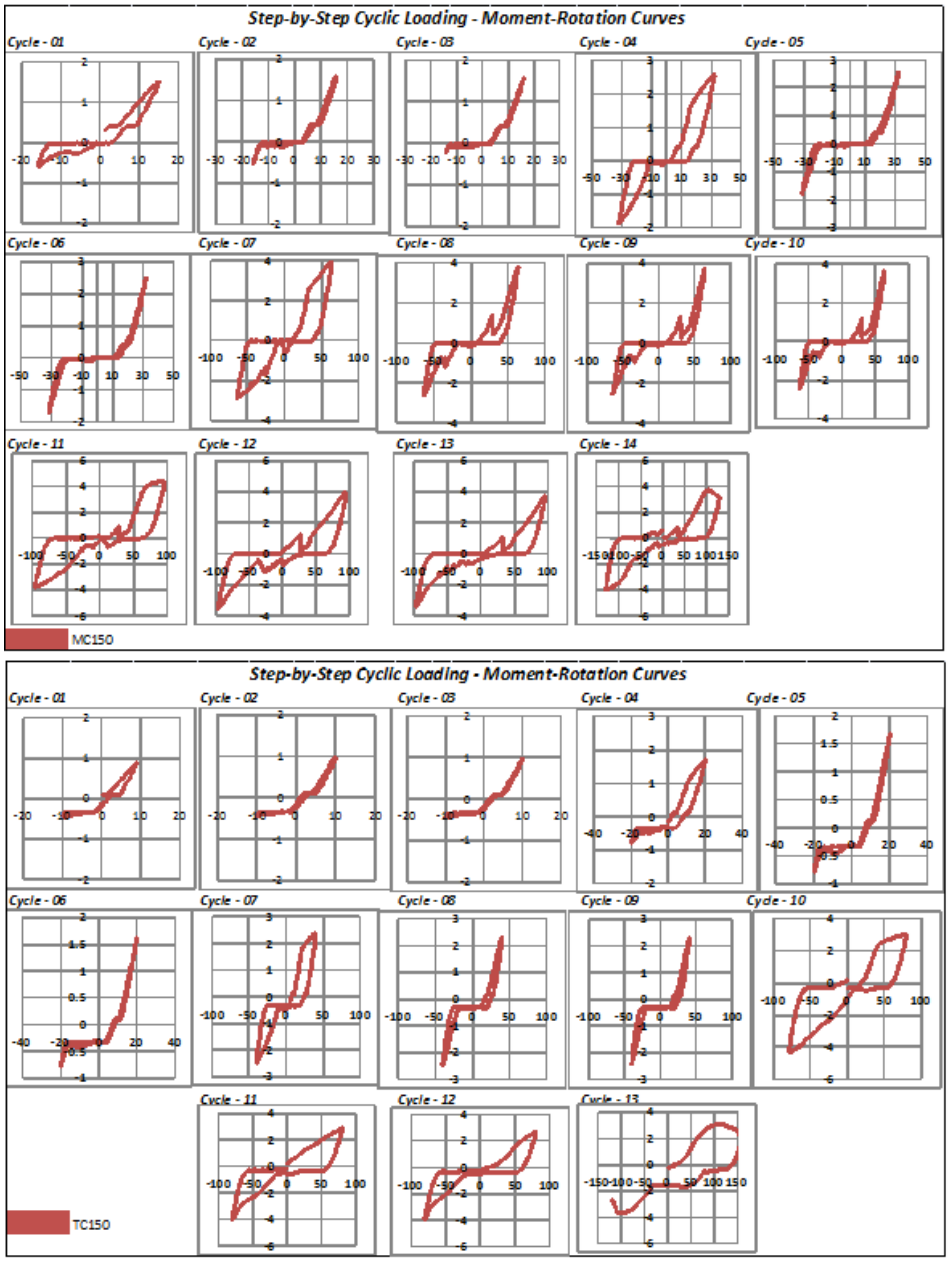

Figure A.4. Step by Step Cyclic Loading Moment Rotation Curves 3.

APPENDIX B: STEP-BY-STEP EVALUATION OF VON-MISES STRESS

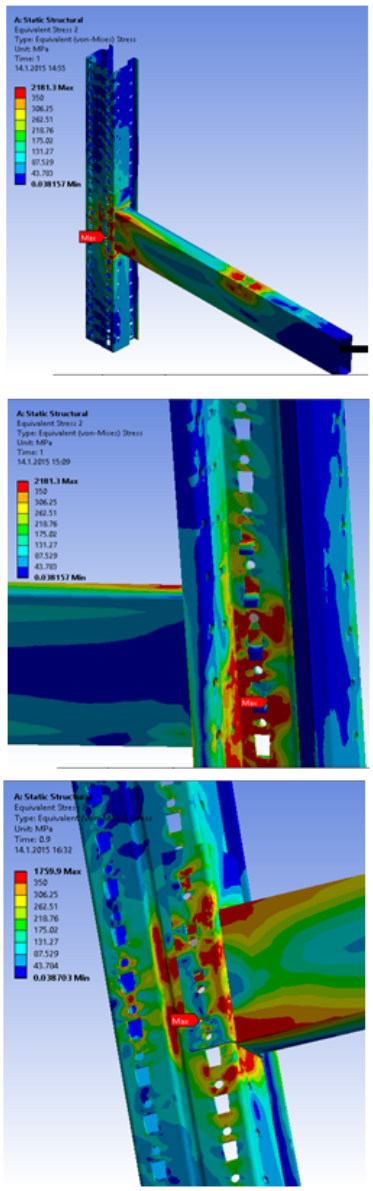

Figure B.1. Step Wise Von-Mises Stress Distribution.

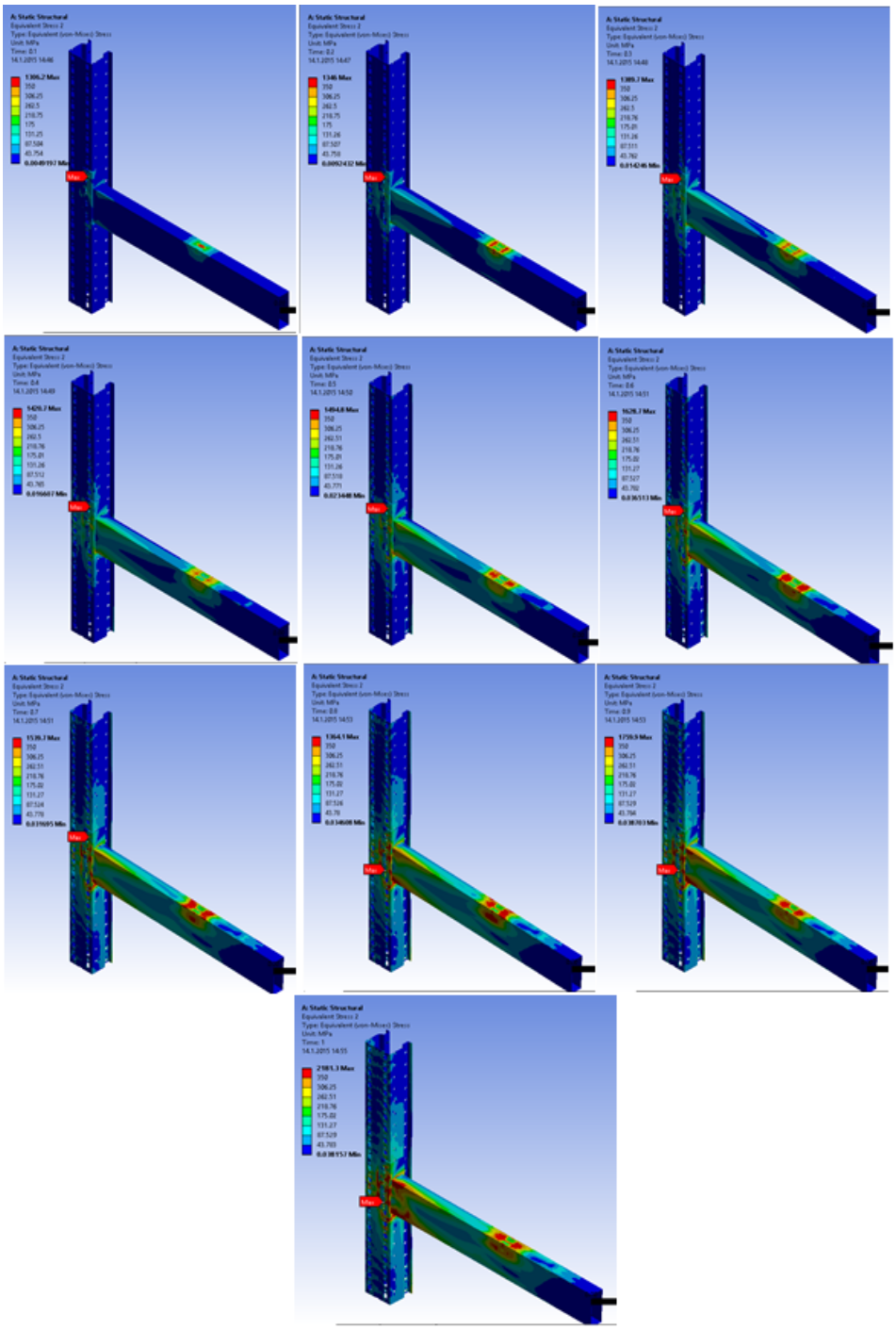

Figure B.2. Step Wise Von-Mises Stress Distribution - Upright.

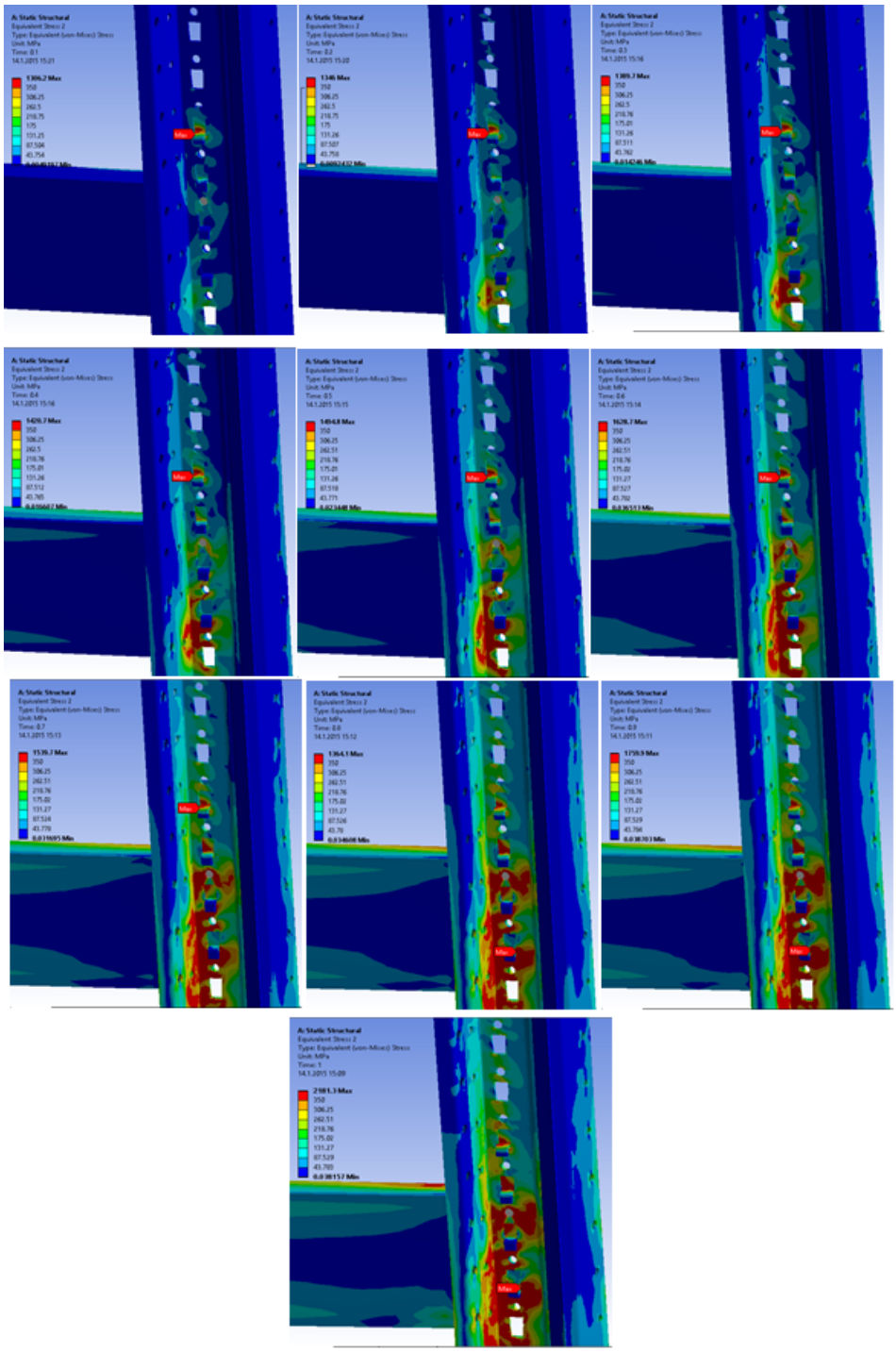

Figure B.3. Step wise Von-Mises Stress Distribution - Taps.

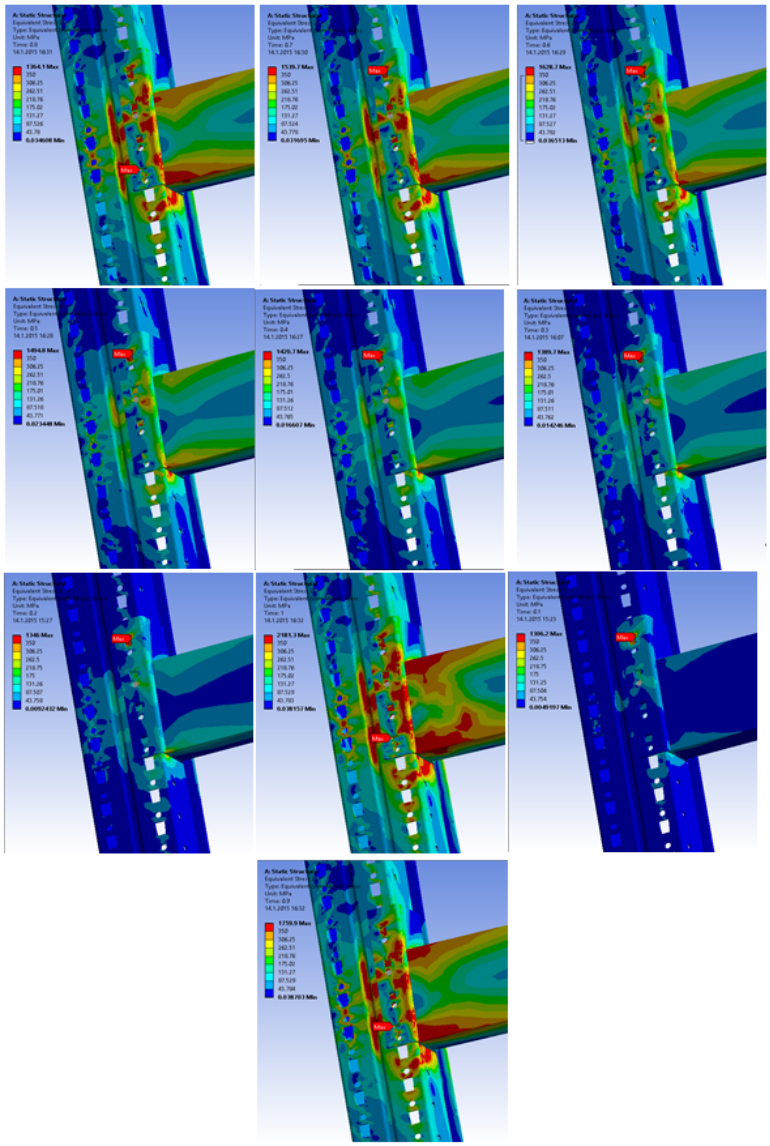

Figure B.4. Step wise Von-Mises Stress Distribution - End-connector.

REFERENCES

Abdel-Jaber, M., R.G. Beale and M.H.R. Godley, 2006, "A Theoretical and Experimental Investigation of Pallet Rack Structures under Sway", *Journal of Constructional Steel Research*, Vol. 62, pp. 68-80.

Agatino M.R., C. Bernuzzi and C.A. Castiglioni, 2001, "Joints Under Cyclic Reversal Loading in Steel Storage Pallet Racks", *Proceedings of XVIII Conference C.T.A.*, Venezia, pp. 105-114.

American Iron and Steel Institute, 2007, *North Amnerican Specification for the Design of Cold-Formed Steel Structural Members*, "American Iron and Steel Institute, Washington", DC 2007 Edition.

American Institute of Steel Construction, 2010, "Specification for Structural Steel Buildings, ANSI/AISC 360-10 an American National Standard", American Institute of Steel Construction, Chicago.

American Society of Civil Engineers, 2012, "Minimum Design Loads for Buildings and Other Structures", American Society of Civil Engineers.

American Society for Testing and Materials, E8 E8M-13a, 2013, "Standard Test Methods for Tension Testing of Metallic Materials", American Society for Testing and Materials International, West Conshohocken, Pennsylvania.

Applied Technology Council -24, 1992, "Guidelines for Cyclic Testing of Components of Steel Structures", Applied Technology Council, Redwood City, California.

Baldassino, N., C. Bernuzzi, 2000, "Analysis and Behavior of Steel Storage Pallet Racks", *Thin-Walled Structures*, Vol. 37 pp. 277-304.

Bajoria, K.M., R.S. Talikoti, 2006, "Determination of Flexibility of Beam-to-Column

Connectors Used in Thin Walled Cold-formed Steel Pallet Racking Systems", *Thin-Walled Structures*, Vol. 44, pp. 372-380.

Beale, R.G., M.H.R. Godley, 2004, "Sway Analysis of Spliced Pallet Rack Structures", *Computers and Structures*, Vol. 82, pp. 2145-2156.

Beattie, G. J. and B.L. Deam, 2006, "Seismic Design of High Level Storage Racking Systems with Public Access", BRANZ Design Guide, Judgefors, New Zealand.

Bernuzzi, C., Castiglioni C.A., 2001, "Experimental Analysis on the Cyclic Behavior of Beam-to-Column Joints in Steel Storage Pallet Racks", *Thin-Walled Structures*, Vol. 39, pp. 841-859.

Bernuzzi, C., C. Chesi and A. Parisi, 2004, "Seismic Behavior and Design of Steel Storage Racks", *13th World Conference on Earthquake Engineering*, No.481, Vancouver-Canada.

Blume, A.J., 1973, "Seismic Investigation of Steel Industrial Storage Racks", *Report Prepared for the Rack Manufacturer's Institute, San Francisco*, California.

British Standards, EN 15512, 2009, "Steel Static Storage Systems - Adjustable Pallet Racking Systems - Principles for Structural Design", Brussels Studies Institute, Brussels.

Calado, L., C.A. Castiglioni and A. Drei, 2012, "Cyclic Tests of Beam-Upright Connections in Racking Systems with a New Hybrid Procedure", Behaviour of Steel Structures in Seismic Areas.

Calderoni, B., A. De Martino, A. Formisano and L. Fiorino, 2009, "Cold Formed Steel Beams Under Monotonic and Cyclic Loading: Experimental Investigation", *Journal of Constructional Steel Research*, Vol. 65, pp. 219-227.

Casafont, M., M.M. Pastor, F. Roure, T. Peköz, 2011, "An Experimental Investigation of Distortional Buckling of Steel Storage Rack Columns", *Thin-Walled Structures*,

Vol. 49, pp. 933-946.

Casafont M., M. Pastor, J. Bonada, F. Roure and T. Peköz, 2012, "Linear Buckling Analysis of Perforated Steel Storage Rack Columns with the Finite Strip Method", *Thin-Walled Structures* Vol. 61, pp. 71-85.

Castiglioni, C.A., 2009, "Seismic Behavior of Steel Storage Racking Systems", *Politecnico di Milano*, Milano, Italy.

Castiglioni C.A., N. Panzeri, J.C. Brescianini and P. Carydis, 2003, "Shaking Table Tests on Steel Pallet Racks", *Proceedings of the Conference on Behavior of Steel Structures in Seismic Areas-Stessa*, Naples, Italy.

Castiglioni, C.A., 2005, "Seismic Behavior of Steel Storage Pallet Racking Systems", Thesis and Dissertation.

Castiglioni, C.A., A. Drei and R. Goncalves, 2010, "A New Hybrid Testing Procedure for the Low Cycle Fatigue Behavior of Structural Elements and Connections", Sloan Digital Sky Survey Rio Stability and Ductility of Steel Structures.

Chen, C.K., R.E. Scholl and J.A. Blume, 1980, "Seismic Study of Industrial Storage Racks", Report prepared for the National Science Foundation and for the Rack Manufacturers Institute and Automated Storage and Retrieval Systems.

Cheng, Y., B.W. Schafer, 2003, "Local Buckling Tests on Cold-Formed Steel Beams", *Journal Structural Engineering*, Vol. 129, pp. 1596-1606.

Cheng, Y., B.W. Schafer, 2006, "Distortional Buckling Tests on Cold-Formed Steel Beams", *Journal Structural Engineering*, Vol. 132, pp. 515-528.

Cheng, Y., B.W. Schafer, 2007, "Simulation of Cold-Formed Steel Beams in Local and Distortional Buckling with Applications to the Direct Strength Method", *Journal of Constructional Steel Research*, Vol. 63, pp. 581-590.

Chung, K.F., L. Lau, 1999, "Experimental Investigation on Bolted Moment Connections Among Cold Formed Steel Members", *Engineering Structures*, Vol. 21, pp. 898-911.

Deng, C.G., O.S. Bursi, R. Zandonini, 2000, "A Hysteretic Connection Element and its Applications", *Computers and Structures*, Vol. 78, pp. 93-110.

Dogangun, A., R. Livaoglu, 2006, "A Comparative Study of the Design Spectra Defined by Eurocode 8, UBC, IBC and Turkish Earthquake Code on R/C Sample Buildings", *Journal of Seismology*, Vol. 10, No. 3, pp. 335-351.

Eoropean Conference on Complex Systems No 45, 1986, "Recommended Testing Procedure for Assessing the Behavior of Structural Steel Elements under Cyclic Loads", European Convention for Constructional Steelwork, First Edition.

The Federation Europeenne de la Manotention, 2001, "The Design of Static Steel Pallet Racks", Federation Europeen de la Manutention.

The Federation Europeenne de la Manotention, 2001, "Guidelines Fot the Safe Use of Static Steel Racking and Shelving", Federation Europeen de la Manutention.

The Federation Europeenne de la Manotention, 2005, "The Seismic Design of Static Steel Pallet Racks", Federation European de la Manutention, Final Draft.

Federal Emergency Management Agency, 2003, "National Earthquake Hazards Reduction Program Recommended Provisions for New Buildings and Other Structures - Part 1: Provisions, Prepared for FEMA by the Building Seismic Safety Council", Washington, District of Columbia.

Federal Emergency Management Agency, 460, 2005, "Seismic Considerations for Steel Storage Racks Located in Areas Accessible to the Public", Building Seismic Safety Council.

Feritas, A.M.S., F.T. Souza, M.S.R. Freitas, 2010, "Analysis and Behavior of Steel

Storage Drive-in Racks", *Thin-Walled Structures*, Vol. 48, pp. 110-117.

Filiatrault, A. and A. Wanitkorkul, 2005, "Shake-Table Testing of Frazier Industrial Storage Racks", Report No., Structural Engineering and Earthquake Simulation Laboratory, Departmental of Civil Structural and Environmental Engineering, SUNY Buffalo.

Filiatrault, A., P.S. Higgins, A. Wanitkorkul and J. Courtwright, 2007, "Experimental Stiffness of Pallet-Type Steel Storage Rack Teardrop Connectors", *Practice Periodical Structural Design Construction*, Vol. 12, pp. 210-215.

Gilbert, B.P., K.J.R. Rasmussen, 2010, "Bolted Moment Connections in Drive-in and Drive-Through Steel Storage Racks", *Journal of Constructional Steel Research*, Vol. 66, pp. 755-766.

Gilbert, B.P., K.J.R. Rasmussen, 2011, "Determination of the Base Plate Stiffness and Strength of Steel Storage Racks", *Journal of Constructional Steel Research*, Vol. 67, pp.1031-1041.

Gilbert, B.P., K.J.R. Rasmussen 2012, "Drive-in Steel Storage Racks I: Stiffness Tests and 3D Load-Transfer Mechanisms", *Journal Structural Engineering*, Vol. 138, pp. 135-147.

Gilbert, B.P., K.J.R. Rasmussen and H. Zhang, 2009, "Impact Tests and Parametric Impact Studies on Drive-in Steel Storage Racks", Research Reports 2013, School of Civil Engineering, University of Sydney, Sydney Australia.

Godley, M.H.R., 1997, "Plastic Design of Pallet Rack Beams", *Thin-Walled Structures* Vol. 29, No. 1-4, pp.175-188.

Godley, M.H.R, R.G. Beale, 2008, "Investigation of the Effects of Looseness of Bracing Components in the Cross-Aisle Direction on the Ultimate Load-Carrying Capacity of Pallet Rack Frames", *Thin-Walled Structures*, Vol. 46, pp. 848-854.

Hancock, G.J., 2003, "Cold-Formed Steel Structures", *Journal of Constructional Steel Research*, Vol. 59, pp. 473-487.

Hanoglu, K., Y. Yuva, O. Yoney and R. Shahshenas, 2010, "Pallet Racking and European and Turkish Earthquake Engineering", Rafder Workshop Presentation on Seismic Behavior of Rack Systems and Design Procedures, Istanbul.

Harris, E., and G.J. Hancock, 2002, "Sway Stability Testing of High Rise Rack: Sub-Assemblages", Proceedings of the 16^{th} Specialty Conference of Cold-Formed Steel Structures, University of Missouri-Rolla.

Jaspart, J.P., 1999, "Semi-Rigid Behavior of Civil Engineering Structural Connections", Recent Advances in the field of Structural Steel Joints and their Representation in the Building Frames Analysis and Design Process, COST C1 European Commission, University of Liege, Brussels Luxembourg.

Krawinkler, H., N.G. Cofie, M.A. Astiz, and C.A. Kircher, 1979, "Experimental Study on the Seismic Behavior of Industrial Storage Racks", Report No. 41, The John A. Blume Earthquake Engineering Center, Department of Civil Engineering, Stanford University, Stanford, California's.

Kotha, R., T., Peköz, 2000, "Cold-Formed Steel Frame and Beam-Column Design", School of Civil and Environmental Engineering, Cornell University, New York.

Kwon, Y.B., H.S. Chung and G.D. Kim, 2006, "Experiments of Cold-Formed Steel Connections and Portal Frames", *Journal of Structural Engineering*, Vol. 132, pp. 600-607.

Lim, J.B.P., D.A. Nethercot, 2003, "Ultimater Strength of Bolted Moment Connections Between Cold-Formed Steel Members", *Thin-Walled Structures*, Vol. 41, pp. 1019-1039.

Lim, J.B.P., D.A. Nethercot, 2004, "Stiffness Prediction for Bolted Moment Connec-

tions Between Cold-Formed Steel Members", *Journal of Constructional Steel Research*, Vol. 60, pp. 85-107.

National Earthquake Hazards Reduction Program, 2003, "Recommended Provisions for the Decelopment of Seismic Regulations for New Buildings", Building Seismic Safety Council, Federal Emergency Management Agency, Washington DC.

Ng, A.L.Y., R.G. Bale and M.H.R. Godley, 2009, "Methods of Restraining Progressive Collapse in Rack Structures", *Engineering Structures*, Vol. 31, pp. 1460-1468.

Pastor, M.M., M. Casafont and *et al.*, 2009, "Optimization of Cold-Formed Steel Pallet Racking Cross-Sections for Flexural-Torsional Buckling with Constraints on the Geometry", *Engineering Structures*, Vol. 31, pp. 2711-2722.

Prabha ,P., V. Marimuthu, M. Saravanan and J.S. Arul, 2010, "Evaluation of Connection Flexibility in Cold Formed Steel Racks", *Journal of Constructional Steel Research*, Vol. 66, pp. 863-872.

Remote Method Invocation, 2004, "Testing Guidelines for Pallet Stacking Frames, Rack Manufacturing Institute", Charlotte, North Carolina.

Remote Method Invocation, 2008, "Specifications for the Design, Testing and Utilization of Industrial Steel Storage Racks", Rack Manufacturing Institute, Charlotte, North Carolina.

Sabbagh, A.B., M. Petkovski, K. Pilakoutas and R. Mirghaderi, 2013, "Cyclic Behavior of Bolted Cold-Formed Steel Moment Connections: FE Modeling Including Slip", *Journal of Constructional Steel Research*, Vol. 80, pp. 100-108.

Sarawit, A., Peköz T., 2006, "Cold Formed Steel Frame and Beam-Column Design", *Research Report RP03-2*, American Iron and Steel Institute.

Sato, A., C.M. Uang, 2008, "Application of Instantaneous Center of Rotation Concept for Cyclic Modeling of Bolted Connections in Special Bolted Moment Frames",

Connections in Steel Structures VI, Chicago.

Sato, A., C.M. Uang, 2009, "Seismic Design Procedure Development for Cold-Formed Steel-Special Bolted Moment Frames", *Journal of Constructional Steel Research*, Vol. 65, pp. 860-868.

Sato, A., C.M. Uang, 2010, "Seismic Performance Factors for Cold-Formed Steel Special Bolted Moment Frames", *Journal Structural Engineering*, Vol. 136, pp. 961-967.

Shifferaw, Y., B.W. Schafer, 2012, "Inelastic Bending Capacity of Cold-Formed Steel Members", *Journal Structural Engineering*, Vol. 138, pp. 468-480.

Uang, C.M., A. Sato, J.K. Hong and K. Wood, 2010, "Cyclic Testing and Modeling of Cold-Formed Steel Special Bolted Moment Frame Connections", *Journal Structural Engineering*, Vol. 136, pp. 953-960.

Wong, M.F., K.F. Chung, 2002, "Structural Behavior of Bolted Moment Connections in Cold-Formed Steel Beam-Column Sub-Frames", *Journal of Constructional Steel Research*, Vol. 58, pp. 253-274.

Yemez, K., 2007, "Experimental Study on the Behavior of an I-Bean to SHS-Column by T-Stub Bolted Connection", Ph.D. Thesis in Civil Engineering, Bogaziçi University.

Yu, W.K., K.F. Chung and M.F. Wong, 2005, "Analysis of Bolted Moment Connections in Cold-Formed Steel Beam-Column Sub-Frames", *Journal of Constructional Steel Research*, Vol. 61, pp. 1332-1352.

Zaharia, R., D. Dubina, 2006, "Stiffness of Joints in Bolted Connected Cold-Formed Steel Trusses", *Journal of Constructional Steel Research*, Vol. 62, pp. 240-249.

Zhang, H., B.P. Gilbert and K.J.R. Rasmussen, 2012, "Drive-in Steel Storage Racks. II: Reliability-Based Design for Forklift Truck Impact", *Journal Structural Engi-*

neering, Vol. 138, No. 2, pp. 148-156.

Zhao, X., T. Wang, Y. Chen, A. Sivakumaran, 2014, "Flexural Behavior of Steel Rack Beam-to-upright Connections", *Journal of Constructional Steel Research*, Vol. 99, pp. 161-175.